

M-Pos94 HYDROGEN EXCHANGE IN M13 COAT PROTEIN: MEASUREMENT OF INDIVIDUAL RAPIDLY EXCHANGING AMIDE PROTONS IN A MODEL MEMBRANE PROTEIN BY A ^{13}C NMR ISOTOPE SHIFT METHOD. Gillian D. Henry, Joel H. Weiner and Brian D. Sykes, Department of Biochemistry, University of Alberta, Edmonton, Alberta, T6G 2H7, Canada.

M13 coat protein is a 50-residue model membrane protein comprising a 19-residue hydrophobic core flanked by hydrophilic terminal regions. Hydrogen exchange rates have been measured for individual assigned amide protons in detergent-solubilized M13 coat proteins as a function of pH using an equilibrium ^{13}C NMR isotope shift technique. In D_2O solutions, a peptide carbonyl resonance undergoes a small (0.08-0.09 ppm) isotope shift; in 1:1 $\text{H}_2\text{O}:\text{D}_2\text{O}$ mixtures the carbonyl lineshape is determined by the exchange rate at the adjacent nitrogen atom. In proteins structural factors, notably H-bonding, can reduce H-exchange by many orders of magnitude over model peptides such as poly-D,L-alanine (PDLA). Using coat protein which has been biosynthetically labelled with ^{13}C at individual carbonyl sites, a map of the exchange rates of the more labile amides has been constructed (1-10⁴-fold retardation over PDLA). These arise mainly from the hydrophilic domains; the more slowly exchanging amide protons (detected by ^1H NMR) have been shown to correspond to those of the hydrophobic core. (see O'Neil *et al.* adjacent abstract). The extreme termini of the protein exchange as rapidly as PDLA, and other NMR experiments have shown these to be the only regions which possess significant backbone mobility on a nanosecond timescale. In the remainder of the N-terminal region, exchange rates are retarded less than 100-fold suggesting this region to be in a state of relatively rapid dynamic flux. By contrast, proceeding inwards from the C-terminus the exchange rates decrease markedly in a way suggestive of a helical segment which may extend throughout the hydrophobic core.

M-Pos95 HYDROGEN EXCHANGE IN M13 COAT PROTEIN; MEASUREMENT OF THE SLOWEST EXCHANGING HYDROGENS BY ^1H NMR SPECTROSCOPY. J.D.J. O'Neil and B.D. Sykes. Department of Biochemistry, University of Alberta, Edmonton, Alberta, Canada, T6G 2H7.

The coat protein of the bacteriophage M13 is inserted into the inner membrane of *E. coli* during infection. The protein consists of a 19-residue hydrophobic core (presumably, a membrane-spanning helix), flanked by N-terminal acidic and C-terminal basic segments of 20 and 11 residues, respectively. In order to obtain information about the structure of this small, model-membrane protein, in a membrane mimetic environment, we have measured peptide amide exchange rates using ^1H NMR spectroscopy of the protein solubilized in dodecylsulfate micelles. During the course of an exchange experiment individual peptide amide resonances are not completely resolved in the NMR spectrum. However, analysis of the *total* protein amide exchange data shows that individual peptide amides belong to one of three kinetically distinguishable sets of amides. This shows that the protein consists of 3 independently unfolding elements of secondary structure. Two of these sets of amides exchange 10⁴ and 10⁵-fold more slowly than unstructured, freely-exchanging amides. From pH 4-9, these two sets show a depressed dependence upon hydroxide concentration ($[\text{OH}^-]^{\frac{1}{2}}$) which supports the idea that these elements of structure are particularly stable and may unfold via global unfolding reactions. Hydrogen exchange measurements on a synthetic peptide corresponding to the acidic N-terminus of the protein (1-21) showed that exchange is very rapid at room temperature. Limited digestion of the protein with proteinase K removes the N-terminal domain, eliminates the rapidly exchanging amides and increases the rates of exchange of the slow sets by 10-100-fold. This shows that the slowest exchanging peptide amides are in the hydrophobic core of the protein.

M-Pos96 THE CONFORMATION AND HYDROPHOBICITY OF THE SUBUNITS OF DIPHTHERIA TOXIN. Jian-Min Zhao and Erwin London, Dept. of Biochemistry, State University of New York at Stony Brook, Stony Brook, NY 11794-5215.

Diphtheria toxin is a protein that penetrates membranes when it encounters the low pH found in acidic organelles. In order to understand the penetration process the pH and thermal dependence of the conformation of the A and B subunits of the toxin was examined using fluorescence techniques. The hydrophobicity of the subunits was assayed by their ability to bind to non-ionic detergents, as detected by a fluorescence quenching method. The A subunit undergoes a major conformational change at both low pH and high temperature. Under these conditions there is an increased exposure of Trp residues to solution as judged by a red shift in the wavelength of maximum emission. In addition, at low pH the A subunit becomes hydrophobic, but not at high temperature. The thermal transition occurs near 45°C, and previous investigators have identified it as the thermal denaturation event by calorimetry. The pH transition occurs near pH 3.5 (at 23°C) or 4 (at 37°C). The B subunit of the toxin does not show a significant change in Trp emission wavelength at low pH or high temperature. However, it does exhibit an increased hydrophobicity at low pH (midpoint about pH 5 at 23°C). It appears that the behavior of the toxin at low pH and high temperature can be partly explained in terms of the behavior of its individual subunits. This work was supported by N.I.H. grant GM 31986.

M-Pos97 PHOTOLABELING OF CALMODULIN WITH p-BENZOYL-PHENYLALANYL PEPTIDES, Susan Erickson-Viitanen, James C. Kauer, Henry R. Wolfe, Jr., and William F. DeGrado, E. I. du Pont de Nemours & Company, Central Research & Development Department, Wilmington, DE 19898.

p-Benzoyl-phenylalanine (Bpa) is a photoreactive amino acid which can easily be incorporated into a peptide by solid-phase peptide synthesis. Previously (Kauer, J. C. et al., *J. Biol. Chem.* 261, 10675, 1986), we have shown that substitution of Bpa for tryptophan in a synthetic calmodulin binding peptide (K-L-Bpa-K-K-L-L-K-L-L-K-K-L-L-K-L-G) results in a 1:1 adduct with calmodulin upon photolysis. We report here studies with the ^3H -acetyl derivative of this Bpa peptide. The acetylated synthetic Bpa peptide gives rise to two 1:1 adducts that can be separated on DEAE-Sephacel followed by HPLC. The ^3H -labeled cyanogen bromide fragments from the two adduct peaks differ in their amino acid composition and indicate that labeling occurs on both the amino and carboxyl terminal halves of the calmodulin molecule. We have also synthesized the photolabile derivative of the calmodulin-binding domain of smooth muscle myosin light chain kinase: R-R-K-Bpa-Q-K-T-G-H-A-V-R-A-I-G-R-L-S-G (Bpa-SMLCK). Upon photolysis, Bpa-SMLCK forms a 1:1 adduct with calmodulin in a Ca^{+2} -dependent manner. This adduct constitutes 76% of the photolysis products separated by HPLC. A cyanogen bromide fragment which appears to contain the SMLCK peptide has been isolated and its sequence is under investigation.

M-Pos98 EFFECTS OF LIGANDS ON THE DOMAIN-DOMAIN INTERACTIONS IN PYRUVATE KINASE. Thomas G. Consler, Edward C. Uberacker, Gerard J. Bunick, Michael N. Liebman, and James C. Lee, Department of Biochemistry, St. Louis Univ. School of Medicine, St. Louis, MO, 63104, Biology and Solid State Divisions, Oak Ridge National Lab, Oak Ridge, TN 37831, and Department of Physiology and Biophysics, Mt. Sinai School of Medicine of the City Univ. of New York, NY 10029.

Rabbit muscle pyruvate kinase (PK) is catalytically active in the presence of Mg^{++} and phosphoenolpyruvate (PEP). The steady-state kinetics are shifted from a hyperbolic to a sigmoidal dependency on PEP concentration by L-phenylalanine (Phe). Structural information obtained from difference sedimentation velocity and small angle neutron scattering experiments indicate Mg^{++} and PEP induce a significant change in the hydrodynamic properties of PK, and this change is reversed by Phe. These hydrodynamic properties indicate a contraction or expansion of the global structure of PK. In order to further elucidate the nature of the structural change at the molecular level, scattering data was calculated using the X-ray crystallographic data obtained in the absence of Mg^{++} . A good agreement was obtained between the calculated and experimental scattering data. In the structure of inactive PK, the active site lies in an open cleft, formed by two of the four domains in each subunit. With the aid of computer graphics, the cleft was closed by rotating one domain with respect to the other, thus simulating the active form. The altered coordinates were used to simulate scattering curves which agree very well with the experimental curves obtained in the presence of Mg^{++} and PEP. Furthermore, peptide sequence analysis indicates that the hinge region between these two domains is preferentially exposed in the presence of Phe. Hence, it can be concluded that the conversion of inactive to active PK is accomplished by domain movements.

M-Pos99 THE INFLUENCE OF GLYCEROL ON HYDROGEN EXCHANGE IN LYSOZYME. Roger B. Gregory. Department of Chemistry, Kent State University, Kent, OH 44242. Andreas Rosenberg, Dept. of Lab. Medicine & Pathology, University of Minnesota, Minneapolis, Minnesota 55455.

Hydrogen isotope exchange rates for lysozyme in glycerol cosolvent mixtures (Knox & Rosenberg, 1980, *Biopolymers* 19, 1049-1068) have been analyzed as functions of solvent viscosity and glycerol activity, in an attempt to determine which solvent properties affect the exchange kinetics. Fast exchanging protons ($60 > H(t) > 25$) are all affected equally by glycerol. Plots of $-\log t$, where t is the time taken to reach a particular number of hydrogens remaining unexchanged, $H(t)$, as a function of $\log \eta$ all have slopes ≈ -1 . The corresponding plots as a function of $\log a_{\text{gly}}$ have slopes ≈ -0.6 . Exchange behavior of the slowest exchanging protons ($H(t) < 20$) is quite different. Slower and slower protons are affected to greater and greater extents by glycerol with limiting slopes of: $-\log t / d \log \eta \approx -3$ and $-d \log t / d \log a_{\text{gly}} \approx -1.6$. Interpreted in terms of EX₂ mechanism of exchange, $-d \log t / d \log a_{\text{gly}}$ is a measure of the difference in the preferential exclusion, $\Delta \epsilon_{\text{gly}}$, of solvent components from the vicinity of the protein in its catalyst accessible and catalyst inaccessible states, the accessible state being the more thermodynamically unfavorable in glycerol-water mixtures. For comparison, $\Delta \epsilon_{\text{gly}}$ for thermal unfolding of lysozyme is between 0 and -0.5. Values of $-d \log t / d \log a_{\text{gly}}$ for exchange are too large to be consistent with exchange occurring from locally unfolded states if $\Delta \epsilon_{\text{gly}}$ is assumed to reflect the size of the unfolding unit. Instead, the value of $-d \log t / d \log \eta \approx -1$ suggests that the fast protons exchange via a mechanism of gated catalyst diffusion within the protein. The large effect of glycerol on the slow exchanging protons cannot be explained in terms of viscosity or preferential exclusion of glycerol alone and involves additional effects. Supported by NSF grants PCM 83-03027 (AR) and DMB 85-18941 (RBG).

M-Pos100 THE EPITOPE FOR MAB G9 ON HUMAN OROSOMUCOID. John S. Ivancic, Ana I. Bencosme, H. Brian Halsall, Dept. of Chemistry and Biomedical Chemistry Research Center, Univ. of Cincinnati, Cincinnati, OH 45221-0172.

Orosomucoid (OMD) is an abundant and heavily glycosylated serum glycoprotein of unknown function but having a strong propensity to bind basic drugs. We are using monoclonal antibodies (MAbs) to monitor access to the protein core and map its surface (Fed. Proc. 45 (1986) 1574). MAb G9 is particularly interesting. Chymotryptides of CNBr II (res 112-183) were separated by HPLC and the peptides screened by immunospot with G9. The smallest immunoreactive peptides were sequenced and overlaps sought. The epitope was localized within the region of res 158 TDWKKDKCEPL 168. Reversible chemical modification with citraconic anhydride indicated an important role for lys 161, 162 or 164. Access to the epitope by G9 was less hindered when the proximal asn 75 was occupied by a biantennary rather than a tri/tetra-antennary glycan chain. Preliminary data using immuno chromatography suggest either that the epitope has a conformational component, or that access to it is conformationally controlled. However, reduction and alkylation, which destroys cys 165 → cys 72, enhances rather than diminishes binding, indicating little direct contribution of the cys 72 containing region. Features of note of this epitope: a) it includes trp 160, which is part of the basic drug binding site, b) it includes cys 165 which participates in a disulphide bond, c) it is part of a very strongly predicted alpha helical region of high antigenicity according to the Hodges method, d) it is close to glycosylation site IV at asn 75.

M-Pos101 SITE DIRECTED MUTAGENESIS OF COLICIN E1 PROVIDES SPECIFIC ATTACHMENT SITES FOR SPIN LABELS WHOSE SPECTRA ARE SENSITIVE TO LOCAL CONFORMATION AND MEMBRANE BINDING. A. Paul Todd*, Veronica Crozel[†], Francoise Levinthal[†], Cyrus Levinthal[†] and Wayne Hubbell*, *Jules Stein Eye Institute and Department of Chemistry and Biochemistry, University of California, Los Angeles, Ca 90024 and [†]Department of Biological Sciences, Columbia University, New York, NY 10027

Colicin E1 is an E. coli plasmid-encoded protein that spontaneously inserts into lipid membranes to form a voltage gated channel. In order to investigate structure and voltage-dependent conformational changes in this channel, we are employing a novel approach in which site directed mutagenesis is used to provide highly specific attachment points for nitroxide spin labels. Thus, a series of colicin mutants, differing only by the position of a single cysteine residue, have been prepared and selectively labeled at that cysteine. The EPR spectra of the labeled protein convey information about local conformation and how it changes upon binding to the membrane and opening and closing of the channel.

For a short sequence outside of the channel-forming region, the mobility of the spin labeled side chain appears to be a periodic function of displacement along the peptide, suggestive of an amphipathic alpha helix. Decreased side chain mobility as well as inaccessibility to aqueous line-broadening agents in liposome suspension indicate that this sequence is buried in the membrane upon binding of colicin to liposomes. Changes in lineshape thus provide a sensitive assay for binding and allow exploration of the effects of pH, ionic strength and lipid composition.

We have developed methods for clamping the transmembrane voltage in a vesicle preparation in the presence of open colicin channels. EPR spectral changes of spin labeled mutant colicins as a function of voltage will provide a unique and powerful tool in elucidating the open channel conformation and gating mechanism.

M-Pos102 POSSIBLE CONFORMATIONS OF THE COLICIN E1 VOLTAGE-SWITCHABLE CHANNEL

P. Youkharibache*, R. Fine, C. Levinthal, Dept of Biol. Columbia Univ. NY NY 10027

Colicin E1, a protein of 522 amino acids, is a bacterial toxin which kills sensitive E. coli cells by making an ion channel in their plasma membrane and thus discharging the transmembrane potential and stopping oxidative phosphorylation. We have isolated and purified short peptides produced by CNBr cleavage after oligonucleotide directed mutagenesis which introduce new methionine codons in the colicin structural gene. With S. Slatin and A. Finkelstein (Liu, et al., "A very short peptide can make a voltage dependent ion channel: The critical length of the channel domain of colicin E1", *Proteins*, vol I, 1986) we have shown that a peptide of less than 88 amino acids can form a voltage-switchable channel in a phospholipid bilayer. With P. Todd and W. Hubbell (F. Levinthal, et al., "One short peptide of colicin E1 can form an ion channel: stoichiometry confirms kinetics", *PNAS*, in press) we have shown stoichiometrically that a single molecule, as monomer, can form a channel and discharge the potential across the membrane of a small 400 Å vesicle. The question we now address is what 3-D structures can form a membrane channel with a lumen size of the order of 8 Å (Raymond, et al., "Channels formed by colicin E1 in planar lipid bilayers are large and exhibit pH-dependent ion selectivity" *J. Membr. Biol.*, vol. 84 1985) using less than 88 amino acids. Three types of beta-barrels, one conventional and two novel, will be presented along with their energy minimized forms and the ways in which they can be tested by using cystine residues inserted by mutation in order to provide binding sites for electron spin resonance labels. (Supported by NIH grant RR-00442. P.I. C. Levinthal)

*NSF grant DMB-8503484. P.I. B. Honig

M-Pos103 MINIMIZATION AND MOLECULAR DYNAMICS DETERMINATION OF ANTIBODY LOOP STRUCTURE UTILIZING MANY RANDOMLY GENERATED STARTING CONFORMATIONS. R.M. Fine, H. Wang, P.S. Shenkin, and C. Levinthal, Dept. of Biology, Columbia University, New York, NY 10027.

We present the results of the application of a new method for searching for the conformation of unknown portions of a protein molecule to the hypervariable loops of the antibody molecule MCPC603. The method is based upon two assumptions. The first of these is that the native conformation of the unknown portion of the molecule will be the global energy minimum for that portion, treating the remainder of the protein as fixed. The second of these is that we can find this minimum by generating a large number of random conformations of the backbone heavy atoms for the portion of the molecule being studied, subjecting these conformations to minimizations and/or to molecular dynamics followed by minimization, and selecting the low energy structures found for further characterization of side chain conformations. For two of the loops studied, this technique was sufficient to select the native conformation. For a third, a lower energy minimum which differed considerably from the native was found. The consequences of this for further energetic modeling of this kind is discussed, with emphasis on electrostatic self energy. The computational cost of ensuring convergence to a global minimum for such structures is also discussed, both with regard to the STAR ST100 array processor we now use and to the FASTRUN processor we are constructing.

M-Pos104 ROLE OF THE AROMATIC SIDE CHAIN RESIDUES IN MICELLE BINDING BY PANCREATIC PORCINE AND EQUINE COLIPASE. FLUORESCENCE STUDIES.* Jon C. McIntyre, Patricia Hundley and W. David Behnke, Dept. of Biochemistry and Molecular Biology, Univ. of Cincinnati Col. of Med., Cincinnati, OH 45267.

NO₂-Tyr-55 of porcine colipase is obtained by reaction of the protein with TNM (in low excess + taurodeoxycholate (TDOC)) followed by gel-filtration on G-50 and DEAE-anion exchange chromatography. Reduction and dansylation of the NO₂-tyr generates a single dansyl-tyr-55 which display an emission max. at 550 nm and is fully twice as active as native colipase. Addition of TDOC causes a 4.3fold increase in band intensity and a 70nm blue shift to 480nm. Scatchard analysis yields a linear plot with $K_d = 6.9 \times 10^{-7}$ and $n = 1.0$ indicating a unique single binding site for TDOC. By comparison to the phospholipase system, the data indicate a possible direct insertion of tyr-55 into the TDOC micelle.

The presence of a single Trp in equine colipase (E.C.) provides a valuable internal fluorescent probe. The emission max. of E.C. is 345nm indicating a relatively solvent accessible trp. Addition of TDOC causes a nearly 2-fold increase in amplitude and a blue shift of 8nm, consistent with a more hydrophobic environment. Studies with fluorescence quenchers: acrylamide, I⁻ and Cs⁺, confirm the above and indicate marked changes in trp accessibility in the presence of TDOC. Whether or not trp is directly involved with TDOC binding must await further study. (*supported by NIH grant HL-30431)

M-Pos105 EFFECTS OF DEGLYCOSYLATION ON THE CONFORMATION OF OVINE SUBMAXILLARY MUCIN R. Shogren, T.A. Gerken, N. Jentoft, A.M. Jamieson, J. Blackwell, Departments of Pediatrics, Biochemistry and Macromolecular Science, Case Western Reserve University, Cleveland, Ohio 44106.

Light scattering and NMR methods have been used to study the conformation of native and deglycosylated (apo) ovine submaxillary mucin (OSM). OSM is a heavily glycosylated glycoprotein in which the majority of its serine and threonine residues are glycosylated by the O-linked disaccharide α -N-acetylneuraminic acid (2-6) α -N-acetylgalactosamine. Solutions of native and modified OSM were fractionated by molecular weight using gel filtration. The radius of gyration (R_g) and hydrodynamic radius (R_h) of OSM were found to be proportional to $N^{0.57}$ (where N is the number of peptide residues) suggesting that the mucin behaves as a linear random coil. The removal of the N-acetylneuraminic acid residue causes a 33% reduction in R_g and R_h , while the complete deglycosylation of OSM causes a 63% reduction in these values. The values for apo mucin are 18% lower than those found for denatured globular proteins extrapolated to the same value of N. Statistical mechanical calculations based on the mucin amino acid composition, which contains 20% gly, predict R_g values in good agreement with the measured values. These results are supported by the measured carbon-13 relaxation times (T_1) which show that the peptide ser, thr and gly α -carbons of apo OSM undergo more rapid motions than those in native OSM, while the removal of the N-acetylneuraminic acid residue alone has little effect on the peptide core mobility. These results together with the lack of detectable secondary and tertiary structures from NMR and the insensitivity of R_g to changes in solvent, suggest that the extended conformation of OSM is controlled primarily by the steric interactions between the N-acetylgalactosamine residue and the peptide core.

M-Pos106 TWO-DIMENSIONAL ^1H NMR STUDIES OF THE STRUCTURE OF PARVALBUMIN IN SOLUTION. T.C. Williams and B.D. Sykes, MRC Group in Protein Structure and Function, and the Dept. of Biochemistry, University of Alberta, Edmonton, Alberta, T6G 2H7, Canada.

In order to understand metal-ion induced structural changes in troponin-C class calcium-binding proteins (CaBPs), we have studied in detail the solution conformation of various metal-bound forms of the single-domain two-site protein parvalbumin (PV). Studies of the solution structures of CaBPs invariably make comparative reference to the solid-state structures of PV, intestinal CaBP, or troponin-C, all of which have been determined by X-ray methods. To extend this structural information to a wider variety of CaBPs and to define pertinent structural features of these proteins in solution, we have begun to assign resonances in the ^1H NMR spectrum of pike III PV to specific residues in its primary sequence. For this we have relied heavily upon the two-dimensional NMR experiments developed by Wuthrich and co-workers for their assignment of resonances in the bovine pancreatic trypsin inhibitor. Because our particular emphasis is the determination of the conformation of the mainchain, we have studied semi-quantitatively the NOEs resulting from dipolar interactions between sequential NH/CH and NH/NH pairs in the metal-binding loops of the diamagnetic forms of PV as was done for the C-terminal domain of calmodulin [Ikura, M., Minowa, O., & Hikichi, K. (1985) *Biochemistry* 24, 4264-4269]. In order to delineate regions of the backbone farther removed from the metal-binding sites, we have also begun to analyze the paramagnetic contributions to the chemical shifts and linewidths of assigned NH and CH resonances in several lanthanide-substituted forms of PV.

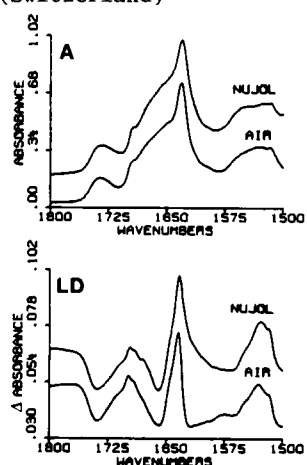
M-Pos107 PHYSICAL STUDIES ON THE STRUCTURE OF SPECTRIN Hwei-Zu Lu¹, Rex P. Hjelm, Jr.^{2,4}, Michael E. Johnson³, P. Thiagarajan² and Leslie W.-M. Fung¹, ¹Department of Chemistry, Loyola University of Chicago, Chicago, IL 60626; ²Chemistry and IPNS Divisions, Argonne National Laboratory, Argonne, IL 60439; ³Department of Medicinal Chemistry and Pharmacognosy, University of Illinois at Chicago, PO Box 6998, Chicago IL 60680; ⁴present address: LANSCE, Mail Stop H805, Los Alamos National Laboratory, Los Alamos, NM 87545.

Spectrin is a major component of the membranes of mammalian erythrocytes and neural tissue and as such is likely to be a major determinant in maintaining the shape of these cell types and the rheological properties of their membranes. We have been studying the structure of this protein using various physical methods. NMR studies using one pulse and spin echo techniques reveal that the structure can be resolved into at least two domains: one relatively rigid, the other flexible. At 25° C about 90% of the protons are estimated to be in the rigid domains of the molecule. CD studies show that a large fraction of the amino acid residues are in alpha helical conformation, and quantitative estimates range from 65 to 85%, depending on the average helical length assumed. Upon heating the sample from 25° C to below 45° C, the number of protons in the flexible segments increases with a concomitant decrease in the CD signal attributable to alpha helix. Neutron scattering studies on spectrin and an 80 KDa fragment derived from the alpha chain in high and low salt give cross-sectional radii of gyration of 3.6 nm in high salt and 3.1 nm in low salt, suggesting cross-sectional radii of 5.1 and 4.2 nm, respectively. The total radius of gyration of the 80 KDa fragment is found to be 6.4 nm in both high and low salt. Comparing these figures to the R_G of spectrin available from light scattering studies indicates that the extension of the fragment may be similar to that of the parent molecule. (Supported in part by grants from NIH and DOE.)

M-Pos108 POLARIZED FOURIER TRANSFORM INFRARED SPECTROSCOPY OF PORIN

E. NABEDRYK⁺, R.M. GARAVITO* and J. BRETON⁺. ⁺Service de Biophysique, CEN Saclay, 91191 Gif-Sur-Yvette cedex (France). *Biozentrum, University of Basel, 4056 Basel (Switzerland)

The degree of orientation of the protein secondary structures of porin is investigated by Fourier transform infrared (FTIR) linear dichroism of oriented multilayers films of porin. The circular dichroism spectrum yields a high β -structure content (68 %). In agreement with Kleffel et al. (EMBO J. 1985, 4, 1589), the FTIR absorbance (A) spectrum shows the amide I band with a major component at 1631 cm^{-1} and several shoulders around 1645-1675 cm^{-1} and at 1695 cm^{-1} . The amide II band is centered around 1525 cm^{-1} . The main dichroic signals (LD) peak at 1738(-), 1660(-), 1633(+) and 1529(+) cm^{-1} . Covering the film with Nujol in order to reduce reflections at the membrane/air interface (Nabedryk et al., Adv. Photosynthesis Res., 1984, vol II, 177) alters neither the dichroism of these signals nor the absorption spectrum but modifies the dichroism around 1600 cm^{-1} . The small magnitude of the 1633 cm^{-1} and 1529 cm^{-1} dichroism bands demonstrates that the transition moments of the amide I and amide II vibrations are tilted at about 45° from the membrane plane. This indicates that the plane of the β -sheets is approximately perpendicular to the bilayer - in agreement with X-rays data (Kleffel et al.) - with the β -strands direction tilted at about 45° from the membrane plane.



M-Pos109 SOLID-STATE NMR STUDIES OF MOUSE EPIDERMAL KERATIN FILAMENT STRUCTURE. James W. Mack and Dennis A. Torchia, NIDR, and Peter M. Steinert, NCI, National Institutes of Health, Bethesda, MD 20892.

The existing dogma of intermediate filament (IF) structure is based on the following principles: the highly conserved rod domains common to all IF chains are thought to form the central backbone or core of the IF; the highly variable end domains of IF chains are thought to occupy positions on the periphery of the IF.

We have explored IF structure using NMR on native mouse keratin IF labelled *in vivo* and *in vitro* by incorporation of carbon-13 enriched glycine (to study end domain organization) and deuterium enriched leucine (to study the packing of the coiled-coil domains). We have performed spin-lattice relaxation experiments and lineshape measurements at three different fields with the objective of determining the extent of motion of the various kinds of residues and the time-scales of these motions. The glycine-rich terminal domains of assembled keratin IF are found by nmr to be highly flexible in nature and lacking in long-ranged order. These observations are consistent with previous suggestions that these domains are extended from the IF periphery. Experiments on leucine labelled keratin IF indicate a surprising degree of mobility of the coiled-coils of the IF, suggesting that these regions, although highly structured, can nevertheless accomodate a high degree of side-chain mobility. It is therefore likely that the coiled-coil rods are quite flexible within the IF.

M-Pos110 DIRECT PHOTOINDUCED CHANGES OF PROTEINS WITH NEAR-UV RADIATION. D.L. VanderMeulen, M.M. Judy, and M. Shanley*, Baylor Research Foundation and SMU*, Dallas, TX 75246.

The potential role of light in the etiology of malignancy and a concern for the side-effects of current and proposed uses of lasers in surgery make the study of photooxidative processes in tissue components a subject of considerable biomedical interest. Moreover, studies of photoinduced protein changes can yield interesting insights into subtleties of structure and conformation.

Using proteins such as egg white lysozyme as a model, we followed changes in the protein induced by direct (no exogenous sensitizer) photochemical changes arising from irradiation at 337.1 nm and 351 nm, utilizing nitrogen and argon-ion lasers, respectively. The time course was monitored by recording enzymatic activity, absorption and fluorescence changes, and photoinduced product formation by means of TLC, HPLC, mass spectrometry, and polyacrylamide gel analysis. Insight into the potential role of singlet oxygen was gained by irradiation in the presence of deuterium oxide and by addition of sodium azide. The percentage loss of tryptophan could be detected by spectral changes, including fluorescence changes "calibrated" by unfolding the protein with GnHCl.

Results suggest the photolysis involves tryptophan loss and the production of N-formyl-L-kynurenine and other daughter products of aerobic photooxidation. Model studies made by others of the direct photolysis of tryptophan in solution were extended in order to aid clarification of the mechanism.

(Supported by ONR FEL Contract N0014-86-K-0186.)

M-Pos111 DISTRIBUTION OF DISTANCES OF MYOSIN S-1 BY ENERGY TRANSFER AND FREQUENCY-DOMAIN FLUOROMETRY. H.C. Cheung, University of Alabama, Department of Biochemistry, Birmingham, M.L. Johnson, University of Virginia, Department of Pharmacology, Charlottesville, J.R. Lakowicz, N. Joshi and I. Gryczynski, University of Maryland, Department of Biological Chemistry, Baltimore.

Fluorescence energy transfer and frequency-domain fluorometry were used to determine the distribution of distances between the two sulfhydryl groups on myosin S-1. The donor on SH₁ was labeled with 1,5-IAEDANS and the acceptor at SH₂ was labeled with DDPM (N-(4-dimethylamino-3,5-dinitrophenyl) maleimide). In the absence of acceptor the donor decay was dominately a single exponential. The donor decay became considerably more heterogenous in the presence of acceptor. We attribute the distribution of decay times to a distribution of donor-to-acceptor distances. The frequency-domain data were analyzed to recover the distance distribution, which was found to be sensitive to Mg-ADP and to denaturation, but appear to be less sensitive to actin. For instance, in the absence of Mg-ADP the average distance and width of the distribution are 29 and 13 Å, respectively. In the presence of Mg-ADP these values change to 20 and 17 Å, and denaturation results in values of 28 and 16 Å.

M-Pos112 FLUORESCENCE ENERGY TRANSFER STUDIES ON LABELED SULFHYDRYL MUTANTS OF STAPHYLOCOCCAL NUCLEASE

Jeanne E. Rudzki, David L. Bain, Amy S. Kimball, Christian B. Anfinsen and Ludwig Brand
Department of Biology, The Johns Hopkins University, Baltimore, MD 21218.

Staphylococcal nuclease consists of a single polypeptide chain with 149 amino acid residues and no sulfhydryl groups. Shortle (Shortle and Lin, *Genetics* (1985) 110, 539) has cloned the gene encoding nuclease from *Staphylococcus aureus* and developed a plasmid-based genetic system utilizing *E. coli* as the host cell. With this methodology, a mutant (R87C) was produced in which a Cys residue replaces Arg 87 at the active site of the enzyme. Mutant R87C is thus a protein with a single Trp residue (Trp 140) and a single sulfhydryl group, and exhibits the same stability and Trp 140 fluorescence kinetics as does the wild type nuclease. The sulfhydryl group in mutant R87C was reacted with di-(1-dimethylaminonaphthalene-5-sulfonate)-L-cystine (didansyl cystine) in a disulfide-sulfhydryl exchange reaction to produce dansyl-R87C. Excess dye was removed by gel filtration on Sephadex G-25, yielding a conjugate with 1 mol of dye bound per mol of protein. Steady-state fluorescence measurements demonstrated energy transfer between the Trp 140 donor and the dansyl-Cys 87 acceptor. From these measurements, a distance of ~ 27 Å between donor and acceptor was calculated, in excellent agreement with that obtained from a model based on the X-ray structure of nuclease. Applications of this energy transfer technique to understanding the folding of nuclease will be presented.

We thank Dr. David Shortle for providing us with the *E. coli* strains required for this work. Supported by NIH grant GM11632 and by an NIH Postdoctoral Fellowship to JER.

M-Pos113 INTERPRETATION OF FLUORESCENCE DECAY IN PROTEINS USING CONTINUOUS LIFETIME DISTRIBUTIONS. E. Gratton, J. R. Alcalá and F. G. Prendergast (*). Department of Physics, University of Illinois at Urbana-Champaign, Urbana, IL 61801. (*) Department of Biochemistry and Molecular Biology, Mayo Foundation, Rochester, MN 55905.

The decay of the tryptophanyl emission in proteins is often complex due to the sensitivity of the tryptophan excited state to its surroundings. The traditional analysis of the decay curve using exponential components is based on the identification of each component with a particular protein conformation. An alternative approach assumes that proteins can exhibit a large number of conformations. Following this assumption, the analysis of the protein emission was performed using continuous distributions of lifetime values. The number of average protein conformations, the range of mobility around each conformation and the rate of interconversion between conformations determines the characteristics of the lifetime distribution. The fluorescence decay from some single tryptophan proteins was measured using multifrequency phase fluorometry and analyzed using a sum of exponentials, unimodal and bimodal probability density functions and the analytical form for lifetime distribution obtained for a model in which the tryptophan residue can move in a single potential well. For ribonuclease T1 and neurotoxin variant 3, the sum of two exponentials and bimodal probability density functions gave comparable results, whereas for phospholipase A2, the description of the decay required three exponentials or bimodal probability density functions. Also the temperature dependence of the fluorescence decay was investigated. It was found that the lifetime distribution was broader and shifted toward longer lifetime values at lower temperature.

M-Pos114 PROTEIN FLUORESCENCE DECAY RATES DUE TO SUBSTATE INTERCONVERSIONS WITH DISTRIBUTED ACTIVATION BARRIERS. N. Silva and E. Gratton. Department of Physics, University of Illinois at Urbana-Champaign, Urbana, IL 61801.

Fluorescence decay from tryptophan residues in proteins is invariably complex even for single tryptophan proteins. We have proposed that the multitude of conformational substates present in proteins is responsible for the heterogeneity of the decay and gives rise to continuous distribution of lifetime values. We have analyzed a model in which only two substates characterized by a different lifetime value are considered. We assumed that the potential energy of this system in the excited state doesn't change from the potential energy of the ground state. Besides the fact that the two states decay there is also the possibility of transition between these two states during the excited state lifetime. Using a distribution of transition rates, simulations have been performed giving a distribution of lifetime values. Also fits to lifetime data, obtained from single tryptophan proteins have been obtained using a predetermined form for the distribution of interconversion rate between the two states. Supported by NSF Minority Fellowship.

M-Pos115 COMPARTMENTAL ANALYSIS OF FLUORESCENCE ANISOTROPY DECAY IN THE PRESENCE OF EXCITED-STATE REACTIONS. D. W. Piston and E. Gratton. Department of Physics, University of Illinois at Urbana-Champaign, Urbana, IL 61801.

Fluorescence anisotropy decay can be complex for anisotropic molecules, or for molecules with restricted rotational mobility. An additional complication can arise due to several emitting species with different lifetimes. Furthermore, anisotropy decay may be governed not only by rotational rates, but also by excited-state reactions such as interconversion between different species. In proteins, complex total intensity decay is frequently observed. It has been proposed that this complexity arises due to the existence of conformational substates and the interconversions between these substates. In the past, analytical approaches to this type of problem have been based on the diffusion equation. However, in proteins the diffusion equation is difficult to use since the potential barriers between substates may be non-uniform. We propose a compartmental model which allows for the calculation of the anisotropy decay in systems undergoing both anisotropic rotations and reactions during the excited-state. In this model, we treat each rotation and excited-state reaction as an interconversion between compartments. A matrix is constructed using the rates of interconversion between substates and the decay rates of each substate. The polarization of each compartment and initial conditions are contained in a vector. The result is a standard eigenvalue problem which can be solved analytically or numerically. This compartmental model is applied to systems which have been solved using the diffusional model. Examples of systems which exhibit complex decay behavior are simulated and the decays of the intensity and anisotropy are obtained. Supported by PHS-IP41-RR-03155 and NSF PCM84-03107.

M-Pos116 RESOLVABILITY OF FLUORESCENCE LIFETIME DISTRIBUTIONS. J. R. Alcala, E. Gratton and F. G. PRENDERGAST (*). Department of Physics, University of Illinois at Urbana-Champaign, Urbana, IL 61801. (*) Department of Biochemistry and Molecular Biology, Mayo Foundation, Rochester, MN 55905.

In the absence of a definite kinetic model, the analysis of the fluorescence decay using discrete exponential components underestimates the uncertainty of the recovered lifetime values. A different approach to determine the lifetime of a population of molecules is the use of probability density functions and lifetime distributions. Fluorescence decay data from continuous distributions of exponentially decaying components were generated. Different magnitudes of error were added to the data to simulate experimental conditions. The resolvability of the distributional model was studied by fitting the simulated data to one and two exponentials. The maximum width of symmetric distributions (uniform, gaussian and lorentzian) which cannot be distinguished from single and double exponential fits for statistical errors of 1% and 0.1% were determined. The width limits are determined by the statistical error of the data. It is also shown that, in the frequency domain, the discrete exponential analysis does not weight uniformly all the components of a distribution. This systematic error is less important when probability and distribution functions are used to recover the decay. Finally, it is shown that real lifetime distribution can be proved using multimodal probability density functions. In the next companion paper we propose a physical approach which provides lifetime distribution functions for the tryptophan decay in proteins. In the following third companion paper we use the distribution functions obtained to fit data from the fluorescence decay of single tryptophan proteins.

M-Pos117 THE ANALYSIS OF FLUORESCENCE ANISOTROPY DECAY IN THE PRESENCE OF EXCITED-STATE REACTIONS. J. M. Beechem and E. Gratton. Department of Physics, University of Illinois at Urbana-Champaign, Urbana, IL 61801.

Complex total intensity decay (multi-exponential, nonexponential, distributions of exponentials) greatly complicates the interpretation of fluorescence anisotropy studies. This is especially true if the origin of the heterogeneous decay results from excited-state reactions (e.g. solvent relaxation, proton transfer, energy transfer, etc.). Analytical methods have been recently developed [Cross et al., *J. Chem. Phys.* 78:6455 (1983); A. Szabo, *J. Chem. Phys.* 81:150 (1984)] solving the coupled linear differential equations describing both the excited-state interconversions and the rotational reorientation. An alternative methodology has been developed using Markov theory to derive the discrete probability distributions associated with the relative amount of time spent in each interconverting state. Within this framework, the complex anisotropy decay can be determined directly by the proper probabilistic combinations of the anisotropy functions of the individual states in the absence of interconversions. Therefore, the large library of anisotropy functions which have been derived for isolated systems can be immediately used to describe interconverting systems. The principal diffusion axes of the various states need not align. In addition, complications which arise from distributions of interconversion rates and time dependent rate constants can be examined within this formalism. Specific examples concerning the anisotropy decay kinetics of tryptophan in proteins will be described both in time and frequency domains. Supported by NIH NRSA GM11163 and PHS-IP41-RR 03155.

M-Pos118 MONOMERIC PROTEIN KINASE C AUTOPHOSPHORYLATES. Alexandra C. Newton and Daniel E. Koshland, Jr., Department of Biochemistry, University of California, Berkeley, CA. 94720

The Ca^{2+} /phospholipid-dependent protein kinase C autophosphorylates in a concentration-independent manner (Mochly-Rosen and Koshland, unpublished observation). In order to establish whether a single peptide is capable of covalently modifying itself, or whether the modification occurs by intramolecular but interpeptide transfer, autophosphorylation was investigated in a detergent micelle system (Triton X-100:phosphatidylserine:dioleoylglycerol). Previous work established that protein kinase C binds to such mixed micelles, in a Ca^{2+} -dependent manner, with a stoichiometry of one protein kinase C to one micelle (Hannun et al., J. Biol. Chem. 260, 10039, 1985). Using this system, we demonstrate that monomeric protein kinase C covalently modifies itself by phosphorylation. The rate of autophosphorylation in the micellar system, where protein kinase C is a monomer, is comparable to that observed in bilayer systems, where the enzyme can exist as an oligomer. This suggests that monomeric protein kinase C may be the predominant form involved in autophosphorylation. Trypsinolysis of the enzyme reveals that the hydrophobic, regulatory domain of the molecule is modified by the phosphorylation. Furthermore, intact protein kinase C cannot phosphorylate the cleaved regulatory domain, either in micellar or bilayer systems, consistent with an intrapeptide event being involved. The intrapeptide modification of protein kinase C has intriguing implications for protein structure and regulation.

M-Pos119 LASER LIGHT SCATTERING STUDIES ON BOVINE SKIN PROTEODERMATAN SULPHATE

D. Zangrando, A.M. Jamieson, J. Blackwell, R. Gupta, Department of Macromolecular Science, Case Western Reserve University, Cleveland, Ohio 44106. P.G. Scott, Department of Oral Biology, University of Alberta, Edmonton, Alberta T6G 2N8, Canada.

Dynamic and static laser light scattering have been used to study the molecular weight (M_w), radius of gyration (R_g), and hydrodynamic radius (R_s) of a bovine skin proteodermatan sulphate (DS-PG) and core protein. Results for the DS-PG in 4M GdHCl indicate a $M_w=65,000$ and $R_g=21.0\text{nm}$. Dynamic light scattering gave an infinite dilution translational diffusion coefficient $D_t^0=20.0 \times 10^{-8} \text{cm}^2/\text{s}$ and hence, using the Stoke's-Einstein equation $R_s=9.70\text{nm}$. For the core protein, $M_w=43,000$ in 4M GdHCl but increased significantly to 450,000 in 0.15M NaCl. The latter solvent has been shown to promote self-association in DS-PG, and our findings suggest that protein-protein interactions may contribute to self-association in addition to interactions of the dermatan sulphate (DS) chains. R_s for the core protein in 4M GdHCl was found to be 9.40nm. Using the values of molecular weight obtained in 4M GdHCl, we calculate a value of 22,000 attributed to the non-protein component of the DS-PG. This value is comparable to previous values for a single dermatan sulphate chain. We have used calculated D_t^0 and R_g values of model shapes for comparison to our experimental findings. Modeling both protein core and DS species as a rigid rod gives $D_t^0=9.30 \times 10^{-8} \text{cm}^2/\text{s}$ and $R_g=34.0\text{nm}$. Conversely, assuming a completely random-coil structure gives $D_t^0=21.3 \times 10^{-8} \text{cm}^2/\text{s}$ and $R_g=15.0\text{nm}$. If however we assume a hatpin structure, as observed from electron microscopy, we obtain $D_t^0=20.0 \times 10^{-8} \text{cm}^2/\text{s}$ and $R_g=17.0\text{nm}$. These studies indicate therefore that the hatpin structure also is present in solution.

M-Pos120 CONFORMATIONAL CHANGES INDUCED IN CAP BY CYCLIC NUCLEOTIDES. J. Michael Hudson, Paul M. Horowitz and Michael G. Fried, Department of Biochemistry, University of Texas Health Science Center, San Antonio, TX, 78284.

The *E. coli* cyclic AMP receptor (CAP) modulates the transcription of a global network of catabolic genes. CAP binds both cAMP and cGMP, but only cAMP is capable of inducing the conformational change in CAP required for promoter binding. To learn the basis of this functional selectivity, we have employed a variety of fluorescence techniques to detect differences in the conformational states induced in CAP by cAMP and cGMP.

Each CAP monomer contains 2 *trp* residues and 6 *tyr* residues, which give a native fluorescence emission spectrum (excitation at 280; $\lambda_{\text{max}} = 349\text{nm}$, $\Delta\lambda = 59\text{nm}$) characteristic of exposed *trp* residues, consistent with the crystallographic structure. Binding cyclic nucleotides decreases emission intensity ($\Delta I_{\text{cGMP}} > \Delta I_{\text{cAMP}}$), however the differential quenching of intrinsic fluorescence by I^- , Cs^+ and acrylamide is not significantly changed. These observations support the notion that functionally inactive cyclic nucleotides are capable of causing conformation changes grossly similar to those induced by cyclic AMP, and that the conformational changes due to cAMP binding occur without major alteration in the surface exposure of fluorescent residues.

We have used the fluorophore Bis-ANS to probe the apolar surfaces of CAP. Our data are consistent with the binding of just one Bis-ANS per CAP monomer, suggesting a unique interaction site. Interaction with CAP increases Bis-ANS fluorescence intensity by ~17 fold; addition of low concentrations of cAMP confers a further increase, but similar concentrations of cGMP decrease intensity. This differential effect may reflect the conformational differences that distinguish the active and inactive states of CAP.

M-Pos121 STEADY-STATE AND DYNAMIC FLUORESCENCE STUDIES OF SUBUNIT INTERACTION AND MOTION IN HUMAN LUTEINIZING HORMONE G. Sanyal, F.G. Prendergast, M.C. Charlesworth, R.J. Ryan, Department of Chemistry, Hamilton College, Clinton, NY 13323 and Department of Biochemistry and Molecular Biology, Mayo Foundation, Rochester, Minnesota 55905

Human luteinizing hormone (hLH) is an $\alpha\beta$ disubunit glycoprotein containing a single tryptophan (W) occurring in position 8 of the β -Subunit (β hLH) sequence. The relative fluorescence intensity (F) of this W-8 is markedly higher in isolated β hLH compared to intact hLH. The fluorescence spectrum of β hLH is also redshifted relative to hLH spectrum. We have exploited this difference in intrinsic fluorescence to study the kinetics of dissociation and reassociation of α - and β hLH. The acid induced dissociation as measured by increase in F followed first-order kinetics, but the reassociation was accompanied by a biphasic decrease in F. The accessibility of W-8 to solvent as measured by D₂O- effect on F was higher in isolated β hLH compared to intact hLH. Consistently, the accessibility of W-8 to the fluorescent quencher acrylamide was also higher in isolated β hLH. The lifetime (τ) dependence of steady-state fluorescence anisotropy (r_{ss}) was studied by oxygen quenching and the τ -resolved anisotropy was determined. These experiments revealed the presence of a limited degree of fast (subnanosecond) segmental motion of W-8 in both free β hLH and intact hLH. The protein correlation times were also obtained from these measurements and from temperature dependence of r_{ss} . Phase-modulation τ (τ_p and τ_m) measurements using modulation frequency (ω) of 18 and 30 MHz suggested conformational heterogeneity of the single W, as $\tau_p < \tau_m$ and both τ_p and τ_m decreased with increasing ω . Multiple frequency phase fluorometry was then undertaken to study the dynamic distribution of W-conformations in β hLH in the free subunit form and in native hLH.

M-Pos122 THE SYNTHESIS OF FLUORESCENT DICHLOROTRIAZINYLAMINOFLUORESCIN-CONCANAVALIN A AND ITS USE AS A GLYCOPROTEIN STAIN ON SODIUM DODECYLSULPHATE POLYACRYLAMIDE GELS. Charles W. Mahoney and Angelo Azzi, Institute of Biochemistry and Molecular Biology, University of Berne CH-3012 Berne / Switzerland.

Dichlorotriazinylaminofluorescein (DTAF), a fluorescent analog of fluorescein, can be reacted with free amino groups of proteins under more gentle and rapid conditions than fluorescein isothiocyanate (FITC), a commonly used fluorescent labeling agent. Con A has been optimally labeled to a maximum stoichiometry of 0.4 mol DTAF/mol con A monomer under mild reaction conditions (pH 8.0, 6 hrs) yielding DTAF-con A preparations with carbohydrate binding ability. This stoichiometry is similar to that for the labeling of con A with FITC under more alkaline conditions which results in preparations which are unable to penetrate 7.5-15% gradient SDS-polyacrylamide gels. DTAF-con A is able to penetrate 7.5-15% gradient SDS polyacrylamide gels allowing for specific staining of glycoproteins. The detection limit of sensitivity for DTAF-con A, which is similar to that of FITC-con A, is in the range of 5-25 μ g of glycoprotein. DTAF-con A will likely have other applications in, for example, fluorescent energy transfer and other structure-function studies.

M-Pos123 KINETICS AND EQUILIBRIA OF EUKARYOTIC RIBOSOMAL SUBUNIT ASSOCIATION. THE EFFECTS OF EUKARYOTIC INITIATION FACTOR 3. ¹D. Rounds, ¹T. Harrigan, ¹D.J. Goss, ²C.L. Woodley, and ²A.J. Wahba (Intro. by M. Tomasz) ¹Dept. of Chemistry, Hunter College of CUNY, 695 Park Ave, New York, NY 10021 and ²Dept. of Biochemistry, Univ. of Miss. Medical Center, Jackson, MS 39216-4505.

Free 40S ribosome subunits are intermediates of the polypeptide synthesis initiation cycle. Eukaryotic initiation factor 3 (eIF-3) binds to the 40S subunits in the absence of other initiation factors and inhibits the reassociation of the 40S with the 60S subunit. eIF-3 ($M_r=700,000$) was isolated from ribosomal washes of rabbit reticulocyte and *Artemia*. The reticulocyte factor affects the subunit association of both reticulocyte and *Artemia* ribosomes. In both systems eIF-3 caused a three-fold increase in the half-time for ribosome association induced by an increase in the $[Mg^{2+}]$ from 0.5 to 6.0 mM. In the presence of eIF-3, Mg^{2+} titration curves showed a shift in the midpoint of the titration (50% association) to about 1.5 mM higher Mg^{2+} relative to titrations in the absence of eIF-3. These results are consistent with eIF-3 shifting the ribosome subunit equilibrium towards dissociation as a result of a decrease in the subunit association rate.

Supported By: American Heart Assoc.-NYC Affil. Investigatorship (DJG), PSC-CUNY Faculty Research Award, Research Corp., NSF 86-007070 and NIH GM 25451.

M-Pos124 ASSEMBLY OF RECOMBINANT DNA DERIVED DES-N ACETYL TOBACCO MOSAIC VIRUS COAT PROTEIN. S.J. Shire^a, D.W. Leung^a, G.J. Cachianes^a, E. Jackson^a, W.I. Wood^a, K. Raghavendra^b, T.M. Schuster^c, and P. McKay^a, ^aGenentech, Inc., So. San Francisco, CA and ^bMolecular and Cell Biology Dept., University of Connecticut, Storrs, CT.

Recombinant DNA derived tobacco mosaic virus (Vulgare strain) coat protein (rTMVP) was characterized with regard to self assembly properties. The rTMVP was obtained by cloning and expression in *E. Coli* and purification by column chromatography and selective precipitation at pH 3.5. Amino acid analysis and N-terminal sequencing verified that the purified protein was TMVP. Isoelectric focusing in 7M urea indicated that the rTMVP has an extra positive charge probably due to a free amino terminus in contrast to TMVP, which is acetylated at the N-terminus. The rTMVP at ~3mg/ml in 0.1M ionic strength orthophosphate pH 7 buffer exhibited temperature reversibility of self association. However, at 20 °C the rTMVP sedimented as 29.5S (63%) and 4.6S (37%) boundaries whereas wild type TMVP sedimented at 19.9S (62%) and 3.7S (38%). Electron microscopy revealed stacked disk rods (on the order of 4 disks) at pH 7.0 and long helical rods at 6.5. The possible role for N-terminal acetylation in TMVP self assembly is discussed in light of these observations.

M-Pos125 HIGH RESOLUTION STUDIES OF HELICAL VIRUSES BY FIBER DIFFRACTION.

Sharon Lobert, Peter Heil, Rekha Pattanayek and Gerald Stubbs,
Dept. of Molecular Biology, Vanderbilt University, Nashville, TN 37235

Macromolecular assemblies often have rod-like or filamentous shapes and helical symmetry. Examples include the helical viruses, cytoskeletal fibers, flagella, nucleic acids and polysaccharides. While parts of these assemblies may crystallize, it is usually the very properties that are inherent in the fibrous form that are of biological interest. It is therefore necessary to use fiber diffraction methods to determine their molecular structures.

Cucumber green mottle mosaic virus (watermelon strain), U2 and aucuba mosaic virus are tobamoviruses. The structure of the type member of the family, tobacco mosaic virus, has been determined at 2.9Å resolution, and refined to an R factor of 0.11. The structures of the other members are being determined by difference methods in conjunction with heavy atom derivatives. In fiber diffraction, molecular replacement methods do not provide sufficient phasing power to determine structures directly, but they can be used to greatly reduce the number of derivatives required, compared to a de novo determination. Two derivatives of CGMMV-W have been made.

In TMV, two charged regions, one including Glu 50 and Asp 77, mediate the assembly and disassembly of the virus. These residues are not present in CGMMV-W. However, lead binds to two sites in CGMMV-W, one of which corresponds to the conserved TMV carboxyl cluster. The other could be close to several new carboxylic acids; the high resolution structure will be needed to verify this. It appears that the mechanism of control of viral assembly is the same in both viruses, but that different amino-acid residues are used.

- M-Pos126** STRUCTURAL STUDIES OF FILAMENTOUS BACTERIOPHAGES BY X-RAY AND NEUTRON DIFFRACTION
Raman Nambudripad, Marc J. Glucksman, Wilhelm Stark & Lee Makowski
Dept. of Biochemistry & Molecular Biophysics, Columbia Univ. P&S, N.Y., NY 10032.

The filamentous single-stranded DNA bacteriophages are structurally similar and can be classified into two groups based on their helical symmetry. The structures of phage M13 from Class I and Pfl from Class II are being investigated using X-ray and neutron diffraction. The coat proteins of these viruses have been shown to be largely alpha-helical. In Pfl, each coat protein consists of two alpha-helical segments arranged as a double layer around the DNA. The positions of these helices were determined by refinement against X-ray diffraction data to a resolution of 7Å. A molecular model for the peptide chains has now been fitted into the 7Å map and this model is being refined using a restrained least-squares refinement procedure. It is not known whether the two alpha-helical segments in Pfl are parallel or antiparallel to each other. Certain residues like valine and methionine are asymmetrically distributed along the sequence. The positions of these residues can be determined from neutron diffraction of Pfl with these residues specifically deuterated, providing information about the orientation and connectivity of the alpha-helical segments. Initial results have determined the radii of the valine residues in the virus and further work is directed at locating their positions in three dimensions. In order to compare the structure of M13 with Pfl, the X-ray data were used to calculate the cylindrically averaged Patterson functions. The results suggest that although the structures of the two virions are similar, the M13 coat protein consists of a single helix which is gently curved. Model building studies underway are aimed at determining the packing of the alpha-helices in the M13 protein coat.

- M-Pos127** MODEL-BUILDING AND REFINEMENT OF THE THREE-DIMENSIONAL STRUCTURE OF HEXON, THE MAJOR COAT PROTEIN OF ADENOVIRUS. Francis K. Athappilly and Roger M. Burnett. Department of Biochemistry and Molecular Biophysics, Columbia University, New York, New York 10032.

The trimeric protein, hexon, is the principal component of the adenovirus virion with 62% of its mass. Hexon crystallizes in space group $P2_13$, $a = 150.6$ Å, with one subunit per asymmetric unit. The chain has been traced in an electron density mini-map at 2.9 Å resolution, phased with five derivatives [M.M. Roberts *et al.*, *Science* **232**, 1148-1151 (1986)]. At 967 residues, hexon is currently the longest polypeptide for which the crystal structure has been determined. Hexon's economical design is evident in its structure. Two similar 8-stranded beta-barrels within each subunit form two corners of a pseudo-hexagonal base with exact threefold symmetry. Hexons close-pack to form a protective coat for the protein-covered core containing the DNA. The barrels have the same topology as those in all known RNA virus structures and, despite different orientations, have a common architectural role as a building block in the formation of a shell of protein.

The geometry of a backbone model of hexon, based on measured coordinates, was regularized using PROLSQ. Side-chains were attached to the backbone in a standard conformation and are being fitted to the electron density using FRODO on an MPS graphics system. Over 60% of the model is complete, including two of the three loops that interweave to form the towers at the top of the molecule. The side chains fit the density well and confirm the original tracing, which has been altered only in one region, where a previous discontinuity has been removed. The results of the refinement, and its implications for the virus structure, will be presented. (Supported by NIH Grant AI 17270).

- M-Pos128** THE STRUCTURE OF *E. COLI* F_1F_0 ATPASE VISUALIZED BY CRYO-ELECTRON MICROSCOPY.
E.P. Gogol, U. Lucken and R.A. Capaldi, Institute of Molecular Biology, University of Oregon, Eugene, OR 97403

The F_1F_0 ATPase from *E. coli* has been isolated and reconstituted into lipid bilayer structures. Preparations are mixtures of asymmetrically-oriented vesicles and small fragments of symmetrically-oriented bilayer sheets, the proportions of which are dependent on the lipid-to-protein ratios employed. Both types of structures have been visualized by transmission electron microscopy in the absence of stain, fixative, or other perturbant. Specimens were preserved and maintained in a thin layer of amorphous ice supported by a holey carbon film.

The F_1 portion of the assembly (the ATPase) is readily visualized with adequate contrast at vesicle edges, in fortuitously-oriented edge-views of small sheets, and in areas free of overlap in two-sided *en face* views. Projections of the F_1 portion are a subset of those seen in similar preparations of the F_1 alone, and define a structure with approximate dimensions $90 \times 90 \times 115$ Å, bisected by a prominent groove or channel. The lipid bilayer profile is well contrasted in edge-views, and differs from that of lipid vesicles mainly in the presence of small discontinuities, particularly in the lipid headgroup region, which are presumably due to the F_0 portion (the proton channel) of the ATPase assembly. A gap of approximately 50 Å separates the F_1 from the lipid bilayer, and is spanned by a stalk approximately 20 Å thick.

Previous models of the F_1F_0 ATPase structure, based on electron microscopy of negatively-stained specimens, are supported by these more direct and less artifactual observations. Further quantitation of molecular mass ratios and a three-dimensional reconstruction are in progress.

M-Pos129 CHARACTERIZATION OF THE HIGH MOLECULAR WEIGHT COMPONENTS EXTRACTED FROM THE CUTICLES OF *CAENORHABDITIS ELEGANS*. Alice J. Burton, Shannon Skarshaug and Emily Clark. Biology Department, St. Olaf College, Northfield, MN 55057.

During the development of *Caenorhabditis elegans*, at least four distinct, stage-specific types of cuticle are synthesized (for review, see Edgar, R.S., Cox, G.N., Kusch, M. and Politz, J. 1982. *J. Nematol.* 14, 248-258). One change we observe is the accumulation, late in the life cycle, of large molecular weight components (>200,000 daltons) among the proteins which can be extracted from cuticle preparations using β -mercaptoethanol. These components become a significant proportion of such proteins extracted from the late larval and adult cuticles of wild type animals; their accumulation begins somewhat earlier in the life cycle of dumpy mutants (obtained from R. Herman) which have major alterations in cuticle morphology. It is unlikely that these large components are primary gene products in view of the relatively small size of most collagen genes and collagen mRNA in *C. elegans* (Cox, G.N., Kramer, J.M. and Hirsh, D. 1984. *Mol. Cell. Bio.* 4, 2389-2395; Politz, J.C. and Edgar, R.S. 1984. *Cell* 37, 853-860). Several laboratories including our own have looked at the effect of inhibitors of cross-linking involving lysine on the construction of the cuticle and have observed no change in the development of the animals. We have considered the possibility that polysaccharide, and perhaps lipid, moieties provide the covalent links permitting the assembly of the high molecular weight components and will present evidence, including the effects of mild acid degradation of cuticle preparations, which supports this view. Supported by the Research Corporation and the National Science Foundation.

M-Pos130 ABSENCE OF THE OUTER FLAGELLIN DOMAIN IN A THREE-DIMENSIONAL RECONSTRUCTION OF THE FLAGELLAR FILAMENT OF *CAULOBACTER CRESCENTUS*. S. Trachtenberg & D.J. DeRosier, Rosenstiel Center, Brandeis Univ., Waltham, MA 02254.

The bacterial cell is propelled through the medium by means of one or more rotating rigid flagella. The flagellum consists of a basal body (rotary motor), hook (universal joint) and filament (propellor). The flagellar filament of *C. crescentus* is unique in being constructed from flagellin of low molecular weight (26-28.5 kD compared to 50-60 kD in other species). We studied the structure of negatively stained filaments by electron microscopy and image reconstruction. The diffraction pattern indexes on an approximate repeat of $1/570 \text{ \AA}^{-1}$. The layer lines present are (n,l) 0,0; 11,1; -5,13; 6,14; 1,27 and the data extended to axial and radial resolutions of 21 Å and 10 Å, respectively. The lattice constant is essentially identical to that of *Salmonella typhimurium* (SJW1660 and 1655), suggesting a common underlying design. Despite the small molecular weight of *C. crescentus* flagellin, about half that of *S. typhimurium*, in the *C. crescentus* filament there is one flagellin subunit per unit cell, not two as suggested by Shirakihara et al. (*Proc. Japan Acad.* 59(B):194, 1983). This was shown by measuring the mass per unit length with the Scanning Transmission Electron Microscope at Brookhaven National Laboratory. A three-dimensional reconstruction of *C. crescentus* filament is similar to that of *S. typhimurium* (S. Trachtenberg & D.J. DeRosier, *Proc. EMSA* 44:298, 1986) and *Rhizobium lupini* (Trachtenberg et al., *Proc. EMSA* 42:638, 1984). Both filaments have 11 segmented columns of density at a radius of about 60-70 Å. In all four maps the inner part of the subunit is weaker consisting of projections persisting radially inward from the 11 columns. The striking difference in the reconstruction of the *C. crescentus* filament is that it lacks the large outer domain found at a radius of ~100 Å in *S. typhimurium* and ~90 Å in *R. lupini*. The absence of the outer domain would explain the lower molecular weight, smaller diameter and smooth appearance of the *C. crescentus* filament. Comparison of the primary amino acid sequences of *C. crescentus* (P.R. Gill & N. Agabian, *J. Biol. Chem.* 258:7395, 1983) and *S. typhimurium* (T.M. Joys, *J. Biol. Chem.* 260:15758, 1985) shows that there is a long interior stretch of sequence in *S. typhimurium* which has no homolog in the shorter *C. crescentus* sequence. This interior segment may correspond to the outer domain.

M-Pos131 SEDIMENTATION EQUILIBRIUM IN MACROMOLECULAR SOLUTIONS OF ARBITRARY CONCENTRATION.

Ronald C. Chatelier and Allen P. Minton, Laboratory of Biochemical Pharmacology, DIR, NIDDK, National Institutes of Health, Bethesda, Maryland 20892.

Relations describing sedimentation equilibrium in solutions of self- and hetero-associating macromolecules at arbitrary concentrations are presented. These relations are obtained using scaled particle theory to calculate the thermodynamic activity of each species present. The results are expected to be valid for solutions of globular proteins under conditions such that the interactions between individual solute molecules may be approximated by a hard particle potential. The results of simulated sedimentation equilibrium experiments are presented in terms of the dependence of apparent weight-average molecular weight(s) upon solute concentration(s). Semi-empirical procedures have been developed that permit the true weight-average molecular weight to be estimated from experimental data to a precision of 10% or better in arbitrarily concentrated solutions, independent of any model for association. These procedures will enable the experimenter to utilize data obtained from measurements of sedimentation equilibrium in highly nonideal solutions to quantitatively characterize mechanisms of self- or hetero-association taking place in such solutions.

M-Pos132 THE ERYTHROCYTE SEDIMENTATION RATES: SOME MODEL EXPERIMENTS. Lawrence C. Cerny, Elaine L. Cerny, Caroline R. Ganley and Frank Compolo. Utica College of Syracuse University and The Masonic Medical Research Laboratory, Utica, N.Y. 13504.

In order to obtain a better understanding of the erythrocyte sedimentation rate (ESR), several models are proposed. The first directs attention to the importance of geometrical models to represent the structure of mixtures. Here it is our intention to understand the effect of the structure on the packing of red blood cells. In this part of the study, "Cheerios" (trademark General Mills) are used as a macroscopic model. Although the "Cheerios" are not biconcave, the central hole has no effect on the packing. It is interesting that a random sampling of "Cheerios" has the same volume distribution curve that is found for erythrocytes with a Coulter Sizing Apparatus. In order to examine the effect of rouleaux formation, the "Cheerios" are stacked one on top of another and then glued. Rouleaux of 2,3,4,5,7 and 10 discs were used.

In order to examine a more realistic biological model, the experiments of Dintenfass (Clin. Hemorheol. 5:917-36, 1985) were used. These investigations were performed in a slit-capillary photo viscometer using whole blood from patients with a variety of diseases. The novel part of this research is the fact that the work performed at 1g and at near-zero gravity in the space shuttle "Discovery." The size of the aggregates and/or rouleaux clearly showed a dependence upon the gravity of the experiment. The purpose of this model was to examine the condition of self-similarity and fractal behavior. Calculations are reported which clearly indicate that there is general agreement in the magnitude of the fractal dimension from the "Cheerios" model, the "Discovery" experiment with those determined with the automatic sedimentimeter (Biorheology 14:145-9, 1977).

M-Pos133 PROTON DEGENERATION AT THE WATER-MEMBRANE INTERFACE: A FEASIBLE MECHANISM FOR LONG RANGE ORDER IN BIOLOGICAL SYSTEMS. Michael Conrad, Departments of Computer Science and Biological Sciences, Wayne State University, Detroit, MI 48202

Water bound to the biological membrane is in some measure analogous to a thin layer of metal spread on the surface of a dielectric, with the mobile protons playing the role of the conduction electrons in a metal and the polar side groups of the membrane playing the role of the lattice nuclei of the dielectric. The motion of the protons induces a wave of electronic polarization in the protruding side groups of the membrane, providing a potential pairing interaction; and the conditions that control pairing and condensation of protons are not less favorable than those that control pairing and condensation of electrons in conventional superconductors (M. Conrad, Biophys. J. 49, 274a, 1986). In order for condensation to occur Bose-Einstein statistics must apply--that is, the protons must form a degenerate system. The condition for strong degeneracy is met if $n \sim (2\pi m^* kT)^{3/2} / h^3$, where n is particle density and $m^* = (d^2E/dp^2)^{-1}$ is the effective mass. This gives a value of $m_p^* \sim m_p/7$ for a hydrogen atom separation of $d \sim 2.5 \text{ \AA}$ (the mean separation in normal water) and $m_p^* \sim m_p/4$ for $d \sim 2 \text{ \AA}$ (the mean separation if close packing of water molecules could occur). Any structures at the water-membrane interface that facilitate the flow of protons would favor degeneration by decreasing effective mass. Under the reduced effective mass assumption a small fraction of the membrane could be covered by degenerated patches and connecting channels in a manner that would allow for condensation and that at the same time would not interfere with normal chemistry over most of the membrane surface.

M-Pos134 SOLUTE PARTITIONING INTO INTERPHASES AND BILAYER MEMBRANES

J. Naghizadeh and Ken A. Dill
Department of Pharmaceutical Chemistry and Pharmacy
University of California, San Francisco, CA 94143

A mean field lattice theory is developed for mixing of short flexible chains and rigid molecules within the interfacial phase of host chain molecules. Interphases considered are bilayer membranes and grafted chains used in reversed phase chromatography. Mixing depends on entropy of mixing, entropy arising from perturbation of chain configurations, and contact interaction between solute and host chains. The theory predicts a stable gradient of solute concentration due to variation of chain organization with depth.

M-Pos135 THE REFERENCE STATE: ITS ROLE IN NETWORK THERMODYNAMIC MODELS OF NONLINEAR KINETIC SYSTEMS. D.C. Mikulecky, F.A. Sauer, and L. Peusner, Department of Physiology/Biophysics, MCV/VCU, Richmond, VA 23298-0001, Max-Planck-Inst. for Biophysics, Frankfurt am Main, West Germany and 181 State Street, Portland, Maine 04101.

Nonlinear systems cannot be totally described by force-flow relations alone. This is in distinction to linear systems which fit the nonequilibrium thermodynamic paradigm [Sauer, Handbook of Physiology: Renal Section - Apdx. to Ch. 12 pp., 399-414 (1973)]. Network thermodynamics has the capacity to provide network representations of nonlinear kinetic systems including carrier models, channel models, biochemical and pharmacological systems, reaction-diffusion systems and many others. [Peusner, Mikulecky, Bunow and Caplan *J. Chem. Phys.* 83: 5559-5566 (1985)]. These representations have been shown to yield a new coordinate system in which the flow-force relations are linear arbitrarily far from equilibrium. [Mikulecky, Sauer and Peusner, *Biophysics of Membrane Transport VIII*, (1986)]. The network representation generates new forces which have some interesting properties, including a smooth transition to the usual thermodynamic forces near equilibrium. For specified reference states, the networks also generate the phenomenological coefficients corresponding to the more traditional nonequilibrium thermodynamic formulation of linear systems near equilibrium. It is possible to incorporate more than one reference state into a network representation using a combination of diodes and sources thereby achieving a piecewise-linear approximation to the actual nonlinear characteristics of a system [Peusner: Studies in Network Thermodynamics, Elsevier (1986)]. Some useful applications of this technique are presented.

M-Pos136 LINEAR STABILITY ANALYSIS OF METABOLIC PATHWAYS. Xianliang Wu and T.G. Dewey.
Department of Chemistry, University of Denver, Denver, CO 80208.

A general theoretical method is presented for analysing the stability of metabolic pathways. This method computes the stability of the linearized differential equations of the coupled enzymatic reactions in a pathway. An approximate method previously used for calculating relaxation times for enzymatic reactions (Hammes & Schimmel, *J. Phys. Chem.*, 71, 917 (1967)) is adapted to the pathway stability problem. General conditions which result in instabilities and in limit cycle behavior are identified for pathways which contain one, two or three coupled slow steps. Uncoupled steps may be treated by standard block diagonalization procedures. Specific examples of pathways involving product inhibition and product activation are considered.

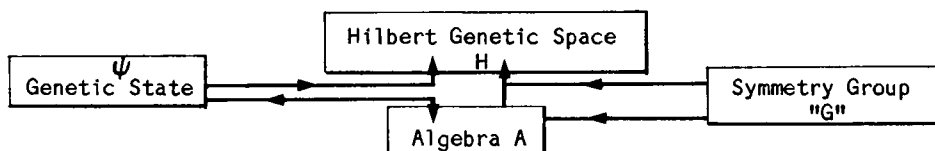
M-Pos137 BROKEN SYMMETRIES OF BIOMOLECULES. Shrikant Mishra and Hara P. Misra, Department of Biosciences, College of Veterinary Medicine, Virginia Tech, Blacksburg, VA 24061

Attempts have been made to rationalize the existence of broken symmetries of biomolecules and to present a model which can bring about a certain level of restored symmetry. A spontaneous dimensional compactification from "n" dimensions to "n-1" dimensions leading to a natural explanation of broken symmetries in the reduced space has been applied to understand dynamical symmetry breaking in L- and D- amino acids as enantiomorphous isomers. The key equations in the above reasoning are:

$$T(X_i) = \sum_{i=1}^n C_i X_i$$

where $X_i = (x_1, x_2, x_3, \dots, x_n)$ in "n" space and $T(x_i)$ is a topological space function, $\sum_{i=1}^n D_i T(x_i) = 0$, is a topological constraint where D_i is the differential operator along the i th axis.

The symmetry breaking mechanism could also be applied to understand the process of genetic mutations as a catastrophic transformation in a SINDF. Mutation, thus, can be likened as a spontaneous breakdown of a certain symmetry subgroup "G", which is some natural invariance group of the genetic state over an appropriate Algebra.



M-Pos138 CORRELATION FUNCTION ANALYSIS OF PATCH CLAMP DATA

Thomas L. Croxton, Oscar J. Riveros, and William McD. Armstrong
Dept. of Physiol. and Biophys., Ind. Univ. Sch. Med., Indianapolis IN 46223

Previous applications of correlation functions to patch clamp analysis have been based on models that do not include noise (Liebovitch and Fischberg, Math. Biosci. 76, 1, 1986). Significant inaccuracies in calculated rate constants developed with increasing noise. We have considered a simple two-state channel model which contains additive Gaussian noise and have derived theoretical expressions for the first- and second-order time correlation functions. For example, the normalized first-order correlation function $g_1(\tau)$ is

$$g_1(\tau) = (\exp(-k_s \tau) + \frac{(1+\beta)^2}{\beta} \alpha^2 \delta_{\tau,0}) / (1 + \frac{(1+\beta)^2}{\beta} \alpha^2)$$

where β is the ratio and k_s the sum of opening and closing rate constants, α is the noise-to-signal ratio and, $\delta_{\tau,0}$ is the Kronecker delta function. The explicit dependence of the correlation functions on α can explain the errors noted by Liebovitch and Fischberg in dealing with noisy data. Based on the above expression for $g_1(\tau)$ and analogous equations, we have developed an alternative scheme that yields accurate rate constants from simulated noisy data. This scheme should be of value for analysis of patch clamp data from certain ion channels. Supported by USPHS grants AM36575 and AM07554.

M-Pos139 MUELLER MATRIX THEORY OF DIFFERENTIAL POLARIZATION IMAGING: SYMMETRY PROPERTIES, Myeonghee Kim, Laura Ulibarri and Carlos J. Bustamante, Department of Chemistry, University of New Mexico, Albuquerque, N.M. 87131

Differential Polarization Imaging (DPI) is a method in which the images of an object, obtained using light of orthogonal incident polarizations, are subtracted point by point from each other. The resulting difference image displays both magnitude and sign which represent the preferential interaction of the object with one polarization over the other. This preferential interaction is due to the optical anisotropy of the object. If an object is optically isotropic, the difference image vanishes identically. Thus, the optical anisotropy of an object within a sample provides the contrast mechanism of DPI. DPI can be applied to microscopy as a method of probing the molecular organization of the specimen.

A theory of Differential Polarization Imaging has been derived in our laboratory using the Mueller matrix formalism. In this theory, an object is described as a collection of polarizable groups and its overall shape is arbitrary. To evaluate the electric fields arriving at the lens surface, the first Born approximation was used. When taking into account the effect of lens, we considered only the paraxial rays and assumed the lens to be thin. For the recombination of the electric fields after the lens, vector diffraction theory was used to form a polarization dependent image. Using this theory, we have investigated the symmetry properties of the difference images upon a rotation of the optical axis of an imaging system.

M-Pos140 EXCITON ORIGIN OF OPTICAL ACTIVITY IN SACCHARIDES. E. S. Stevens and B. K. Sathyanarayana, Department of Chemistry, University Center at Binghamton, State University of New York, Binghamton, NY 13901

Kirkwood's polarizability theory of optical activity is modified to make explicit reference to electric dipole allowed transitions deep in the vacuum ultraviolet. The transition moments are then coupled according to exciton theory. The model is applied to representative saccharides. Relatively simple CD spectra result and indicate that the local symmetry within saccharides is sufficient to generate exciton-like features. Calculated sodium D rotations display the same dependence on saccharide structure as is observed experimentally. The calculated rotations are however uniformly too small by a factor of two-to-three, which reflects limitations either in polarizability theory, i.e., the omission of electric dipole-magnetic dipole coupling, or in the parameterization of the model, or both.

M-Pos141 LIVER LENGTH/WIDTH ON RADIONUCLIDE IMAGES: A STUDY IN BIOLOGICAL CONSTRAINTS. Richard P. Spencer, Jonathan R. Arnow. Department of Nuclear Medicine, University of Connecticut Health Center, Farmington, CT 06032.

Organ size and shape are likely determined both by genetic information and the constraints imposed by neighboring structures. For example, during thyroid enlargement ("goiter"), the fascial planes restrict growth laterally and the organ grows forward thus producing the anterior neck mass. We investigated the relationship between liver length and width, during life, by means of radionuclide liver images obtained after intravenous administration of Tc-99m-sulfur colloid (a reticulo-endothelial probe). Gamma cameras that carried out the imaging were calibrated as to their image minification; hence actual size could be determined from the anterior images. We studied 97 consecutive adults who were sent in for liver imaging. The ages were 22 to 90 years (mean: 50 years). There were 55 females and 42 males. The length of functional liver tissue varied from 12 to 29 cm (normal range is 14-20 cm). The liver width varied from 13-28 cm. We first analyzed the relationship between liver length and width in all 97 individuals, using a linear assumption ($L = a.W + b$). The result was $L = 0.35W + 11.3$. The correlation coefficient of 0.35 indicated little relationship. Separate analysis was carried out for the 67 patients with livers of normal length, and without any hepatic defects. The correlation coefficient was 0.32 for the length-width relationship. The correlation in the 30 patients with very large or small livers, or with defects, was 0.31. These low values suggest little coupling between liver length and width. A further approach was taken by logarithmic analysis; again the correlation was low. The liver is apparently free to expand downward (Length) but is constrained laterally. (Supported by USPHS CA 17802).

M-Pos142 LOW EXTERNAL SODIUM DECREASES MECHANICAL THRESHOLD IN FROG SKELETAL MUSCLE. R. Godínez*, M.C. García[†] and J.A. Sánchez*. Dept. of Pharmacology*, CINVESTAV-IPN and Biophysics[†], ENCB-IPN, Mexico, D.F.

It is well known that the absence of extracellular sodium does not induce contractures in twitch skeletal muscle. The present experiments show however, that low external sodium decreases the mechanical threshold.

Single fibers from *Rana pipiens* or *Rana montezumae* were used at 20–22°C. Strength-duration curves were constructed by visually measuring the mechanical threshold in voltage clamp experiments using the vaseline gap technique for cut fibers. The sodium in the external Ringer's was substituted by N-methylglucamine and TTX (10^{-6} M) was added. Internal solutions contained (mM): Cs-Aspartate=104, $MgCl_2$ =6.5, EGTA=0.2 at MOPS=4 at pH=7.2. Low external sodium shifted the rheobase by 12 mV (2) towards more negative potentials the effect is reversible and fully develops in ca 15 min. Amiloride in the presence of sodium (0.4 mM) had a similar effect: 10.8 mV (2). Increasing external Na^+ to 260 mM increased the threshold by 5 mV (2). Potassium contractures in single intact twitch fibers also depend on external sodium: Half maximum tension was obtained at 46 mM $[K]_e$ in full external sodium and at 37 mM in low external sodium.

The results are in line with a role of sodium-calcium exchange in skeletal muscle.

Supported by CONACYT PCCBNA-022593 and J. Ricardo Zevada grants.

M-Pos143 MEASUREMENT OF INTRACELLULAR CALCIUM BY QUIN2 OR FURA2 IN CARDIAC MYOCYTES OF RAT VENTRICLES: INTERACTION BETWEEN ISOPROTERENOL, BAY K 8644 AND PROPRANOLOL. Ö.G. Björnsson, K. Kobayashi and J.R. Williamson. Dept. of Biochem. & Biophys. Univ. of Penn. Philadelphia, PA.

Isoproterenol and the dihydropyridine calcium agonist BAY K 8644 both exert a positive inotropic effect on the heart but through different receptor mechanisms. We measured free intracellular calcium in ventricular myocytes, using the fluorescent indicators Quin2 and Fura2, and studied the response of $(Ca^{2+})_i$ to activation by isoproterenol and/or BAY K 8644 in the presence or absence of propranolol. Cells were loaded with varying amounts of Quin2 (0.3 – 3.0 nmol/mg drw) or Fura2 (0.1 – 0.9 nmol/mg drw). $(Ca^{2+})_i$ increased significantly upon electrical stimulation in both Quin2 cells (72 ± 7 nM to 145 ± 13 nM, SEM, $n = 24$) and Fura2 cells (64 ± 5 nM to 147 ± 12 nM, $n = 34$) ($P < 0.01$). In Quin2 cells and cells loaded with Fura2 of high conc. (> 0.6 nmol/mg drw), isoproterenol (10^{-10} – 10^{-6} M) increased $(Ca^{2+})_i$ in a dose-dependent manner (max. 192%). At lower Fura2 loading the effect of isoproterenol was not detected. During electrical stimulation BAY K 8644 (10^{-10} – 10^{-6} M) caused dose-dependent an upward shift in baseline and attenuation of superimposed Ca^{2+} transients. With termination of electrical stimulation the baseline fell towards previous levels. The effect of BAY K 8644 was augmented by isoproterenol. Pretreatment with propranolol (10^{-6} M) attenuated the effect of BAY K 8644 and abolished the effect of isoproterenol, and in cells incubated with propranolol alone, $(Ca^{2+})_i$ was suppressed. Propranolol has calcium antagonistic effects in cardiac ventricular myocytes, interferes with BAY K 8644 and abolishes the effect of isoproterenol. Similar resting and stimulated $(Ca^{2+})_i$ levels were measured in Quin2 and Fura2 cells but the response to isoproterenol in Fura2 cells was critically dependent on high indicator loading.

M-Pos144 SOME FEATURES OF (i) CONTRACTILE ALTERNANS & (ii) SPONTANEOUS, ASYNCHRONOUS CONTRACTION IN THE VOLTAGE-CLAMPED, DIALYZED HEART CELL. Barry London & John Krueger. The Albert Einstein College of Medicine, Bronx, N.Y. 10461

We analyzed some aspects of irregular contraction in dialyzed, voltage-clamped heart cells isolated from Guinea Pigs. The internal perfusate was weakly buffered at pCa=7 with 0.5mM EGTA and also contained (in mM) ATP 3.3, CP 12, cAMP 0.03, DTT 0.1, and CPK 30 U/ml, at pH 7.1. 30 μ M TTX in the extracellular sol'n and holding potentials of -50 mV minimized the Na^+ current through the fast channels. (i) Alternating weak and strong twitch contractions could be induced reversibly by stimulus patterns which raised the intracellular $[Ca^{++}]$: i.e., high stimulus rates, prolonged or large depolarizations. The magnitude of the peak inward currents which triggered the alternate contractions appeared similar, while the internal dialysis probably minimized changes in [ATP] or other metabolites. This demonstrates that the contractile alternans arises in the sarcoplasmic reticulum and/or in the mechanism of Ca^{++} release (ii) Spontaneous asynchronized waves of shortening (presumably caused by localized SR Ca^{++} release) were occasionally seen and were accompanied by a small transient inward current at holding potentials of -50mV. Replacement of external Na^+ by Li^+ and removal of internal Na^+ increased the amplitude of shortening and, by inference, the spontaneous release of Ca^{++} . The larger asynchronized contractions were no longer associated with a transient inward current. The absence of a transient inward current in the presence of a small molecule like Li^+ suggests that this current (or the spontaneous afterdepolarization which would have been seen in the absence of a voltage clamp) is not mediated by a nonspecific cation channel. An electrogenic Na^+/Ca^{++} exchange could explain these results. Supported, in part by HL 21325, T32 GM7288, & the NYHA.

M-Pos145 EFFECTS OF SODIUM NITROPRUSSIDE (NP) AND CYCLIC GMP (cGMP) ON SKINNED AORTIC STRIPS. Judy Y. Su, Department of Anesthesiology, University of Washington, Seattle, WA 98195

NP, a vasodilator, has been shown to increase cGMP by stimulating guanylate cyclase. If cGMP is a second messenger for NP-induced vasodilation we would expect that they have similar mechanisms of action. Accordingly, we examined the intracellular mechanisms of action of NP and cGMP on chemically skinned aortic strips of rabbits. Medial layers (200 μm x 500 μm x 1-2 mm) of aortic strips were mounted on photodiode force transducers and skinned with 500 $\mu\text{g}/\text{ml}$ saponin in relaxing solution for 5-10 min. The effects of the drugs were studied on Ca^{2+} -activated tension development of the contractile proteins (CP), and Ca^{2+} uptake and release from the sarcoplasmic reticulum (SR) using caffeine-induced tension transient. The bathing solution contained (in mM) K^+ Na^+ = 70, Mg^{2+} = 1 (for CP) and 0.1 (for SR), MgATP^{2-} = 2, creatine phosphate $^{--}$ = 15, EGTA total = 7 (for CP) and 0.05 or 7 (for SR), PIPES = 50, and $-\log [\text{Ca}^{2+}](\text{M}) = > 8 - 3.8$. Propionate (for CP) and methanesulfonate (for SR) were major anions to achieve ionic strength of 0.15 and pH of 7.00 ± 0.02 at $23 \pm 2^\circ \text{C}$. We found that > 0.1 mM cGMP decreased, and > 1 mM NP increased the submaximal and maximal Ca^{2+} -activated tension of the contractile proteins. Ca^{2+} uptake by the SR was decreased by 0.1 μM - 10 mM cGMP and NP (0 - 83%, 0 - 33% respectively) and Ca^{2+} release from the SR was decreased by 0 - 41% by cGMP (0.1 μM - 10 mM) and increased by NP (32% and 300% for 1 & 10 mM respectively). The effects were dose-dependant. We conclude that < 0.1 mM cGMP and NP have similar mechanisms of action, decreasing Ca^{2+} uptake by the SR which may be responsible for NP-induced vasodilation mediated through cGMP. (Supported by grants from Washington Heart Association and HL 20754 and HL 01100 from NIH.)

M-Pos146 CHANGES IN MUSCLE LENGTH PRIOR TO OR DURING ACTIVE CONTRACTION AFFECT INTRACELLULAR Ca^{2+} IN AEQUORIN-LOADED TRACHEAL SMOOTH MUSCLE. Susan J. Gunst, Dept. of Physiology, Mayo Foundation, Rochester, MN 55905.

Canine tracheal smooth muscle strips (5 mm long x 2 mm wide) were suspended vertically in a tissue bath between a small clamp and a servo-controlled electromagnetic lever. The length of maximal active contraction, L_0 , was determined using electrical field stimulation (60 Hz, 30 V). Muscles were then loaded with aequorin using a modification of the method of Morgan and Morgan (J. Physiol. 357:539, 1984). Intracellular Ca^{2+} was evaluated by recording light emitted by the muscle during 20-30 s tonic isometric contractions produced by electrical field stimulation. Ca^{2+} increased rapidly coincident with the onset of stimulation, and then either remained nearly constant or slowly increased further over the course of the contraction. When the stimulus was stopped, the fall in force lagged the fall in light by 1-2 s. Isometric muscle force decreased when muscle length prior to contraction was decreased from L_0 to lengths of 60 to 90% L_0 , but the light increased at shorter muscle lengths. When a rapid step decrease in muscle length (10-40% of L_0) was imposed during isometric contraction, light rose coincident with the onset of isometric force redevelopment at the shorter muscle length. The rise in light following a quick release was greatest when the length step was performed early in the contraction (1-7 s after the onset of stimulation). Light also rose following an isotonic quick release but the rise did not occur until several seconds after the release. We conclude that intracellular Ca^{2+} increases when muscle length during active contraction is decreased. The increase in Ca^{2+} could be caused by a length-dependent change in the Ca^{2+} affinity of the contractile filaments. Supported by USPHS grant HL29289.

M-Pos147 FURA-2 LOADS INTO MITOCHONDRIA IN MAMMALIAN VASCULAR SMOOTH MUSCLE CELLS.

Tia T. DeFeo, G. Maurice Briggs, and Kathleen G. Morgan. Dept. of Medicine and Cardiovascular Division, Beth Israel Hospital, Harvard Medical School, Boston, MA 02215

We have previously shown that, with the appropriate loading conditions, Fura-2 intracellularly compartmentalizes in isolated ferret portal vein cells. Caffeine (10 mM) which is known to deplete calcium from the sarcoplasmic reticulum, causes a decrease in the overall ratio image but causes an apparent enhancement of punctate bright spots of 1-2 μm in size. These "hotspots" are of similar size to that which has been reported for mitochondria from portal vein cells. To investigate the possibility that Fura-2 loads into the mitochondria of these cells, in 8 experiments, we co-loaded the same individual cells with Fura-2 and Rhodamine 123 (R-123); a vital dye which has been shown to specifically fluorescently label mitochondria. The excitation wavelength for Fura-2 was 350 or 390 nm and for R-123 was 485 nm. There was no detectable crossover of the fluorescence of the two indicators. The Fura-2 ratio image and the R-123 image were remarkably similar in that individual identifiable "hotspots" could be seen in both images. To further test the idea that the "hotspots" were mitochondria, the effects of the mitochondrial uncoupler FCCP (which depletes calcium from the mitochondria) were tested. The "hotspots" disappeared and the control digital ratio decreased from 3.2 ± 0.2 to 0.7 ± 0.3 in the presence of FCCP (n=6). These data strongly support the idea that Fura-2 loads into mitochondria in mammalian vascular smooth muscle cells and suggest that Fura-2 may give a signal which is a function of ionized [Ca] in the mitochondrial matrix.

Support: Established Investigatorship and NIH HL 31704.

M-Pos148 ANGIOTENSIN RAPIDLY DECREASES TOTAL CELL CALCIUM BY STIMULATING SODIUM/CALCIUM EXCHANGE IN CULTURED SMOOTH MUSCLE CELLS. Jeffrey Bingham Smith, Bryan L. Higgins, and Lucinda Smith. Dept. Pharmacology, University of Alabama at Birmingham, Birmingham, AL 35294.

Total cell Ca was measured in rat aortic muscle cells after equilibrium labeling with ^{45}Ca (overnight in culture medium). One min after adding 100 nM angiotensin II (ANG) total cell Ca decreased by $27 \pm 2.9\%$ ($n=15$). Cell Ca returned to the initial level about 10 min later in the continued presence of ANG. ANG rapidly increases cellular inositol 1,4,5-trisphosphate (IP₃) which opens an intracellular Ca channel by a ligand-binding reaction (Am. J. Physiol. 250:F759, 1986). The increase in free Ca that is produced by ANG is due largely to the release of sequestered Ca since the removal of external Ca has a minor effect on the free Ca transient measured with fura-2. The following evidence suggests that the Ca that is released from the IP₃-sensitive compartment rapidly exits the cell via Na/Ca exchange: 1) the replacement of external Na with other monovalent cations strongly decreases ANG-evoked ^{45}Ca efflux and almost prevents the decrease in total cell Ca 1 min after adding ANG; 2) the relative potency of 7 congeners of amiloride was similar for Na/Ca antiport activity and ANG-evoked ^{45}Ca efflux. The assay of Na/Ca antiport activity in Na-loaded cells by ^{45}Ca influx and ^{22}Na efflux indicates that it is abundant in this cell type and has a stoichiometry of 3:1. In conclusion the data provide evidence for a Ca cycle that consists of the following 3 events: 1) a rapid opening of the intracellular Ca channel by IP₃ which transiently increases free Ca; 2) the exodus of the released Ca by Na/Ca exchange; 3) a slow restoration of total cell Ca and refilling of the inositol trisphosphate-sensitive compartment. (Supported by Grants HL32508 and HL01671 from the National Institutes of Health.)

M-Pos149 MEASUREMENT OF $[\text{Ca}^{2+}]_{\text{cyto}}$ BY FURA-2 IN INTACT CONTRACTING SMOOTH MUSCLE. B. Himpens & A.P. Somlyó, U. of Pennsylvania Sch. of Med., Phila., PA

$[\text{Ca}^{2+}]_{\text{cyto}}$ was measured, in sheets of the longitudinal smooth muscle of guinea-pig ileum, by fluorescence emission (510nm) of intracellular Fura-2¹, excited at 340 and 380nm through narrow bandpass filters mounted in an air driven turbine, alternating at 35Hz. Exciting light was passed through and the fluorescence collected by one leg each of a bifurcated randomized light pipe. The tension trace and the fluorescence emitted at the two exciting wavelengths were stored in an IBM AT computer; the 340/380nm ratio signal (FR) was calculated offline to avoid artifacts in the FR due to unequal shifts in the same direction of the 340 and 380nm signals. Parallel fluctuations in $[\text{Ca}^{2+}]_{\text{cyto}}$ accompanied spontaneous, rhythmic contractions. Carbachol (10^{-4}M) or depolarization with high K^{+} (1.2mM Ca^{2+}) increased $[\text{Ca}^{2+}]_{\text{cyto}}$ and caused force development; both the light signal and contraction were less sustained after C than K^{+} . The force response to 70mM K^{+} was $81 \pm 10.3\%$ and the fluorescence $80 \pm 13.8\%$ of these responses to 140mM K^{+} . 35mM K^{+} evoked $55 \pm 9.7\%$ of the force and $61 \pm 10.2\%$ of the light signal ($n=16$). Transient reduction of K^{+} from 140mM to 35mM K^{+} caused relaxation without, however, a significant change in the FR. In Ca^{2+} -free solution the FR fell below resting levels and an intracellular Ca^{2+} -store could be released by C. Verapamil (10^{-5}M) reduced the force response to C to $30 \pm 4.5\%$ and that to 140mM K^{+} to $6 \pm 2.5\%$; the FR peak response to C was reduced to $78 \pm 12.5\%$ ($n=7$) and that to K^{+} to $18 \pm 5.3\%$ ($n=6$).
1. Grynkiewicz, G. et al. J. Biol. Chem. 260:3440, 1985. Supported by HL15835 to the Penna Muscle Institute. B.H. is a Res. Asst. of the NFWO (Belgium).

M-Pos150 FREE CALCIUM MEASUREMENTS WITH FURA 2 IN CONTRACTING STRIPS OF EMBRYONIC SMOOTH MUSCLE. Marilyn R. James-Kracker (Intr. by G. Kracker). SUNY Health Science Center at Syracuse, N.Y. 13210.

Contraction of ileal circular smooth muscle was observed from the 10th to 14th day of development in chicken embryos. Ileal segments (diameter 1 mm, length 8 mm) were cut helically so that the predominant circular layer was oriented longitudinally. The adventitia and mucosa are easily separated at this stage of development. At 10 days old, carbachol (100 μM) induced a small phasic contraction (peak tension 25 mg at 30 sec). By 13 days old, the muscle is more sensitive to carbachol. The phasic contraction is larger (80 mg tension) and peaks earlier (20 sec), and a second tonic component appears. Strips were loaded with fura 2 (0.5 μM fura 2/am for 1 hr) and washed while pinned across a frame which fits into a cuvette. Changes in intracellular free calcium concentration ($[\text{Ca}^{2+}]_i$) were calculated every 9.4 sec in a Perkin Elmer MPF-66 spectrofluorimeter by the ratio method which cancels photobleaching and contraction artifacts. Unlike suspensions of embryonic smooth muscle, in which fluorescent changes indicative of Ca^{2+} changes were never observed to carbachol, muscle sheets always responded, which indicated that surface receptors may be easily removed by agitation or collagenase. With perfusion of medium through the cuvette (not feasible with suspensions of cells), recovery of the muscles on frames after activation by carbachol, histamine, and high K^{+} could be monitored. The resting level of $[\text{Ca}^{2+}]_i$ (120 nM) was reduced in Ca-free medium (80 nM) and, in this medium, responses to carbachol and high K^{+} were blocked. Caffeine (10 mM) increased $[\text{Ca}^{2+}]_i$ indicating that Ca^{2+} in sarcoplasmic reticulum is present as early as the 10th day of development.

M-Pos151 MEASUREMENTS OF FORCE AND CYTOSOLIC CALCIUM IN SINGLE SMOOTH MUSCLE CELLS FOLLOWING ELECTRICAL STIMULATION. S. Yagi, P.L. Becker, and F.S. Fay. Department of Physiology, University of Massachusetts Medical School, Worcester, MA, 01605.

The relationship between force and calcium concentration in smooth muscle cells (SMCs) is key to understanding the role of calcium in the control of smooth muscle contractility. The calcium sensitive dye fura-2 has allowed for the first time the simultaneous measurement of force and calcium in single SMCs. A single SMC was loaded with fura-2, attached to a force transducer, and viewed in a microspectrofluorimeter (MSF). The MSF allowed determination of cell fluorescence at 500 nm (band pass 30 nm) when alternately excited with 340 and 380 nm light (frequency: 250 Hz). The 340/380 fluorescence ratio was converted to calcium concentration by calibration with fura-2 free acid in standard calcium solutions. Cells were stimulated by single 50-100 V, 100 μ sec duration DC electrical pulses via platinum wire electrodes positioned 100 μ m on either side of the cell. Following single stimulus, $[Ca^{++}]$ increased rapidly and peaked within 5 sec. The onset of force development following maximal stimulation lagged behind that of calcium by approximately 200 msec, which suggests that a process subsequent to the change in $[Ca^{++}]$ determines the initiation of contraction. The rate of rise of $[Ca^{++}]$ (dCa/dt), and the peak value attained, could be controlled somewhat by varying the stimulation voltage. Force increased with increasing $[Ca^{++}]$. The rate of rise of force (dF/dt) increased as a function of dCa/dt up to a dCa/dt of around 1000 nM/sec, beyond which dF/dt did not increase further. This is presumably due to the kinetics of the reaction responsible for the delay between force and calcium. Grant support from NIH HL-14523 and the MDA. PLB supported by an NIH fellowship (AM07807).

M-Pos152 CYTOSOLIC CALCIUM TRANSIENTS IN SINGLE SMOOTH MUSCLE CELLS: KINETIC CHARACTERISTICS. P.L. Becker, D.A. Williams and F.S. Fay. Dept. of Physiol., U. Mass. Med. Sch., Worc.

Single smooth muscle cells from the toad stomach were loaded with fura-2 and observed in a microspectrofluorometer which allowed determination of cell $[Ca^{++}]$ at a frequency of up to 250 Hz. Cells were activated either by local K^+ or acetylcholine (ACh) application or by single electrical pulses (100 V, 100 μ sec). Resting cell $[Ca^{++}]$ was found to be 110 ± 33 nM. In response to prolonged stimulation with K^+ or ACh peak $[Ca^{++}]$ did not exceed 800 nM despite the fact that following electrical stimulation a $[Ca^{++}]$ in excess of 1.5 μ M could be achieved. Following electrical stimulation $[Ca^{++}]$ increased rapidly for 100 msec and then often showed a transition to a much slower rate of increase at a $[Ca^{++}]$ that coincided with the ceiling seen in response to K^+ and ACh. We propose that the $[Ca^{++}]$ ceiling may reflect either negative feedback of Ca^{++} on cytoplasmic gating mechanisms or the strong activation of Ca^{++} pumps at this $[Ca^{++}]$. The onset of shortening was determined by observing cell length in video images of the cell. Cells shortened following electrical stimulation with a delay of 186 ± 36 msec. The delay following K^+ application was longer but represented the diffusion and mixing kinetics for K^+ in the cell micro-environment. Two basic types of Ca^{++} transients were observed following K^+ application. Type 1 showed either a slow or no decline from peak $[Ca^{++}]$ (620 ± 55 nM) in the face of continued K^+ application while type 2 showed a more rapid decline and a lower peak $[Ca^{++}]$ (330 ± 20 nM). This behavior could be indicative of heterogeneity in the inactivation rates of the voltage dependent Ca^{++} channels that are activated by K^+ application. Fellowship support: PLB from NIH (AM07807), DAW from AHA (Mass. Affil.) Grant support: NIH HL-14523 and MDA.

M-Pos153 SIMULTANEOUS RECOVERY OF CHARGE MOVEMENT AND Ca RELEASE IN SKELETAL MUSCLE. G. Pizarro, R. Fitts, G. Brum*, M. Rodriguez and E. Rios, Department of Physiology, Rush Medical College, Chicago, IL and *Departamento de Biofisica, Facultad de Medicina, Montevideo.

Intramembrane charge movement is regarded as a necessary step in coupling T-tubule membrane depolarization to Ca release from the sarcoplasmic reticulum. Questions remain regarding its nature, components and mechanism. After prolonged depolarization Ca release disappears (inactivation) and the voltage dependence of charge movement changes so that very little charge moves in the range positive to -70 mV (charge 1) whereas more charge moves in a more negative voltage range (charge 2). (Brum and Rios, J. Physiol., in press). Upon repolarization charge 1 and release reappear ("repriming"). We measured the time course of repriming of charge 1, repriming of Ca release and disappearance of charge 2 in voltage clamped cut skeletal fibers that contained Antipyrilazo III. The time course of these changes was fit by single exponential functions. In 8 fibers at 8 to 12°C the mean time constant (τ) for reappearance of charge 1 was 47.4 s (s.e.m. = 11.7 s.). τ for reappearance of release was 41.1 s (9.43). τ for disappearance of charge 2 was 32.26 s (15.1). The extracellular $[Ca^{2+}]$ had an effect on the extent but not the rate of recovery. These parallel changes in Ca release and charge movement are consistent with the concept that charge 1 is caused by transitions of a voltage sensor that controls Ca release. Opposite changes in charges 1 and 2 are consistent with charge 2 being caused by transitions between inactivated states of the voltage sensor. Supported by NIH grants AR 32808 and AR 07575.

M-Pos154 THE POSITIVE AND NEGATIVE INOTROPIC ACTIONS OF ADRENERGIC AND CHOLINERGIC AGENTS IN THE FROG HEART. Fouad Yousif, Lars Cleemann and Martin Morad. University of Pennsylvania, Philadelphia, PA 19104.

Epinephrine, which normally potentiates the twitch force, has a negative inotropic effect when 1-2 mM Ni^{2+} is added to block the Ca^{2+} current and prolong the action potential. Carbachol, a cholinergic agent, was found to have the opposite effect, i.e. it reduced the twitch in normal Ringer's solution but potentiated the twitch in the presence of Ni^{2+} . KCl-contractures and tension-voltage relations were measured to explore the extent of this reciprocity. A phasic component of tension evoked by action potentials and brief voltage clamp depolarizations was enhanced by epinephrine and reduced by carbachol. The tonic component of force development observed with long voltage clamp depolarizations, KCl-contractures and Ni^{2+} action potentials was suppressed by epinephrine. Dibutyryl cAMP had only positive inotropic effects, whereas sodium nitroprusside, which is known to increase cellular cGMP levels, had only negative inotropic effects. These observations are consistent with the notion that the phasic component of force development is mediated by a cAMP/cGMP sensitive Ca^{2+} current. Carbachol had no effect on the KCl-contracture or the tension voltage relation in normal Ringer's solution and had a positive inotropic effect in the presence of Ni^{2+} only when the plateau of the action potential was not blocked by TTX. Experiments with single isolated voltage clamped cells showed that Ni^{2+} shifts the excitatory Na^+ current to a range of potentials where it may support the plateau of the action potential. Carbachol was found to increase the conductance of the inward rectifying K^+ channel. It is possible therefore that the positive inotropic action of carbachol is related to Na^+ loading brought about by simultaneous increases in the Na^+ and K^+ conductances caused by Ni^{2+} and carbachol respectively.

M-Pos155 EFFECTS OF IONIC BACKGROUND ON EGTA STABILITY CONSTANTS. Milton L. Pressler¹ and Paul W. Schindler² Krannert Institute of Cardiology¹, Indiana University School of Medicine, Indianapolis, IN and Department of Chemistry², University of Berne, Berne, Switzerland

Accuracy in measuring intracellular free Ca^{2+} concentration depends upon the precision of Ca^{2+} -buffered solutions. We used a potentiometric technique to determine stoichiometric stability constants for the binding of the 3rd and 4th protons ($\text{K}_{a3}, \text{K}_{a4}$), Ca^{2+} (K_{Ca}) and Mg^{2+} ($\text{K}_{\text{Mg}}, \text{K}_{\text{MgH}}$) to 2 mM EGTA at $25.0 \pm 0.1^\circ\text{C}$. Background solutions were altered in KCl and NaCl content to test for salt effects on cation affinity. Ionic strength (I) varied from 0.060-0.500 M. Glass electrodes were calibrated for $[\text{H}^+]$ in unbuffered solutions; EGTA purity was $\geq 99.5\%$; titration curves were fitted by non-linear regression. Mean results for I = 0.1, 0.175 & 0.5 M KCl or NaCl were:

I (M)	Salt	$-\log K_{a3}$	$-\log K_{a4}$	$\log K_{\text{Ca}}$	$\log K_{\text{Mg}}$	$\log K_{\text{MgH}}$
0.100	KCl	8.917	9.347	10.802	5.288	3.532
0.175		8.795	9.224	10.535	5.007	3.316
0.500		8.642	9.068	10.103	4.559	2.964
0.100	NaCl	8.790	9.132	10.461	-	-
0.175		8.661	9.026	10.141	-	-
0.500		8.439	8.765	9.577	-	-

As shown, the affinity of EGTA for H^+ , Ca^{2+} , and Mg^{2+} decreased with increasing ionic strength. However, Na^+ affected cationic binding more than K^+ . Calculation of free $[\text{Ca}^{2+}]$ at submicromolar levels should include these salt effects. (Supported by grants from the NHLBI and IN Heart Assn)

M-Pos156 THE MEASUREMENT OF K'_{Ca} OF EGTA, BAPTA, AND DI-BROMO-BAPTA AT A RANGE OF IONIC STRENGTHS AND TEMPERATURES. Simon M. Harrison and Donald M. Bers. Division of Biomedical Sciences, University of California, Riverside, CA 92521, U.S.A.

The calcium buffering ability of the organic ligands EGTA, BAPTA and Di-Br-BAPTA is modified by temperature, ionic strength and pH. This study evaluates the influence of temperature (1-36°C) and ionic strength (0.1-0.3M) on the apparent association constant of the above ligands for calcium (K'_{Ca}). Solutions contained 25mM HEPES, 1mM ligand, KCl (95-295mM) to make up the desired ionic strength and titrated to pH 7.00. A calcium sensitive macroelectrode was used to measure $[\text{Ca}^{2+}]$ and then K'_{Ca} and ligand purity were calculated from Scatchard plots. An increase in temperature from 1 to 36°C led to a nearly linear increase in K'_{Ca} of EGTA from 1.22 to $2.93 \times 10^4 \text{ M}^{-1}$. An Arrhenius plot of these data yields a straight line, the slope of which equals $-\Delta H/2.3R$. This plot generated a value of ΔH for K'_{Ca} of EGTA of 14.2 KJ/mol. Similarly, the K'_{Ca} of BAPTA increased from 2.34 to $4.65 \times 10^4 \text{ M}^{-1}$ ($\Delta H = 13.9 \text{ KJ/mol}$) and K'_{Ca} for Di-Br-BAPTA increased from 2.48 to $5.62 \times 10^4 \text{ M}^{-1}$ ($\Delta H = 16.7 \text{ KJ/mol}$) over the same temperature range (1-36°C). The purity of the three ligands was found to be 96.2% for EGTA (Sigma) 79% for BAPTA (Mol. Probes) and 97% for Di-Br-BAPTA (Mol. Probes), the impurity in BAPTA found to be water. Increasing ionic strength from 0.1 to 0.3M at 22°C led to a decrease in the K'_{Ca} of BAPTA from 5.99 to $1.70 \times 10^4 \text{ M}^{-1}$. Similar results were obtained with Di-Br-BAPTA. Experimental results were compared to theoretical predictions of K'_{Ca} for each ligand, calculated from the individual association constants corrected for the test conditions using the Debye Huckel limiting law and Van't Hoff isochore for ionic strength and temperature respectively. The experimental values of K'_{Ca} for EGTA agree well with those in the literature and with the theoretically derived values. The characterization of these new calcium buffers will enable them to be used accurately under a wide range of physiological conditions.

M-Pos157 TETRACAINE RELEASES Ca^{2+} FROM THE SARCOPLASMIC RETICULUM (SR) OF AMPHIBIAN AND MAMMALIAN SKINNED SKELETAL FIBERS. G. Pike, J. Abramson† and G. Salama* (Intr. by Jim Collins)

*Department of Physiology, University of Pittsburgh, School of Medicine, Pittsburgh, PA 15261 and †Department of Physics, Portland State University, Portland, OR 97207.

Local anesthetics such as tetracaine and procaine have previously been found to either block, induce, or potentiate Ca^{2+} release from the SR of intact fibers, skinned fibers or vesicles, depending upon experimental conditions or design. Furthermore, tetracaine has been found to abolish the Q γ component of charge movement in frog skeletal fibers as well as the optical signal arising from a postulated SR membrane potential change using voltage sensitive dyes. Tetracaine and procaine are now shown to elicit Ca^{2+} release from the SR of skinned fibers of both frog and rabbit. Following Ca^{2+} loading of the SR, tetracaine (1mM) produces a tonic contraction with a time to half-peak tension of 15-20s and a magnitude about 80% of control Ca^{2+} contractures. Ca^{2+} release by tetracaine is dependent on Ca^{2+} concentration, being inhibited as free Ca^{2+} is lowered. With Ca^{2+} -loaded SR and low external free $[\text{Ca}^{2+}]$, procaine (10mM) and tetracaine (1mM) produce little Ca^{2+} release and inhibit slightly Ca^{2+} -release induced by caffeine (2mM). At high external free $[\text{Ca}^{2+}]$, tetracaine induces Ca^{2+} release from the SR which could not be blocked by Ruthenium Red (25 μ M). The results suggest that tetracaine acts via an alternative site different from that in Ca^{2+} -induced and caffeine-induced Ca^{2+} release. In addition, the actions of tetracaine could not be attributed to displacement of Ca^{2+} bound to membrane or other sites, because fibers lacking functional SR due to treatment with Quercetin (100 μ M) or Triton X-100 (0.5%) did not contract after additions of tetracaine. These results suggest that the actions of these local anaesthetics cannot be merely interpreted in terms of blocking SR Ca^{2+} release, but are considerably more complex.

Supported by Western PA AHA, NIH NS 18590 and RCDA to G.S., a MDA postdoctoral fellowship to G.P., and a AHA Alaska affiliate to J.A., who is also an established investigator of the AHA.

M-Pos158 EFFECT OF MAGNESIUM ON $[\text{Ca}^{2+}]_i$ IN MALIGNANT HYPERTHERMIA SUSCEPTIBLE SWINES. J.R. López (a), V. Sánchez(a), M. Mendoza (a), Allen, P., Ryan J., F. Sreter (b). (a) IVIC, Apartado 21827, Caracas, Venezuela; (b) BBRI, Boston, MA 02114, USA.

It is now well established that the pathophysiology of the MH syndrome is related to a malfunction of the intracellular calcium homeostasis. Magnesium plays important roles in the basic contractile properties of muscle and many of its actions are antagonistic to that of calcium. The aim of this study was to determine the effectiveness of Magnesium sulphate to prevent the MH episode in susceptible animals, and correlate its effects with the $[\text{Ca}^{2+}]_i$. The experiments were carried out in 4 MH susceptible crossbred swines (Poland China x Pietran)¹. Magnesium sulphate was used at a dose of 100 mg/kg (IV). The resting intracellular free $[\text{Ca}^{2+}]$ determined by means of Ca^{2+} selective microelectrodes (Biophys. J., 43:1-4, 1983). was $0.19 \pm 0.01 \mu\text{M}$ ($m \pm$, $n=16$) which was not modified by treatment with MgSO_4 ($0.20 \pm 0.01 \mu\text{M}$ ($M \pm \text{SEM}$, $N=16$)). The exposure to halothane (1.5%) triggered the episode, which was associated with an increment in $[\text{Ca}^{2+}]_i$ lesser than the observed in those animals without any pretreatment with MgSO_4 . The intravenous administration of dantrolene sodium (0.25 mg/kg) provoked a reversion of the clinical manifestations associated with the MH episode and also a reduction of $[\text{Ca}^{2+}]_i$ to $0.13 \pm 0.06 \mu\text{M}$ ($M \pm \text{SEM}$, $n=4$). These results indicate that MgSO_4 was not able to prevent the MH episode. However, it was able to reduce the increment in $[\text{Ca}^{2+}]_i$ associate with the clinical manifestation of the syndrome. This effect might be related to the ability of Mg^{2+} to modify the release of calcium from the sarcoplasmic reticulum. (Supported by MDA).

M-Pos159 VERAPAMIL IS NOT ABLE TO PREVENT OR REVERSE THE SYNDROME OF MALIGNANT HYPERTHERMIA.

López, J.R.¹, Mendoza, M.¹, Sánchez, V.² & Sreter F.¹ ¹Centro de Biofísica y Bioquímica, IVIC, Apartado 21827-Caracas 1020-A., ²Boston Biomedical Research Institute, Boston, MA 02114.

Malignant hyperthermia (MH) is a genetic syndrome whose pathophysiology has been associated to abnormal Ca^{2+} homeostasis in skeletal muscle (López et al., Muscle and Nerve 1985). We have used verapamil, a Ca^{2+} channel blocker, in MH susceptible swine (Pietrian) to study its effect on the $[\text{Ca}^{2+}]_i$ and correlate it with the effectiveness of this agent in preventing and reverting the MH syndrome. The Ca^{2+} selective microelectrodes were prepared and calibrated as described previously (López et al., Biophys. J., 1983). We used only those microelectrodes that showed a Nernstian response between pCa 3 and 7 (30.5 mV per decade at 37°C). The administration of verapamil (0.15 mg/Kg) did not induce a significant change either in the $[\text{Ca}^{2+}]_i$ or in the resting membrane potential. Thus, the mean value for the $[\text{Ca}^{2+}]_i$ was $0.48 \pm \mu\text{M}$ ($M \pm \text{SEM}$) before and $0.46 \pm 0.02 \mu\text{M}$ ($M \pm \text{SEM}$) after the verapamil treatment. Verapamil administered during the hyperthermic episode induced by halothane (2%) did not modify either the high level of $[\text{Ca}^{2+}]_i$ or the clinical manifestations of the syndrome. The administration of dantrolene (2.5 mg/kg) produced a complete reversal of the muscle contracture as well as significant reduction in the $[\text{Ca}^{2+}]_i$. These results support the hypothesis that the Ca^{2+} involved in the muscle contracture during the episode is released from intracellular stores and is not related to an increase in Ca^{2+} influx from extracellular space. Supported by Muscular Dystrophy Association, CONICIT S1-1277 and NIH, Center Grant GM 15904-19.

M-Pos160 DANTROLENE REDUCES THE $[Ca^{2+}]_i$ INCREASE IN STRETCHED SKELETAL MUSCLE FIBERS. Alamo L., López, J.R., Caputo, C. CBB, IVIC, Apartado 21827, Caracas 1020-A, Venezuela. We have previously reported that when a muscle fiber is stretched from 2.1 μ m to 3.0 μ m, $[Ca^{2+}]_i$ increases by about threefold. We have conducted further studies to characterize the possible origin of the Ca involved in this phenomenon. Experiments were carried out in small bundles of stretched semitendinosus muscles from *Rana pipiens*. The intracellular free $[Ca^{2+}]_i$ was measured by means of Ca selective microelectrodes which were prepared and calibrated as described previously (López et al., *Biophys. J.* 43:1-4, 1983). Sarcomere length was determined by laser diffraction technique. We consistently found that stretching the muscle fibers induced an increase in $[Ca^{2+}]_i$, from $0.12 \pm 0.01 \mu$ M (n=32) to $0.38 \pm 0.09 \mu$ M (n=47). Addition of the Ca channel blocker Nifedipine (50 μ M) after muscle fibers have been stretched did not block the effect of enhancement of $[Ca^{2+}]_i$ ($0.35 \pm 0.07 \mu$ M, n=5). On the other hand dantrolene (50 μ M) was able to revert the increase in intracellular $[Ca^{2+}]_i$ to $0.17 \pm 0.04 \mu$ M (n=8) observed with stretching. These results suggest that the Ca involved in this phenomenon seems to be released by the sarcoplasmic reticulum. (Supported by CONICIT S1-1277, S1-1148 and Muscular Dystrophy Association).

M-Pos161 RECORDING OF LOCAL CALCIUM TRANSIENTS IN SINGLE MUSCLE FIBERS FROM THE BARNACLE, *BALANUS NUBILUS*. E. B. Ridgway and A. M. Gordon. Department of Physiology, Medical College of Virginia, Richmond, VA 23298; and Department of Physiology and Biophysics, University of Washington, Seattle, WA 98195.

We have used image-intensification and video image-enhancement techniques to record local (100 μ X 100 μ) calcium transients from various regions of aequorin-C injected barnacle muscle fibers. These techniques complement the usual technique of recording global calcium transients (with a photomultiplier) and we therefore combined measurements of the global and the local calcium transients in the same fiber to obtain a more complete picture of the barnacle preparation. Cross-sectional profiles of the intensity of the light emission at the peak of the calcium transient show that the aequorin is uniformly distributed to the edge of the fiber. The longitudinal profile shows little spread of the aequorin beyond the injected region, except for slight leakage along the injector track. Several fibers showed well defined hot spots probably due to damage caused by the internal electrode. Such hot spots usually disappear with time, but it is important to detect them because they contribute to the resting glow of the fiber interfering with quantitative measurements. The threshold for detection of the local calcium transient is much higher than that for the global calcium transient owing to the smaller fiber volume. The wave forms of local calcium transients from various regions of the fiber are essentially similar to each other and to the global calcium transient leading us to conclude that the fibers are uniformly activated under these conditions. Supported by NIH grants AM-35597 and NS-08384 and the American Heart Association Virginia Affiliate.

M-Pos162 MYOFILAMENT SPACE CALCIUM CONCENTRATION AFFECTS THE CALCIUM RELEASE RATE FROM THE SARCOPLASMIC RETICULUM OF SKINNED, SKELETAL MUSCLE FIBERS OF THE FROG. Wai-Meng Kwok and Philip M. Best, Department of Physiology and Biophysics, University of Illinois, Urbana, 61801. The effect of myofilament calcium concentration on the rate of calcium release from the sarcoplasmic reticulum (SR) of skinned, skeletal muscle fibers was determined. Fibers were mechanically skinned (sarcolemma removed) and preincubated in a solution containing elevated calcium ion concentration before calcium release from the SR was induced by 7.5 mM caffeine. The release rate was calculated from the rate of change in absorbance of a calcium sensitive dye, antipyrilazo III (0.5 mM). Solutions contained 2 mM MgATP, 15 mM creatine phosphate, 1 mM Mg, 100 mM monovalent cation, and approximately 35 mM MOPS buffer (pH=7 at 10°C), $I=0.15$. A standard procedure was used to load the SR with calcium before each release was stimulated. Three successive releases (control, test, control) were obtained from each fiber. The rate of calcium release during the test was compared with the average of the control releases. Release rates obtained from fibers exposed to solutions with pCa=8 were used as controls. Test releases were obtained from fibers exposed to solutions containing either pCa=6, 6.5 or 7. The calcium release rate decreased to approximately $83.6 \pm 2.1\%$ (\pm SEM, n=27) of its control level when the myofilament calcium concentration was pCa=6 and to approximately $75.7 \pm 2.7\%$ (n=14) when it was pCa=6.5. No significant differences were observed at pCa=7 (n=10). Control experiments ruled out any significant effect of the calcium concentration in the prerelease solutions on SR calcium loading. Therefore these results suggest a calcium dependent inactivation of the SR calcium channel in skeletal muscle fibers. Supported by AR32062 and the M.D.A.

- M-Pos163** EFFECT OF La^{+++} AND TETRACAINE ON CHARGE MOVEMENT INACTIVATION IN SKELETAL MUSCLE FIBERS. C. Caputo and Pura Bolaños, Centro de Biofísica y Bioquímica, IVIC, Apartado 21827, Caracas, 1020A.

We have measured intramembrane charge movement in cut skeletal muscle fibers from *L. insularis* and *R. pipiens* using the triple vaseline gap voltage clamp technique, and the WAD-UCLA system for data acquisition and analysis. The internal solution contained Cs or K Aspartate and 10 mM EGTA, while the external medium contained $(\text{TEA})_2\text{SO}_4$, Rb_2SO_4 , CaSO_4 , and MgSO_4 . TTX was added to block sodium currents. Temperature was 8-10°C. When $[\text{Ca}]$ was low, a large inward current was observed which disappeared when $[\text{Ca}]$ was raised to 1 or 2 mM. Tetracaine 0.5 or 1 mM enhanced this current, and higher $[\text{Ca}]$ had to be used to abolish it. Usually the charge movement signal contained a fast transient component, which disappeared with conditioning depolarizing prepulses. This component possibly associated with Na gating current, amounted to 10-15% of total charge measured. Tetracaine and Lanthanum both, at 0.5-1 mM, did not substantially affect the charge-membrane potential relationship but changed the time course of the intramembrane current. However, La decreased sodium currents and shifted the INa activation and inactivation curves by about +25 mV. When the fibers were depolarized at different M.P. values for 2 minutes total charge was diminished in a potential dependent way. At -20 mV charge was diminished to 30% and 10% in the absence and presence of 0.5 mM tetracaine respectively. Reduction was to 25% and 45% in the absence and presence of 0.5 mM La. Thus tetracaine shifted the steady state inactivation curve of charge movement by about -20 mV, while La had the opposite effect. Supported by MDA and CONICIT S1-1148.

- M-Pos164** RECTIFICATION IS A PROPERTY OF THE OPEN CHANNEL IN THE INWARD RECTIFIER POTASSIUM CHANNEL OF RAT SKELETAL MUSCLE TRANSVERSE TUBULES. Jeffrey S. Smith and Roberto Coronado. (Intr. by Michael Hines) Department of Physiology and Molecular Biophysics, Baylor College of Medicine, Houston, TX 77030

Inwardly rectifying K channels were recorded in planar bilayers using a new membrane preparation in which rat muscle transverse tubules are purified from intact triads dissociated in high salt. The shape of the open channel vs. voltage curve coincides strikingly well with the macroscopic current vs. voltage curve in frog muscle and the theoretical fit of Standen and Stanfield, 1978. Open channels have a slope conductance that (i) is positive at voltages more negative than E_K (80ps in 250 mM Ki/50 mM K^+); (ii) is zero at voltages moderately above E_K ; and (iii) is negative at voltages >50 mV positive to E_K . This rectification of the open channel is observed in buffers containing KCl as the only salt, thus the possibility of channel blockade by a diffusible ion other than K (Cl is impermeant) is ruled out. Single channel currents were blocked by external Cs and Ba and internal Mg. Cs blockade was steeply voltage-dependent and produced a lowering of single channel amplitudes. At -120 mV ($E_K = -53$ mV), 50% block was elicited by 0.4 mM Cs. External Ba in the range of 0.05-0.1 mM shortened the duration of open events. At -70 mV ($E_K = -44$ mV), channel lifetime was reduced from 10 ms (0 Ba) to 4 ms (0.1 mM Ba). Internal Mg partially blocked outward currents by reducing single channel amplitudes. At 0 mV ($E_K = -35$ mV), 50% block was elicited by 10 mM Mg. This finding suggests that blockade by internal Mg may enhance inward rectification in the intact cell. Supported by MDA postdoctoral fellowship and NIH grants GM 36852 and HL 37044.

- M-Pos165** CALCIUM RELEASE CHANNEL OF RAT SARCOPLASMIC RETICULUM: ACTIVATION BY CAFFEINE AND CURRENT-DEPENDENT ACTIVATION BY CALCIUM. Jeffrey S. Smith and Roberto Coronado.

Department of Physiology and Molecular Biophysics, Baylor College of Medicine, Houston, TX 77030

Similar to calcium channels previously studied in rabbit SR (Smith et al., 1985. *Nature* 316,446), we find high conductance calcium channels in rat skeletal muscle SR which are activated by micromolar Ca and/or millimolar ATP. In rat, pretreatment of channels with 10 mM caffeine induced a new state unresponsive to activation by nucleotide (10 mM ATP) in low free Ca (<10 nM). Subsequent raising of free Ca to approximately 100 nM partially activated the ATP-insensitive channel. Thus apparently, caffeine abolishes the nucleotide-dependent but not the Ca-dependent activation. At high free Ca (2 μM), 3-10 mM caffeine activates the channel only in cases where several channels are recorded simultaneously, i.e., when open probability (p_o) is high, but not in single channel recordings when $p_o < 0.01$. Thus, (i) activation by caffeine may require a partially open channel, or (ii) it is cooperative and requires several channels. When Ca, but not Ba, is used as current carrier kinetic analysis of single channels demonstrates a negative correlation between the duration of an open event and the duration of the closed event that immediately follows. For openings <2 ms, following closed times have a mean of about 100 ms. For openings >50 ms, following closed times last 20 ms. Thus, the rate at which channels reopen increases if channels are previously open for a long time. This facilitation of channel opening by Ca current may be a mechanism which in-vivo sustains high rates of Ca release. Supported by MDA postdoctoral fellowship and by NIH grants GM 36852 and HL 37044.

M-Pos166 DIHYDROPYRIDINE AND D-600 INDUCED PARALYSIS OF CONTRACTURES IN SKINNED MUSCLE FIBERS: TEMPERATURE AND CONCENTRATION DEPENDENCY OF BLOCK, Michael Fill and Philip M. Best, Department of Physiology and UICOM, University of Illinois, Urbana, IL 61801.

Calcium channel antagonists cause paralysis of skinned fibers stimulated by ionic substitution. The effects of two Ca^{++} channel blockers, D-600 and nitrendipine (Nitr) were explored. Fibers from the semitendinosus of *Rana pipiens* were stimulated by replacing K propionate for choline chloride ($\text{K} \times \text{Cl}$ product constant) in the bathing solution. Solutions contained in mM; 125 monovalent cation, 2 MgATP, 1 Mg, 5 CP, .5 EGTA ($\text{pCa}=7.3$), and approximately 30 MOPS buffer ($\text{pH}=7$) to make $\text{I}=-.15$. The character of Nitr paralysis was temperature dependent. At 10°C , Nitr paralysis resembles that of D-600 in that inactivated fibers are more susceptible to drug induced paralysis. In contrast, at 22°C Nitr paralyzed inactivated and reprimed fibers equally well. A simple 1:1 binding scheme was used to fit the concentration-response relationship for Nitr at 22°C , but could not account for that of D-600 or Nitr at 10°C . These data were fit using a two state (inactivated and reprimed) concerted scheme. It predicts that the inactivated state has much greater affinity for drug. To test this reprimed fibers were paralyzed with nisoldipine before being exposed to an intense light flash which was assumed to photodynamically destroy the drug's action. After this treatment fibers were found to be inactivated demonstrating that the dihydropyridines paralyze fibers by locking them into the inactivated configuration. Furthermore, both 202-791(+) (an agonist) and 202-791(-) (an antagonist) paralyzed reprimed fibers suggesting that the blockade of calcium channel conductance is not important for the paralytic action of the dihydropyridines. Supported by NIH AM32062, MDA and PHS training grant 5-P32GM07283.

M-Pos167 SULFHYDRYL REAGENTS TRIGGER RAPID Ca^{2+} RELEASE FROM THE SARCOPLASMIC RETICULUM (SR) OF SKINNED SKELETAL FIBERS. G. Pike, J. Abramson† and G. Salama*

*Department of Physiology, University of Pittsburgh, School of Medicine, Pittsburgh, PA 15261 and †Department of Physics, Portland State University, Portland, OR 97207.

Heavy metals have previously been shown to induce Ca^{2+} release from heavy sarcoplasmic reticulum (SR) vesicles by binding to a critical sulfhydryl group of an SR protein. Mercaptans such as cysteine also release Ca^{2+} when applied in the presence of Cu^{2+} , which catalyzes the oxidation by cysteine of sulfhydryl groups on the SR. The nature of Ca^{2+} release induced by various sulfhydryl reagents has been further investigated by monitoring isometric tension in chemically skinned rabbit psoas fibers. The addition of a heavy metal (5-50 μM) triggered Ca^{2+} release from the SR leading to a phasic contraction. The metals have the following order of potency: $\text{Cu}^{2+} > \text{Hg}^{2+} > \text{Cd}^{2+} > \text{Ag}^+ > \text{Ni}^{2+}$. Higher concentrations of these metals ($>50\mu\text{M}$) lead to elevated levels of tonic tension due to a maintained higher Ca^{2+} permeability of the SR. The release of Ca^{2+} caused by heavy metals bears a resemblance to Ca^{2+} -induced Ca^{2+} release (CICR) and Cl-induced release; for example, Ca^{2+} release induced by Cu^{2+} is dependent on free Ca^{2+} concentration and is blocked by 25 μM Ruthenium Red (RR).

In the presence of Hg^{2+} or Cu^{2+} , additions of cysteine (5-25 μM) elicited rapid contractions, Ca^{2+} release being dependent upon free Mg^{2+} concentration and blocked by 25 μM RR or 5 mM glutathione (GSH). On the other hand, oxidized glutathione (GSSG) did not block Ca^{2+} release by cysteine. In the presence of 5 μM Hg^{2+} , the addition of low concentrations (10 μM) of cysteine produced a small tonic tension, whereas subsequent addition of cysteine (100 μM) caused further Ca^{2+} release followed by a rapid relaxation, back to baseline tension. This rapid reduction of SR Ca^{2+} permeability by high [cysteine] suggests that a second sulfhydryl group with lower reactivity may participate in Ca^{2+} channel closure. In some fibers (10%), the addition of cysteine (5-50 μM) alone produced rapid twitches without the prior addition of Hg^{2+} or Cu^{2+} .

Supported by Western PA AHA, NIH NS 18590 and RCDA to G.S., a MDA postdoctoral fellowship to G.P., and a AHA Alaska affiliate to J.A. who is also an established investigator of the AHA.

M-Pos168 PATCH CLAMP OF SARCOPLASMIC RETICULUM WITHIN MUSCLE FIBERS. J.M. Tang, J. Wang and R.S. Eisenberg, Department of Physiology, Rush Medical College, Chicago, IL 60612.

Ionic channels in the sarcoplasmic reticulum (SR) of the second antenna remotor muscle of *Homarus americanus* were studied using the patch clamp technique. A single muscle fiber is skinned in relaxing Ringer (high K^+ , low Ca^{++} with EGTA and ATP), leaving the SR exposed for patching. Transmission and scanning electron microscopy confirm the large volume fraction of SR and absence of sarcolemma in this unusual skinned preparation. Some 10% of patches contain a K^+ -selective channel with a mean open time of seconds and at least one subconductance state. The open probability is weakly voltage dependent, large at zero and positive potentials (cytoplasm minus SR lumen), decreasing at negative potentials. The open channel conductance $\gamma(\text{K}) \approx 200$ pS in symmetrical 470 mM K^+ solution and the current-voltage relation of the open channel is linear over a range of ± 100 mV. The lobster SR K^+ channel is similar to, but distinct from, that of vertebrates: it is blocked (in a voltage-dependent manner) by hexamethonium from the cytoplasmic side but not from the SR lumen side. It has higher selectivity: $\text{P}(\text{K})/\text{P}(\text{Na}) \approx 8$, determined from reversal potential measurements, while $\gamma(\text{K})/\gamma(\text{Na}) \approx 14$, determined from open channel conductance measurements in symmetrical 470 mM solutions.

The patch clamp technique evidently can be used to study internal membranes of suitable cells.

M-Pos169 Na/Ca EXCHANGE AND EXCITATION-CONTRACTION COUPLING IN FROG STRIATED MUSCLE. Brian A. Curtis, University of Illinois College of Medicine at Peoria, Peoria, IL 61656.

Dichlorobenzamil (10 μ M) (Merck), a Na/Ca exchange blocker, slows the rate of rise of contracture tension; in 190 mM K Me SO₃ the ratio of rates of rise, drug/control was 0.41 in bundles of 4-6 fast fibers. To confirm that this effect was upon a Na/Ca exchanger, contractures were induced in 95 mM K Me SO₃ and either 95 mM Na ($\Delta=103$ mV, Ca in) or 90 mM TRIS, 5 mM Na ($\Delta=327$ mV, Ca in). The paired ratio of rates of rise in TRIS/Na was 1.61, clearly the rate of rise is greater when the net inward force on Ca increases, in this case by creating an outward force on Na. Increasing internal Na by inhibiting Na/K ATPase with 10 μ M ouabain should also increase the net inward force on Ca in a 95 mM K Me SO₃ contracture ($\Delta=-140$ mV, Ca in). After one hour in 10 μ M ouabain, the ratio of rates of rise, ouabain/control was 1.45. After an overnight soak in ouabain, the rate of rise of tension was rapid and slowed after 1 hr in Ringer at 12°C, the ratio of rates of rise, ouabain/recovery was 1.84. I conclude that the Na gradient is an important factor in determining the rate of tension rise and may have its influence on a 3Na/Ca exchanger in the t wall which rotates once upon depolarization, presenting Ca to the t-SR junction to initiate contraction via Ca induced Ca release. The single rotation of a fixed number of 3Na/Ca exchanger sites could generate a rapidly decaying electrical signal very similar to the observed "charge movement" signal.

M-Pos170 CALCIUM REGULATION OF PHOSPHATIDYLINOSITOL PHOSPHORYLATION IN TRANSVERSE TUBULE MEMBRANES FROM FROG SKELETAL MUSCLE. M. Angélica Carrasco, Karin Magendzo, Cecilia Hidalgo^a and Enrique Jaimovich. Depto. Fisiol. Biofis., Fac. Med. U. de Chile and C.E.C.S.^a, Santiago, Chile, Muscle Dept., Boston Biomed. Res. Inst. and Dept. Neurol., Harvard Med. Sch., Boston, MA, U.S.A.

Highly purified transverse tubule (T-T) membranes isolated from frog skeletal muscle phosphorylate phosphatidylinositol (PI) to phosphatidylinositol 4-monophosphate (PIP) and phosphatidylinositol 4,5-bisphosphate (PIP₂). The two phosphorylation reactions have different calcium requirements. Phosphorylation of PI to PIP, which takes place both in isolated T-T and sarcoplasmic reticulum membranes, is independent of calcium in a range of concentrations from 10⁻⁹M to 10⁻⁶M, and is progressively inhibited to 10% of the maximal values by increasing the calcium to 10⁻⁴M or higher ($K_{0.5} \sim 5 \times 10^{-6}$ M). In contrast, phosphorylation of PIP to PIP₂, a reaction exclusively present in T-T membranes, is maximal at calcium concentrations higher than 2×10^{-6} M and decreases to 30% of maximal values at calcium concentrations of 2×10^{-7} M or lower ($K_{0.5} \sim 10^{-6}$ M). The effect of varying calcium concentrations on the hydrolysis of PIP₂ to inositoltrisphosphate (IP₃) is currently under investigation. IP₃ has been proposed recently as a chemical messenger in E-C coupling (Vergara et al PNAS 82, 6352, 1985). Calcium regulation of the synthesis of PIP₂, the membrane-bound precursor of IP₃, might have physiological implications regarding modulation of E-C coupling by intracellular calcium levels.

Supported by NIH grants GM 35981 and HL 23007, by NDA, DIB grants 2149 and 2123, and by the Finker Foundation, Inc.

M-Pos171 EFFECT OF ORGANIC CALCIUM BLOCKERS ON Ca²⁺ UPTAKE BY AND RELEASE FROM THE SR OF FROG PHASIC MUSCLE CELLS. *Ortega, A., Gonzalez-Serratos, H. and Rogers, T. *Department of Biochemistry School of Medicine, National University of Mexico, and Departments of Biophysics and Biochemistry School of Medicine, University of Maryland, Baltimore, Maryland, 21201.

It has been reported previously that the Ca-blockers diltiazem and verapamil used in concentrations that block the slow inward calcium currents (I_{Ca}) in frog skeletal twitch muscle fibers do not affect the contractility of these types of muscle cells. Diltiazem potentiates twitch tension and none of them affect K-contractions (J. Gen. Physiol. 84:34a, 1984).

In the present study, we have investigated the effects of diltiazem (DI), verapamil (VP+), carboxy verapamil (CVP-) and its quarternary ammonium derivative (ACVP+) on the calcium uptake by and release from the SR. The experiments were done in split open single muscle cells isolated from the semitendinosus muscle of the frog rana temporaria. The release of calcium was assessed as the force produced due to either caffeine or high Cl⁻ exposure following an adequate period of Ca²⁺ load. The results can be summarized as follows: Calcium uptake by the SR was strongly inhibited by diltiazem in concentrations similar to the ones that block I_{Ca} and potentiates twitches. In contrast VP, CVP and ACVP did not affect the Ca uptake substantially. However, VP, CVP and ACVP decreased release of Ca²⁺ from SR when this release was induced by either caffeine or high Cl⁻ concentration. Further, preliminary data demonstrate that diltiazem and CVP decrease the passive efflux of Ca²⁺ from the SR. Taken together, these suggest that the potentiating effect of diltiazem on the twitch tension can be due to an inhibition of Ca²⁺ uptake by the SR and the decrease of its passive Ca²⁺ efflux. Supported by NIH Grant R01-NS17048.

M-Pos172 **LENGTH DEPENDENT CHANGES IN SENSITIVITY AND SLOPE OF FORCE-CALCIUM RELATIONS IN SKELETAL FIBERS: EFFECTS OF MYOFILAMENT LATTICE SPACING, PH AND IONIC STRENGTH.** D.A. Martyn and A.M. Gordon. Center for Bioengineering and Dept. of Physiology and Biophysics, University of Washington, Seattle, Washington, 98195.

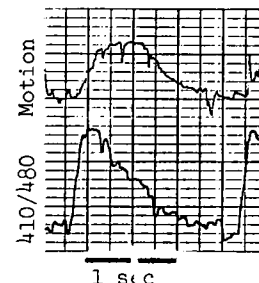
Calcium sensitivity of force was measured in glycerinated rabbit psoas fibers at sarcomere lengths (SL) from 2.3 to 3.4 μm . Increasing SL caused calcium sensitivity to increase and the slope of the F-Ca relation to decrease. We have hypothesized that length dependent changes in myofilament lattice spacing and the presence of fixed charge on the myofilaments are important in determining calcium sensitivity. Lattice spacing changes were monitored by measuring fiber diameter (D). D was altered by changing SL (increasing SL caused D to decrease), bathing solution pH (changing pH over a range from 7.5 to 5 caused D to decrease at all SL) and by osmotic compression with 3% PVP in the bathing solutions. 3% PVP caused D to decrease 20-25% at all SL's and pH's. Force-Ca relations were measured at different SL's and pH's, with and without PVP in the bathing solutions. It was found that the relative value of D at SL 2.3 μm with 3% PVP was comparable to the value at 3.4 μm without PVP. The Ca sensitivity was the same at both SL, although the slope of the force-Ca relation was less at the longer SL. The similarity of the calcium sensitivity at the same D but much different SL, indicates that lattice spacing is important in determining calcium sensitivity, while SL and the degree of myofilament overlap are important in determining the slope of F-Ca relations. In order to test for the role of myofilament charge in determining Ca sensitivity, bathing solution pH and ionic strength ($\Gamma/2$) were varied. Decreasing pH causes decreased maximal force and a decrease in calcium sensitivity. In addition the influence of SL on calcium sensitivity decreased as pH was lowered with no SL dependence at pH 5.5, even though lattice spacing decreased with increased SL. When D was decreased with PVP calcium sensitivity increased at all SL's in pH 7.5 and 7.0, while the same lattice spacing changes at pH 6.0 and 5.5 resulted in no changes in calcium sensitivity. These results indicate that at lower pH myofilament calcium sensitivity becomes independent of lattice spacing. At pH 7.0 lowering $\Gamma/2$ from 200 to 120 mM caused calcium sensitivity, at a given SL, to increase by .5 pCa units. At pH 6.0 the same change in $\Gamma/2$ caused a .1 pCa unit increase. Although changes in pH and ionic strength can alter crossbridge binding and kinetics, and the binding of Ca to troponin, as well as the magnitude of fixed charge, the results taken together with the diameter measurements are consistent with an importance for both changes in lattice spacing and the presence of fixed myofilament charge in determining muscle sensitivity to calcium.

M-Pos173 VOLTAGE DEPENDENT RELAXATION IN VENTRICULAR MUSCLE. John H.B. Bridge* (Introduced by K.W. Spitzer) Nora Eccles Harrison CVRTI, University of Utah, Salt Lake City, Utah 84112

Papillary muscles cooled to 0°C for 10 min in modified Tyrode solution exhibit contractures. Abrupt reheating to 30°C produces prompt relaxation. Muscles were cooled in Tyrode solutions containing either 144, 44 or 0mM Na (Li replacement) for 10 min to allow equilibration in the extracellular space. Reheating caused relaxation ($t_{1/2}$ = 700 msec) that was independent of the $[Na]_o$. Apparently, relaxation occurs by rapid internal sequestration of Ca by the SR. If muscles are cooled for 10 min in the aforementioned Tyrode solutions containing in addition 10.0mM caffeine relaxation upon rewarming shows a striking dependence on the composition of the cooling (and rewarming solution). In 144mM Na, the presence or absence of caffeine makes little difference to relaxation. However, in 44 Na or 0 Na (10.0mM caffeine) relaxation is dramatically slowed (≈ 6 fold in 44 Na and ≈ 30 fold in 0 Na). Caffeine, therefore, makes relaxation dependent on external $[Na]_o$. This is consistent with the idea that caffeine prevents the SR from sequestering Ca and that under these circumstances relaxation occurs by Ca extrusion via Na/Ca exchange. However in the presence of caffeine relaxation rates are normal if Na and Ca are simultaneously reduced (44mM and 78 μ M respectively). This indicates a competitive effect of Na and Ca on relaxation in the presence of caffeine and further implies the involvement of Na/Ca exchange. Using solutions containing 44mM Na, 78 μ M Ca and 10.0mM caffeine I examined the effect of various $[K]$ (5.4–100mM) on relaxation. Plots of relaxation rate vs $\ln K_o$ indicate that in the presence of caffeine relaxation is steeply dependent on voltage between approximately -80 and -10mV. Either the process (presumably Na/Ca exchange) producing relaxation is voltage dependent or an electroneutral relaxation process opposed by a voltage dependent Ca leak produces voltage sensitive relaxation.

M-Pos174 MEASUREMENT OF CALCIUM TRANSIENTS AND CELL MOTION IN CULTURED CHICK AND ISOLATED ADULT RABBIT VENTRICULAR CELLS. George A. Peeters*, John H.B. Bridge* and William H. Barry* (Introduced by John L. Walker), Nora Eccles Harrison CVRTI, University of Utah, Salt Lake City, Utah 84112

We exposed spontaneously contracting cultured chick embryo ventricular cells and isolated rabbit ventricular cells to indo-1 AM (10 μ M) for 15 minutes. Using an inverted 40X objective epifluorescence system, washed cells containing Ca²⁺ sensitive indo-1 were excited at 360nm, and the fluorescence ratio 410nm (+ with + Ca²⁺) and 480nm (+ with + Ca²⁺) was recorded with photomultiplier tubes. Cell motion (video motion detector) was recorded simultaneously. An example of motion and the 410/480 ratio for rabbit ventricular cells (27°C) is shown in the inset. Signals with similar temporal relationships were recorded in cultured chick ventricular cells. Calibration of the $[Ca^{2+}]_i$ signals was achieved in cultured cells with Ca²⁺ buffered solutions containing the non-fluorescent ionophore, Bromo A23187. Calculated diastolic and systolic $[Ca^{2+}]_i$ were 241 ± 62 and 779 ± 289 nM (mean \pm se, $n=9$). These results indicate that indo-1 may be used to detect $[Ca^{2+}]_i$ transients in enzymatically dissociated and cultured myocytes.



M-Pos175 TRANSIENT MECHANICAL RESPONSES TO CAFFEINE IN ARTERIALLY PERFUSED RIGHT VENTRICLE AND TRITON X-100 TREATED VENTRICULAR MYOCYTES OF RAT. D.W. Hilgemann, K.P. Roos and A.J. Brady. Department of Physiology, UCLA School of Medicine, CHS A3-381, Los Angeles, CA 90024.

Mechanical responses to caffeine were determined in quiescent, arterially perfused rat right ventricle and isolated ventricular myocytes. In the ventricle, the first application of 20 mM caffeine (2.5 mM external calcium) transiently increased resting tension to $\sim 10\%$ of twitch tension. Subsequently, it decreased incompletely toward baseline over 2 to 5 minutes. After removal of caffeine, contraction amplitude was decreased relative to control. Subsequent exposures to caffeine increased resting tension to the previous steady state level in caffeine, while its removal resulted in rapid tension return to baseline. Similar protocols were then carried out in 1% Triton X-100 treated ventricular myocytes. Stiffness measurements were obtained by oscillatory length perturbations applied to the myocyte through attached concentric double-barreled suction micropipettes as described by Brady and Farnsworth (Am. J. Physiol. 250:H932-943, 1986). In Ca-free relaxing solution (10 mM EGTA; pH 7.1) application of caffeine was without effect on stiffness or unattached myocyte length. Increasing the pCa to 6.8 had no effect on stiffness or length. Subsequent application of 20 mM caffeine resulted in an irreversible hypercontracted state in unrestrained myocytes and at least a 50% increase of stiffness in restrained myocytes. As in ventricle, the stiffness decreased incompletely toward baseline. Stiffness responses to subsequent applications of caffeine were substantially less. Caffeine did not enhance rigor development in ATP-free, Ca-free, 0.19M KCl solution. However, caffeine treatment blunted subsequent rigor responses. These results suggest that the slow transitory mechanical responses to caffeine described here may be caused by processes other than intracellular calcium release.

M-Pos176 SPATIAL DISTRIBUTION OF ACTIVATION IN ISOLATED CARDIAC MYOCYTES. Robert S. Danziger, Harold A. Spurgeon and Mark Sharnoff. Laboratory of Cardiovascular Science, Gerontology Research Center, National Institute on Aging, Baltimore, MD and Physics Department, University of Delaware, Newark DE

Myocytes isolated from collagenase-treated rat hearts (Am J Physiol 245:H491, 1983) were suspended at 37°C in HEPES buffer containing 0.5 mM Ca^{2+} (pH 7.4) and plated on a petri dish. The dish was placed under a microscope and transilluminated with a laser beam of wave-length 5147 Å. Field electrical stimulation at 0.4 Hz was provided and used to reference occasional, paired flashes of the laser beam. Differential holograms were recorded and interpreted by the usual method (J Opt Soc Am A 2:1619, 1985). The optical signature of initial activation in myocytes entrained in the stimulation cycle became visible within 15 msec of stimulus and consisted of a rapid, strong brightening confined within one or two sarcomeric layers of a syncytial end and a slower, much weaker, less uniform brightening of the myocyte as a whole, often marked along myofibrillar lines. Most of the myocytes became visually quiescent after suppression of the electrical pulses, and their differential images gave no evidence of spontaneous myofilamentary oscillation exceeding 100 Å in amplitude. On rare occasions a spontaneous Ca^{2+} -dependent contraction wave (Circ Res 57:844, 1985) would be seen. The signature of such a wave appears to be confined to a band several sarcomeres wide and extending transversely across the myocyte, of contrast not so marked as the syncytial response of entrained cells.

M-Pos177 NOREPINEPHRINE INDEPENDENTLY INCREASES SARCOPLASMIC RETICULUM CALCIUM CONTENT AND SARCOLEMMA CALCIUM INFLUX IN RESPONSE TO DEPOLARIZATION OF CARDIAC MYOCYTES BY KCl.

Robert S. Danziger, Edward G. Lakatta, Richard G. Hansford. Gerontology Research Center, NIA, NIH, Baltimore, MD

Depolarization of rat cardiac myocytes with KCl (45mM) increases intracellular free Ca^{2+} (Ca_i) with a $T_{1/2}$ of 16.1 ± 3.2 sec ($n=15$), when Ca_i is monitored in suspensions of cells loaded with the fluorescent indicator Quin 2. Part of this increase in Ca_i is due to sarcoplasmic reticulum (SR) release, because caffeine (10mM) which causes a large release from the SR when given prior to KCl, prolongs $T_{1/2}$ by 100% for the Ca_i increase occurring in response to KCl (table). The neurotransmitter, norepinephrine (NE) (10^{-5}M) accelerates the rate of rise of cytosolic Ca^{2+} in response to KCl. In the absence of KCl depolarization, NE augments the release of Ca^{2+} into the myoplasm in response to caffeine (peak fluorescence 1.8 ± 0.4 times control and area under the curve 2.2 ± 0.2 times control). The rise in Ca_i caused by addition of KCl in the presence of caffeine and NE is both more rapid than in the absence of NE and inhibited by verapamil. Thus (1) the increase in Ca_i with KCl depolarization is a result of both SR release and sarcolemmal influx and NE enhances both; (2) NE augments SR calcium loading even in the absence of depolarization.

	($T_{1/2}$)/ $T_{1/2}$ KCl*	* of Suspensions
NE+KCl	0.5 ± 0.04	3
Caffeine+KCl	4.0 ± 0.6	3
Caffeine+NE+KCl	2.4 ± 0.5	3

*Each ratio with respect to $T_{1/2}$ for KCl depolarization in same suspension.

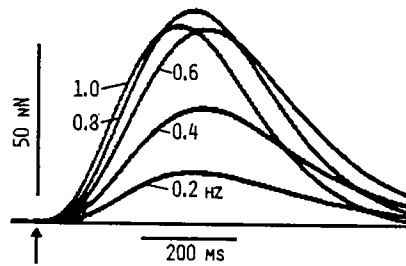
M-Pos178 CALCIUM TRANSIENTS AND CELL SHORTENING IN INDO-1 LOADED ISOLATED FELINE VENTRICULAR MYOCYTES. W.H. duBell and S.R. Houser. Department of Physiology, Temple University

School of Medicine, Philadelphia, PA, 19140.

The calcium transient that causes twitch contractions in cardiac muscle has usually been studied using aequorin that has been injected into a multicellular preparation. Recently, however, Ca^{2+} -sensitive dyes such as indo-1 have been developed that should allow cytosolic Ca^{2+} to be monitored in single myocytes. In the present study the objective was to relate the fluorescence transients recorded using indo-1 to the twitch properties of single feline ventricular myocytes. After loading myocytes with indo-1 acetoxymethyl ester (AM, 10 μM) for 30 min, an aliquot of cells was placed in a chamber on an inverted fluorescence microscope. The cells were superfused with normal Tyrode solution (2 mM Ca^{2+}) at 37°C and field stimulated at 0.22 Hz. Fluorescence excitation was at 355 nm (10 nm BW). Emission was monitored at 420 nm (10 nm BW, \uparrow w/ \uparrow Ca^{2+}) and 490 nm (10 nm BW, \downarrow w/ \uparrow Ca^{2+}). The results of the experiments showed that following stimulation, fluorescence at 490 nm decreased, fluorescence at 420 nm increased and cell shortening occurred. Importantly, the transients and twitches were longer than observed previously. The peak of the transient occurred within 400-1000 msec while peak shortening occurred within 700-1200 msec. In all cases the calcium transient preceded the twitch and peaked earlier. However, the downstroke of the transient sometimes followed, rather than led relaxation. These experiments show that the prolonged transient is accompanied by a prolonged twitch. These findings could result from the release of products from the indo-1 AM reaction or be due simply to the presence of indo-1 free acid within the cytosol. (Supported by NIH Grants HL 33921 & HL33648. W.H.D. is supported by a fellowship from Berlex Laboratories, Inc.)

M-Pos179 FORCE-FREQUENCY RELATION IN SINGLE FROG VENTRICULAR HEART CELLS. Leslie Tung, Department of Biomedical Engineering, Johns Hopkins School of Medicine, Baltimore, MD 21205

Single cardiac cells lack the restricted extracellular spaces (ES) present in multicellular muscle strips where accumulation or depletion of charge carriers may occur, thus simplifying the analysis of membrane currents and potentials (Tung and Morad, *Pflugers Arch* 405:274, 1985). This property of single cells may be used advantageously in contractile studies of the force-frequency relation. Twitch force of cardiac muscle generally increases with frequency up to a characteristic f_C above which force declines (in frog $f_C \approx 0.8$ Hz). One interpretation for the fall-off is that at high stimulus rates, sufficient K^+ accumulates and/or Ca^{2+} depletes in the ES to reduce tension either by a direct negative inotropic effect or by altering action potential configuration (thereby mediating Ca influx). This hypothesis is best tested in frog heart, where tension is highly sensitive to both of



these factors. Twitches were elicited in the single frog ventricular cell and recorded using an optic fiber-based cantilever beam force probe (Tung, *Pflugers Arch* 407:109, 1986). The inset shows the tenth beat following step increases to different stimulus rates. Both the rate of rise (dp/dt) and peak of tension increase monotonically with frequency. However, although dp/dt continues to increase from 0.8 to 1.0 Hz, peak tension declines, time-to-peak decreases, and rate of relaxation increases. These results are similar to those observed in muscle strips and suggest that in frog heart accumulation or depletion of charge carriers in the ES is not the major determinant of the peak of the force-frequency relation.

M-Pos180 HOW CHANGES IN INTRACELLULAR MILIEU ASSOCIATED WITH SHORT-TERM HYPOXIA AFFECT Ca^{2+} LOADING OF THE SARCOPLASMIC RETICULUM IN SKINNED CARDIAC MUSCLE FIBERS. T. M. Nosek, R.E. Godt & H. Kammermeier. Dept. of Physiology & Endocrinology; Med. College of Georgia; Augusta GA 30912 and Dept. of Physiology; Aachen Techn. U.; Aachen Fed. Rep. of Germany.

In intact hearts, short-term hypoxia leads to the following changes in intracellular milieu (in mM): ATP, from 6.18 to 4.7; ADP, 0.05 to 0.7; phosphocreatine (PC), 14.16 to 1.42; inorganic phosphate (Pi), 0.88 to 17.38; creatine, 11.28 to 22.34; affinity for ATP hydrolysis (A), 60.5 to 46.1 kJ/mol (Kammermeier et al., *J. Mol. Cell. Cardiol* 14:267, 1982). We used saponin-skinned bundles (less than 200 μ m diameter) from guinea-pig papillary muscles to assess the effects of these changes on calcium uptake by the sarcoplasmic reticulum (SR). Skinned fibers were bathed in a sequence of solutions (cf. Nosek et al., *Am. J. Physiol.* 250:C807, 1986): (i) to remove Ca^{2+} from the SR (25 mM caffeine, 7 EGTA), (ii) to load the SR with Ca^{2+} (1 min in 3.2 μ M Ca^{2+} and desired milieu), and (iii) to release Ca^{2+} from the SR (25 mM caffeine, 0.05 EGTA, 0.1 μ M Ca^{2+}). The amount of calcium taken up by the SR in solution (ii) was estimated from the transient force in solution (iii). The overall milieu change associated with short-term hypoxia had no significant effect on Ca^{2+} loading by the SR. Tested individually, changes in ATP, ADP, and creatine had no effect. Lowering PC, however, decreased Ca^{2+} loading by 38 (+9)%, while 30 mM Pi increased loading by 113 (+24)%. Decreasing A to 45 kJ/mol had no influence, however a decrease to 42 kJ/mol decreased loading by 20 (+3)%. We conclude that changes in Ca^{2+} loading by the SR do not significantly contribute to the decline in muscle force with short-term hypoxia. (Support: MCG & DAAD to TMN; NIH/AR 31636 to REG; DFG-Ka337/7-6 to HK).

M-Pos181 ATRIOPEPTIN III PROMOTES MYOCARDIAL RELAXATION - AND DOES IT THROUGH THE ENDOCARDIUM

Ann L. Meulemans, Karin R. Sipido, Stanislas U. Sys and Dirk L. Brutsaert
(Intr. by George McClellan)
University of Antwerp, Antwerp, Belgium

While the vasorelaxant and natriuretic properties of atrial natriuretic peptide (ANP) are well established, a direct action of ANP on the ventricle has not been described, despite the presence of receptors for ANP on the endocardial endothelium.

We studied the effects of atriopeptin III (synthetic rat ANP, 10^{-7} M) on papillary muscle isolated from cat right ventricle ($n=20$, 29° C, 0.2Hz) and from rat left ventricle ($n=13$, 29° C, 0.1Hz).

Atriopeptin III induced early relaxation of isotonic and isometric contractions without affecting the velocity of contraction. A similar early relaxation without changes in velocity was also seen when intracellular cyclic guanosine 3',5'-monophosphate (cGMP) was increased by the addition of dibutyryl-cGMP (db-cGMP, 10^{-4} M) and sodium nitroprusside (SNP, 10^{-5} M).

Damaging the endocardial endothelium of rat papillary muscle ($n=7$), either by exposure (1-2s) to 1% Triton X-100 or by gentle rubbing of the muscle surface, significantly blunted the response to atriopeptin III, but not the response to db-cGMP ($n=7$) and SNP ($n=6$).

Thus, early relaxation of cardiac muscle is induced by ANP, and may be mediated through endocardial receptors.

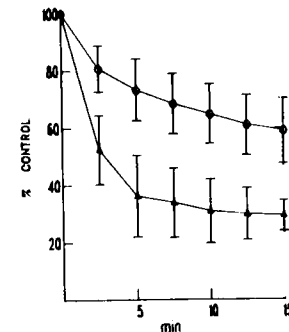
M-Pos182 THE ROLE OF SIALIC ACID IN THE CONTROL OF MYOCARDIAL SARCOLEMMA Ca^{2+} PERMEABILITY.

Hal F. Yee, Jr. and Glenn A. Langer, Cardiovascular Research Laboratory, UCLA School of Medicine, Los Angeles, CA 90024.

The regulation of Ca^{2+} movement across the heart cell membrane is critically important to excitation-contraction coupling. Thus, the role of sialic acid, an anionic membrane sugar, in controlling sarcolemmal Ca^{2+} permeability was evaluated. Using the scintillation disc-flow cell technique, Ca^{2+} flux was measured in cardiocytes before and after a number of interventions. It was determined that removal of sialic acid by sialidase alters the amount of Ca^{2+} associated with heart cells; release of increased amounts of sialic acid leads to increased cell Ca^{2+} uptake. Cleavage of the carbon side chain (carbons 8-9) of sialic acid does not alter cell associated Ca^{2+} which would seem to implicate the carboxyl group of the sugar in this phenomena. Since the rate constants for K^{+} washout do not change following removal of sialic acid residues, this effect does not appear to be due to changes in general membrane permeability. There are only two recognized systems for Ca^{2+} specific entry into the myocardial cell, the Ca^{2+} channel, and the $\text{Na}^{+}/\text{Ca}^{2+}$ exchanger. Experiments were conducted which revealed that nifedipine, a specific Ca^{2+} channel blocker, decreases the Ca^{2+} influx associated with sialic acid removal. A video-monitoring system was also used to evaluate this phenomena. Removal of sialic acid leads to myocardial inotropy. This is consistent with the increased Ca^{2+} influx seen in association with sialic acid removal. Thus, it appears that sialic acid plays a role in the specific regulation of transsarcolemmal Ca^{2+} transport and consequentially excitation-contraction coupling. This phenomena may be related to the negative charge of sialic acid, and may be modulated through the Ca^{2+} channel. (Supported by NIH MSTP grant GM08042 to HFY, Jr., NIH grant HL28539 to GAL, and the Castera and Laubisch endowments.)

M-Pos183 PHORBOL ESTER TRANSLOCATES PROTEIN KINASE C AND HAS A NEGATIVE INOTROPIC EFFECT IN RAT CARDIAC MYOCYTES. M. C. Capogrossi, T. Kaku, D. J. Pelto, C. Filburn, R. G. Hansford, H. Spurgeon, E. G. Lakatta. Gerontology Research Center, NIA, NIH, Baltimore, MD

α_1 -Adrenergic agonists increase 1,2-diacylglycerol which activates protein kinase C. The functional significance of this effect, which can be simulated by phorbol ester, on myocardial contractility is unknown. In suspensions of Ca^{2+} tolerant, single, rat cardiac myocytes (37°C , $[\text{Ca}^{2+}]$ of 1.0 mM, pH 7.4) the ratio of protein kinase C in the membranous fraction to that of the total cell (PKAR) in either 5 (n=7) or 30 (n=3) mM KCl was respectively (\pm SEM) 0.143 ± 0.017 and 0.177 ± 0.022 . Following the addition 10^{-7}M PMA it increased respectively to 0.366 ± 0.026 and 0.497 ± 0.048 at 30 sec ($p < 0.05$). At 10 min PKAR had further increased to 0.686 ± 0.036 and 0.781 ± 0.044 . Twitch amplitude was measured via videomicroscopic edge motion detection in individual myocytes during electrical stimulation at 60 min^{-1} . PMA (10^{-7}M) had a negative inotropic effect which was more marked in higher KCl (see Fig.). Control twitch amplitude (expressed as % resting cell length) was 2.26 ± 0.37 (0; KCl 5 mM; n=5) and 3.0 ± 1.89 (Δ ; KCl 30 mM; n=3). A similar contractile response could be induced in either KCl by 10^{-5}M dioctanoyl glycerol. Thus, PMA, in rat cardiac myocytes (1) increases PKAR, (2) decreases myocardial contractility and (3) in high KCl, a perturbation which increases myoplasmic Ca^{2+} , the change in PKAR is faster and the negative effect on twitch amplitude is greater.

**M-Pos184 HOG CAROTID LACTATE DEVELOPMENT AS OBSERVED WITH H-NMR** J.F. Clark and P.F. Dillon, Departments of Physiology and Radiology, Michigan State University, E. Lansing, Michigan 48824

The methyl resonance of lactate at 1.13 ppm increases markedly during K^{+} stimulation in the presence of low phosphate (0.1 mM) in a single perfused-oxygenated carotid artery. Over the same 12 hr time course no significant decline in ATP or PCr was noted as observed using ^{31}P -NMR. The proton spectra were obtained using a ^1H resonance frequency of 400.131 MHz. Water was suppressed using a 10 sec. presaturation pulse of .0317 Watts. A total of 800 free induction decays (FID) were added together using a 90° pulse of 8.5 usec, and Fourier transformed with an exponential multiplier of no more than 5Hz. A single carotid was perfused continuously while held in a 5mm coil within the probe. The ^{31}P experiments were conducted at 161.9 MHz using a 10mm diameter phosphorus probe and a single artery. 600 1 second scans were acquired using a pulse width of 8.5 sec, and transformed using a line broadening of 30 Hz. The perfusion solution consisted of a modified Krebs solution including 0.1 mM Pi, 0.6 mM Ca^{++} , and 80 mM K^{+} to depolarize the membrane. When the carotid arteries were exposed to 50 mM Pi for the same duration, no change in lactate was found, but a dramatic increase in the resonances at 2.77 and 3.2 ppm was observed. There was no marked change in the ATP or PCr under these conditions. We conclude that (1) the lactate varies as a function of external Pi, but not in a directly proportional manner as reported by Kutchai and Geddes and (2) ^{31}P -NMR spectra do not entirely reflect the metabolic state of the tissue. We suggest that there may be several parallel methods of maintaining high energy phosphate levels in vascular smooth muscle. Supported by AM34885 and the Whitaker Foundation.

M-Pos185 EFFECTS OF ACETYLSTROPHANTHIDIN (ACS) ON CARDIAC MUSCLE TWITCHES, RAPID COOLING CONTRACTURES AND MICROSCOPIC TENSION FLUCTUATIONS. Donald M. Bers and John H.B. Bridge. University of California, Riverside, CA 92521 and University of Utah, Salt Lake City, UT 84112.

ACS increased twitch tension in rabbit ventricular muscle in a concentration dependent manner up to 4-6 μ M. At higher concentrations twitch amplitude progressively declined and resting force began to increase. Rapid cooling contractures (RCC) induced 2 sec after the last stimulation were used as an index of SR Ca available for release. RCC amplitude increased monotonically with increasing [ACS] such that RCC magnitude was maintained at [ACS] at which twitch amplitude was depressed. RCC could be eliminated by pre-treatment with 10mM caffeine ($K_1=1$ mM). RCC magnitude also declined with increasing rest intervals prior to cooling ($t_1=1$ min) and this "rest decay" of RCC magnitude was prolonged by ACS ($t_1>5$ min in 4 or 8 μ M ACS). These observations are consistent with the "lag hypothesis" of glycoside action. Microscopic tension fluctuations (measured with an AC coupled tension transducer) became apparent at about the same [ACS] at which twitch tension began to decline (prior to any increase in resting force or aftercontractions). Fourier analysis of these fluctuations revealed an underlying frequency of 2-4 Hz. Spontaneous oscillations of Ca between the SR and the cytoplasm are believed to underlie these tension fluctuations. Twitch tension may decline in part because mechanical fluctuations in series can decrease the transmission of force to the ends of the muscle. These oscillations may also contribute to the decline in twitch force by decreasing the ability of the SR to release Ca upon stimulation or decreasing the time averaged SR Ca content. If these fluctuations do represent Ca moving from SR to cytoplasm and back, then the sum of SR + cytoplasmic Ca at rest may not change. The RCC magnitude is probably determined by the sum of SR + cytoplasmic Ca and as such would not be influenced by these oscillations. This might explain why the RCC do not decline at high [ACS] where twitch amplitude decreases.

M-Pos186 CARDIAC STIMULANT EFFECT OF PROGESTERONE DERIVATIVES. T. Kobayashi, D. Bose, D. Elliot, J.F. Templeton, S. Kumar, R.S. Kim & F.S. LaBella (Intr. by Ratna Bose), Dept. of Pharmacology & Therapeutics & Internal Medicine, University of Manitoba, Faculty of Medicine, Winnipeg, Man, Canada, R3E 0W3.

Previous studies done by us and others have shown that certain progesterone derivatives, e.g. chlormadinone acetate (CMA) resemble the cardiac glycosides (CG) and are inhibitors of Na-K ATPase as well as of the sodium pump. Furthermore, these compounds interact at the CG receptor site. However their effect on cardiac contractility is either inhibitory or at best only transiently excitatory. The present study was done with a new derivative, 14-beta-hydroxy-progesterone (14OHP), which is more consistently inotropic and has a greater efficacy than other progesterone derivatives. In isolated canine ventricular trabecula, isometric contractions were consistently depressed by progesterone (PROG), usually depressed but occasionally transiently stimulated by CMA and consistently stimulated by 14OHP. High concentrations of 14OHP caused aftercontractions and contracture in a manner similar to cardiac glycosides (CG). Asynchronous Ca release during diastole (studied by intensity fluctuation of 'speckle pattern' obtained by laser light scattering and is a characteristic of CG but not of several other inotropes, e.g. isoproterenol or BAY K 8644) was increased by 14OHP but was decreased by PROG. Sodium pump inhibition was studied by observing the effect of the compounds on potassium-induced relaxation in potassium deprived canine portal vein. The potency order for inhibition of relaxation was ouabagenin > 14OHP > CMA > PROG. Membrane stabilization was studied by measuring erythrocyte hemolysis in a hypotonic medium. PROG reduced hemolysis while ouabagenin and 14OHP had no effect. It is concluded that although progesterone and a number of its derivatives interact at the CG receptors, positive inotropic effect may only be seen with compounds that do not, in addition, stabilize the sarcolemma, an action which may tend to antagonize any positive inotropy. (Supported by Manitoba Heart Foundation and MRC of Canada).

M-Pos187 EFFECTS OF HOLDING POTENTIAL ON PEAK Ca^{2+} CURRENT FOLLOWING REST INTERVALS IN CAT VENTRICULAR MYOCYTES. L.S. Miller and S.R. Houser, Department of Physiology, Temple University School of Medicine, Philadelphia, Pennsylvania 19140.

Previous studies have shown that the first beat following a 2 minute rest period has a prolonged action potential duration and decreased contraction magnitude. The objective of this study was to examine the role of the slow inward Ca^{2+} current in this phenomenon. Cells were isolated from adult cat heart by standard enzymatic digestion and perfused with normal Tyrode solution (2 mM Ca^{2+} , 35° C). Single cells were impaled by suction pipette and subjected to a series of constant voltage-clamp steps (500 msec, 1 Hz) in the presence of 50 μ M TTX. Cells were held at -73 mV or -40 mV and stepped to 0 mV. At a holding potential of -40 mV, peak current was approximately 0.8 nanoamps at 0 mV. Following a 2 minute rest interval, current during the first step was increased approximately 1.4 X steady state. From a holding potential of -73 mV, peak current was approximately 0.5 nanoamp at 0 mV. Following 2 minutes of rest, the current was decreased in the first step (approximately .7 X steady state) with a gradual increase to steady state upon subsequent steps. The apparent positive staircase at negative holding potentials could reflect either a true beat-dependent increase in inward current, or a marked beat-dependent contribution of a transient outward current observable only at the more negative holding potential which masks actual inward Ca^{2+} current. (Supported by NIH grants HL 33921 and HL 33648; AHA SE Pennsylvania Chapter Research Fellowship)

M-Pos188 TWO TTX-INSENSITIVE INWARD CURRENTS IN FELINE VENTRICULAR MYOCYTES. A. Bahinski, R.B. Kleiman, H. Hartman and S.R. Houser. Physiology Dept., Temple Univ. Sch. of Med. Phila. PA 19140.

Studies in atrial and ventricular muscle have observed two types of calcium channel currents. The purpose of the present study was to: 1) determine if more than one TTX-insensitive inward current exists in feline ventricular myocytes and 2) to examine the respective roles of Na and Ca as current carriers through these channels. Micropipettes were filled with 100 mM Cs, 10 mM EGTA, 5 mM ATP to block outward K and intracellular Ca activated current. Holding potentials were between -70 to -80 mV and 50 μ M TTX was used to block inward current through Na channels. Myocytes were superfused with either a normal Tyrode solution (in mM; 150 Na, 5.4 K, 2 Ca^{++} 5 Hepes) or a zero Na solution in which Na was replaced by TEACl. In Na containing solutions depolarizing voltage clamp steps (500 msec duration) elicited two distinct inward current peaks. The first was of a rapidly activating and inactivating (with 5 msec) current (I_{fast}) elicited on depolarization to values positive to -45 mV with peak current around -35 mV. The second inward current peak (I_{slow}) was activated when the membrane was pulsed to values positive to -25 mV with peak current around 0 mV. In zero Na solutions the voltage-current relationships for both I_{fast} and I_{slow} were similar to those in solutions containing Na. However the magnitude of I_{fast} was greatly reduced. The results indicate the presence of two TTX-insensitive inward currents in ventricular myocytes. The reduction in magnitude of I_{fast} in Na free solutions may indicate either 1) a role for Na as a charge carrier through the channel responsible for I_{fast} or 2) the presence of a contaminating inward current through a very TTX-insensitive Na channel. (Supported by NIH grants HL 33921 and HL 33648 to SRH).

M-Pos189 MEASUREMENT OF DIVALENT CATION KINETICS USING FLUORESCENT CHELATORS. Lynn A. Selden, Henry J. Kinoshian, James E. Estes and Lewis C. Gershman. Research and Medical Services, Veterans Administration Medical Center, Albany, and Departments of Physiology and Medicine, Albany Medical College, Albany, NY 12208.

Measurement of Ca^{++} binding to proteins has traditionally included use of atomic absorption or radioisotopes. Studies of Ca^{++} binding kinetics by these methods are difficult, however, since temporal resolution is limited by the speed with which samples may be fractionated into bound and free components for assay. Other methods, such as use of specific ion electrodes, have slightly better temporal resolution but poor sensitivity. Measurements of Mg^{++} binding are further hampered by the lack of a "convenient" Mg radioisotope.

The fluorescent Ca^{++} chelator Quin2 has been extensively used for *in vivo* studies of Ca^{++} effects. We recently reported the use of Quin2 to measure the affinity and kinetics of the tight-binding of Ca^{++} to actin, noting that actin appears to be the highest affinity Ca^{++} -binding protein yet reported (Biochem. Biophys. Res. Comm. 135:607-614, 1986). Here we describe more fully the characteristics of Quin2 and its utility in binding studies of Ca^{++} . We also characterize the fluorescent Mg^{++} chelator 8-OH quinoline-5-sulfonic acid and describe its use in the study of Mg^{++} binding kinetics. Use of these fluorescent chelators permits accurate determinations of free Ca^{++} and Mg^{++} concentrations in solution and of the affinity and kinetics of divalent cation binding. Supported by the Veterans Administration and NIH grant GM-32007-02.

M-Pos190 CHARACTERIZATION OF DIVALENT CATION-FREE ACTIN by Lewis C. Gershman, Lynn A. Selden, and James E. Estes. Research and Medical Services, Veterans Administration Medical Center, Albany and Departments of Physiology and Medicine, Albany Medical College, Albany, NY 12208.

We have previously reported that the polymerization characteristics of actin are affected by the tightly-bound divalent cation: Mg -actin nucleates and polymerizes more readily than Ca -actin and produces a more stable polymer (Biochem. Biophys. Res. Comm. 116:476-485, 1983; J. Muscle Res. Cell Motility 7:215-224, 1986). We have recently determined that the high-affinity binding of Ca^{++} and Mg^{++} to actin is much stronger than previously thought (Biochem. Biophys. Res. Comm. 135:607-614, 1986). Pollard (Calcium Regulation in Biological Systems, Ed. by S. Ebashi, M. Endo, K. Imahori, S. Kakinchi, and Y. Nishizuka, Academic Press, Japan, 1984) has shown that, in the presence of EGTA, Ca -actin polymerizes like Mg -actin. Using the Ca^{++} specific chelators BAPTA or EGTA, we have succeeded in preparing divalent cation-free actin (DCF-actin). DCF-actin denatures spontaneously with a half-life which is about 5-10 min at pH 7 and much shorter at higher pH. However, the half-life at pH 7 is sufficiently long to permit measurements of polymerization kinetics. DCF-actin polymerized in 20 or 100 mM KCl has both a low critical concentration and a low calculated rate constant of dissociation similar to Mg -actin. Furthermore, from studies on actin labelled with 1,5-I-AEDANS, the fluorescence of DCF-actin is more similar to that of Mg -actin than to that of Ca -actin. Thus, DCF-actin probably has a conformation unlike that of Ca -actin but more similar to the conformation of the more "physiologic" Mg -actin. (Supported by the Veterans Administration and NIH grant GM-32007-02).

M-Pos191 DIVALENT CATION EXCHANGE ON MONOMERIC ACTIN. James E. Estes, Lynn A. Selden, and Lewis C. Gershman. Research and Medical Services, Veterans Administration Medical Center, Albany, and Departments of Physiology and Medicine, Albany Medical College, Albany, NY 12208.

We have reported that monomeric actin binds Ca^{++} and Mg^{++} much more tightly than previously thought (Biochem. Biophys. Res. Comm. 135:607-614, 1986). More recently, using the fluorescent Ca^{++} chelator Quin2, we have observed that the kinetics of Ca^{++} dissociation from actin parallel the fluorescence intensity changes in 1,5-I-AEDANS-labelled actin, suggesting that the 1,5-I-AEDANS fluorescence intensity change reflects slow cation exchange rather than a slow Mg^{++} -induced isomerization as proposed by Frieden (J. Biol. Chem. 257:2881-2886, 1982). The isomerization model incorporates a phase of rapid pre-equilibration at the onset of divalent cation exchange. Experiments in our laboratory suggest that this rapid pre-equilibrium phase does not take place and that over the pH range 7-8, the changes in 1,5-I-AEDANS-labelled actin fluorescence intensity upon exchange of the divalent cation are directly related to the binding or release of Mg^{++} or Ca^{++} as indicated by fluorescent chelators. The observed exchange kinetics - the association and dissociation rate constants for Mg^{++} are smaller than those for Ca^{++} by factors of about 40 and 10, respectively - result in large part from the character of the Mg^{++} aquo-ion. We conclude that divalent cations bind tightly to actin by a simple first-order mechanism which does not require a "slow isomerization" step. Since the binding is very strong, exchange is slow, and thus the associated change in 1,5-I-AEDANS-labelled actin fluorescence intensity is slow. (Supported by the Veterans Administration and NIH grant GM-32007-02)

M-Pos192 DYNAMIC LIGHT SCATTERING USING LATEX SPHERES AS A PROBE OF PORES IN FILAMENTOUS ACTIN SOLUTIONS Jay Newman, Kenneth L. Schick, Physics Department, Union College, Schenectady, N.Y. 12308, Lynn A. Selden, Lewis C. Gershman, and James E. Estes, Research and Medical Services, Veterans Administration Medical Center, Albany, and Departments of Physiology and Medicine, Albany Medical College, Albany, N.Y. 12208

Actin polymerization was studied by dynamic light scattering experiments in the presence and absence of 0.109 μm diameter polystyrene latex spheres (PLS). The PLS were added to G-actin solutions (in the concentration range of 0.1-10 μM ; prepared with Mg^{++} as the bound cation) so that the light scattered at 90° from the spheres was in excess of that to be produced by the polymer by fixed ratios greater than about 20. Upon the addition of 100 mM KCl the average apparent diffusion coefficient of the PLS decreases from the expected monodisperse value observed in water. With increasing actin concentration, the rate and extent of the decrease are greater and the apparent distribution of diffusion rates is broader. At the lowest concentrations little or no restricted diffusion or broadening of the diffusion rates is observed over a period of several hours, while at 10 μM actin the diffusion coefficient decreases by a factor of 4 in about 10 minutes. The kinetics agree with those found by monitoring the scattered intensities in the absence of the PLS and thus reflect the early polymerization rates. Control experiments show that there is no association between PLS and actin polymer. The decrease and broadening of the apparent diffusion coefficient of the PLS reflects the distribution of pore sizes in filamentous actin and provides a direct method for studying the nature of the network state in actin. Supported by NSF grant DMB-8607031.

M-Pos193 ASSEMBLY OF CHICKEN GIZZARD MYOSIN: PHOSPHORYLATED, THIOPHOSPHORYLATED AND UNPHOSPHORYLATED. P. Chowrashi, H. Miyata, S. Chacko and F. Pepe. Dept. of Anatomy, School of Medicine and Dept. of Pathology, School of Veterinary Medicine, Univ. of Penn. Phila. PA 19104.

Chicken gizzard myosin was purified by gel filtration in the unphosphorylated (U), 100% phosphorylated (P) and 100% thiophosphorylated (T) forms as described previously (Chacko, Biochem. 20 702, 1981). Assembly was studied both in the presence and absence of 1 mM MgATP under conditions which, for skeletal myosin, produce a length of 1.5 μ m and which sharpens around that same length with time (Chowrashi and Pepe, J. Mus. Res. Cell Mot. 7, 1986). The assembly was observed in electron microscopy by negative staining. In addition to the assembly at 0.15, 0.08 M KCl was studied. No aggregation of U-myosin was observed in the presence of MgATP either at 0.15 or at 0.08 M KCl. In the absence of MgATP, U-myosin formed paracrystals with a 14 nm axial repeat, with some short filament present. The paracrystals were more numerous at 0.08 than at 0.15 M KCl. Both the T-myosin and P-myosin assembled into short filaments (0.5-0.7 μ m) in the absence of MgATP. In the presence of MgATP filaments with a mean length of about 1 μ m were obtained for both T-myosin and P-myosin immediately on reaching 0.15 or 0.08 M KCl. On standing there was little change for both myosins at 0.08 M KCl. At 0.15 M KCl the P-myosin length changed to give a mean of 1.5 ± 0.2 μ m (110 fil) while the length of the T-myosin changed to a mean of 1.2 ± 0.3 μ m (100 fil). We conclude that a) the assembly of P-myosin gives a length distribution comparable to that of skeletal myosin filaments, b) this assembly is dependent on the presence of 1 mM MgATP, 0.15 M KCl and sufficient time at 0.15 M KCl for redistribution of length to occur, c) the assembly of T-myosin gave shorter filaments and d) U-myosin did not readily assemble into filaments.

M-Pos194 AFFINITY LABELING OF GIZZARD MYOSIN WITH 5'- ρ -FLUOROSULFONYLBENZOYLADENOSINE.

Gary Bailin, UMDNJ-School of Osteopathic Medicine, Piscataway, NJ 08854.

Treatment of chicken gizzard myosin with the ATP analog, 5'- ρ -fluorosulfonylbenzoyladenine[14 C], FSO₂BzAdo[14 C], resulted in 50% inhibition of the K⁺-ATPase (ATP phosphohydrolase, EC 3.6.1.32) activity when 2 mol of the reagent were bound per 4.7×10^5 g protein. Inactivation of myosin occurred when one mol of the label was bound to the light chain of Mr 20,000 and only 0.4 mol was bound to the heavy chains or light chain of Mr 17,000. Substrate MgATP prevented the inactivation whereas MgADP had no protective effect. It is noteworthy that in all cases there was no change in the extent of incorporation of the FSO₂BzAdo[14 C]. By way of contrast, when gizzard myosin was pretreated with the myosin light chain kinase catalyzed phosphorylating system and then incubated with FSO₂BzAdo[14 C] the heavy chains were modified predominantly. Phosphorylation induced changes in the conformation of gizzard myosin that altered its reactivity with the affinity label. Thiolysis of the modified myosin with dithiothreitol resulted in a loss of nearly one mol of the label from the heavy and light chains (Mr 17,000) but there was little restoration of the ATPase activity. Studies on the FSO₂BzAdo[14 C] labeling of myosin in the presence of gizzard actin suggest that the light chain of Mr 20,000 is more closely associated with the ATP binding sites on gizzard myosin. Supported, in part, by the American Heart Association (N.J. Affiliate), Foundation of UMDNJ and the American Osteopathic Association.

M-Pos195 EFFECT OF PARTIAL PROTEOLYSIS ON THE SELF-ASSEMBLY OF SMOOTH MUSCLE MYOSIN.

Sarkis S. Margossian, James R. Sellers & Henry S. Slayter. Departments of Biochemistry and Orthopedic Research Montefiore Medical Center, Bronx, NY 10467; Laboratory of Molecular Cardiology, National Institutes of Health, Bethesda, MD 20892 & Dana Farber Cancer Institute, Boston, MA 02115.

Removal of the regulatory light chains by a neutral protease resulted in a reversible shortening of skeletal and cardiac myosin synthetic thick filament length. Treatment of gizzard myosin with the hamster protease cleaved the heavy chains instead, at a site about 70 kDa from the N-terminal end with no degradation of the regulatory light chains (Margossian, *et al.*, (1984) J. Biol Chem. 259, 13534). It was decided to investigate the effect of heavy chain cleavage on the self-assembly of smooth myosin. Both phosphorylated and unphosphorylated myosins, control and protease-treated, were dialyzed against a buffer containing 10-25 mM MgCl₂ and 1 mM MgATP at pH 7.2. Control, unphosphorylated myosin precipitated as ordered aggregates with cross-striations having a 13.5 nm periodicity, and a thickness of about 40-50 nm. The unphosphorylated, protease-treated myosin on the other hand, formed side polar filaments. When these aggregates were fixed and sectioned, cross bridges could be seen projecting at 90° to the filament axis. In contrast, neither of the phosphorylated myosins formed ordered aggregates. Occasionally, a side polar filament was found. These results parallel those reported earlier (Ikebe and Ogihara, (1982) J. Biochem. (Tokyo) 92, 1973). Moreover, they also indicate that cleavage of the heavy chains generates new cross-linkages that seem to favor formation of side polar filaments. (Supported by NIH Grants HL 20569 (SSM) and GM 14237 (HSS).

M-Pos196 A DOMAIN-LIKE ORGANIZATION OF SMOOTH MUSCLE MYOSIN HEAVY CHAIN. Sudhir Srivastava, Department of Physiology and Biophysics, Medical College of Virginia, Virginia Commonwealth University, Richmond, VA 23298.

Recently, Mornet et al. (Proc. Natl. Acad. Sci. 81, 736-739, 1984), using the approach of limited proteolysis with proteases of different specificities, have shown that the three tryptic peptides (25 kDa, 50 kDa and 20 kDa) are the functional domains of skeletal myosin subfragment-1 (S1). This interpretation was based on the assumption that domains of folded polypeptide chains are separated by well defined structureless boundaries (regions) which are susceptible to proteolytic cleavages by various proteases. Using a similar approach, we have shown that smooth muscle S1, like its skeletal counterpart, also has a domain-like structure. Smooth muscle S1 prepared from gizzard myosin was digested with the following proteases with their site specificities noted: trypsin (arg-lys), V8 protease (glutamyl and aspartyl residues), subtilisin (non-specific), plasmin (trypsin-like) and thermolysin (tyrosine and phenylalanine). The three major peptides obtained as a result of limited digestion were 25 kDa, 29 kDa and 50 kDa. The further cleavage of the 50 kDa peptide was significantly reduced when the proteolysis of S1 was carried out with trypsin in the presence of Mg-ATP. Mg-ATP had no effects on digestion by other proteases. Our earlier studies have shown that the 50 kDa peptide contains the ATP-binding site (Srivastava et al. Eur. J. Biochem. 156, 447-451, 1986). The results of these studies will be discussed in terms of a domain-like organization for smooth muscle myosin. Supported by American Heart Association, Virginia-affiliate.

M-Pos197 ENHANCEMENT OF TRYPTOPHAN FLUORESCENCE OF SMOOTH MUSCLE MYOSIN AND HEAVY MEROMYOSIN BY ATP. Jan Sosinski and John C. Seidel, Dept. of Muscle Res., Boston Biomed. Res. Inst., Boston, MA 02114.

Hydrolysis of ATP by gizzard heavy meromyosin (HMM) is accompanied by a decrease in digestibility by papain in the 9S form but not in the 7.5S form (Suzuki et al. (1986) Biophys. J. 49, 184a). Addition of 0.2 mM ATP in the presence of Mg^{2+} produces a 18-22% enhancement of tryptophan fluorescence of phosphorylated (PHMM) or dephosphorylated HMM (DHMM), that is independent of ionic strength, indicating that the enhancements of the 9S and 7.5S forms are the same. The rate of decay of fluorescence of PHMM on addition of a stoichiometric concentration of ATP follows the same dependence on ionic strength as do the steady state rate of ATP hydrolysis and the sedimentation velocity. The decay rates were $0.004\ s^{-1}$ for DHMM and $0.012\ s^{-1}$ for PHMM at 0.025 M NaCl and increased to $0.028\ s^{-1}$ at 0.3 M NaCl. Phosphorylation also shifted the dependence of the decay rates on the concentration of NaCl to lower concentrations. ATP produces a 17-22% increase in fluorescence intensity of phosphorylated (PM) or unphosphorylated myosin (UM) between 0.3 and 0.5 M NaCl where myosin is in the 6S conformation. The apparent enhancement of UM decreases to 10% at 0.1 M NaCl. This decrease in the apparent enhancement is accompanied by an 80% decrease in light scattering on addition of ATP, which may account for the decreased enhancement. Decay rates of PM are $0.004\ s^{-1}$ at 0.1 M NaCl and $0.013\ s^{-1}$ at 0.3 M NaCl. Changes in decay rates parallel changes in steady state rate of ATP hydrolysis.

M-Pos198 PROTEIN KINASE C PHOSPHORYLATION SITES IN THE SMOOTH MUSCLE MYOSIN LIGHT CHAIN. A. Resai Bengur¹, Elizabeth A. Robinson², Ettore Appella² and James R. Sellers¹ NHLBI¹ and NCI², NIH, Bethesda, MD 20892.

One of the mechanisms that has been shown to regulate smooth muscle contraction is the reversible phosphorylation of serine 19 in the 20,000-Da myosin light chain by the Ca^{2+} -calmodulin dependent enzyme, myosin light chain kinase. It has been demonstrated that protein kinase C, a Ca^{2+} -activated, phospholipid-dependent enzyme, can also phosphorylate the myosin light chain on a threonine residue and that this phosphorylation may play a role in modulating the phosphorylation dependent regulation of smooth muscle contraction (Nishikawa et al., J. Biol. Chem. 258, 14069, 1983). Through indirect evidence it has been proposed that the threonine site is either threonine 9 or 10 (Hassell et al., BBRC 134, 240, 1986). In order to better understand the role of protein kinase C in the phosphorylation dependent regulation, we have sequenced the phosphorylation sites in the turkey gizzard smooth muscle myosin light chain. Unexpectedly, two-dimensional tryptic peptide maps of both heavy meromyosin and the isolated myosin light chain showed two phosphopeptides; one containing phosphoserine and the other phosphothreonine. We have purified the succinylated tryptic phosphopeptides using HPLC reverse phase and HPLC DEAE chromatography. The serine peptide, residue 1-4 (SSKR), is the N-terminal peptide. Amino acid analysis after carboxypeptidase digestion showed that serine 1 is phosphorylated. The threonine peptide, residue 5-16, yielded the sequence: AKAKTTKKRPQR. Preliminary analysis of the yields and radioactivity of the products from automated Edman degradation suggest that threonine 9 is the phosphorylation site.

M-Pos199 DEPENDENCE OF CONFORMATION OF SMOOTH MUSCLE MYOSIN ON THE PHOSPHORYLATION AND DEPHOSPHORYLATION OF 20,000 DALTON LIGHT CHAIN. Mitsuo Ikebe and David J. Hartshorne*, Dept. of Physiology and Biophysics, Case Western Reserve Univ. and *Dept. of Biochem Nutrition and Food Sci. Univ. of Arizona.

Smooth muscle myosin forms two distinct conformations. One is a folded conformation and the other is an extended conformation. We studied phosphorylation and dephosphorylation of smooth muscle myosin by myosin light chain kinase (MLCK) and myosin light chain phosphatase (MLCP). At 1mM MgCl₂ and 85mM KCl pH 7.5 where P-myosin forms a folded conformation, P-myosin was hardly dephosphorylated by MLCP. The rate of dephosphorylation was increased above 150mM KCl and reached a maximum rate at 200-250 mM KCl. The rate again decreased above 250mM KCl. This dual phase KCl dependence was not observed when S-1 and isolated 20,000 dalton light chain was used as a substrate. Conformational transition of myosin from 10S to 6S monitored by the change in viscosity was correlated to the increase in the rate of dephosphorylation between 150mM to 200mM KCl. Therefore, it was concluded that the dephosphorylation of myosin is inhibited when P-myosin forms a folded conformation. Inhibition of dephosphorylation was not observed when P-myosin forms thick filaments. The rate of phosphorylation of myosin by MLCK was also affected by the conformation of myosin. The rate of phosphorylation was increased above KCl concentration of 150mM and reached its maximum at 250mM KCl and decreased above 300mM KCl. This dual phase KCl dependence was not observed when S-1 or isolated light chain was used. When the data is normalized by the KCl effect on MLCK, the rate of phosphorylation was found to be correlated to the conformational transition of DP-myosin from a folded to an extended. Supported by NIH grants AR38431 to M.I. and HL23615 and HL20984 to D.J.H. and by American Heart Assoc. North Ohio Affil. to M.I.

M-Pos200 INTRACELLULAR PHOSPHORYLATION OF MYOSIN HEAVY AND LIGHT CHAINS IN ANTIGEN-STIMULATED BASOPHILS. Itzhak Peleg, Russell I. Ludowyke, Michael A. Beaven and Robert S. Adelstein, NHLBI, NIH, Bethesda, MD 20892.

A rat basophil leukemic cell line (RBL-2H3) exhibited phosphorylation of both the 200,000 and 20,000-dalton chains of myosin following antigenic stimulation. Cells were primed with specific IgE and labeled with ³²P-orthophosphate and then stimulated with DNP-bovine serum albumin. Cells were then disrupted and myosin was selectively removed by immunoprecipitation with anti-platelet myosin antibodies. Scanning of the heavy chains in Coomassie-blue stained polyacrylamide gels revealed 1.1 µg of myosin per 10⁶ cells. Cells, stimulated at 37°C for 0.5 to 5 min, released increasing amounts of histamine, 32% of the total cellular histamine being released in 5 min. Scanning of autoradiograms suggested that the amount of radioactive phosphate associated with the myosin heavy and light chains increased 2-3 fold over that present in nonstimulated controls, during the same time period. Two-dimensional maps of tryptic digests indicated that the light chains were phosphorylated by myosin light chain kinase. Whether this phosphorylation of myosin within intact basophils plays a role in the secretory process is under investigation.

M-Pos201 ISOFORMS OF THE SMOOTH MUSCLE 20 kD MYOSIN LIGHT CHAIN ARE DISTINGUISHED BY POLYCLONAL ANTISERA. B. Gaylinn and R.A. Murphy, Department of Physiology, School of Medicine, University of Virginia, Charlottesville, VA 22908.

Two dimensional gel electrophoresis of swine carotid media preparations reveals four or more apparent forms of the 20 kD myosin light chain (LC₂₀) despite precautions taken to inhibit charge modification [1,2,3]. These include the dephosphorylated and phosphorylated smooth muscle LC₂₀ and two or more "satellite" species which have variously been suggested to represent multiply phosphorylated LC₂₀, charge modified forms, non-myosin species or proteolytic artifacts. When blotted to nitrocellulose only the two species of highest pI were recognized by polyclonal antisera to purified smooth muscle LC₂₀. The satellite species did not react with the antisera. This was true with antisera prepared to avian gizzard LC₂₀ (gift of Dr. David Hathaway) or antisera to canine tracheal smooth muscle LC₂₀ (gift of Dr. James Stull). When the antigenically recognized LC₂₀ was purposefully charge modified (carbamylated) or proteolyzed, antigenicity remained strong. Several lines of evidence suggest that the satellites are forms of LC₂₀: (1) copurification with smooth muscle myosin, (2) reversible Ca²⁺ dependent phosphorylation, and (3) peptide mapping [3]. In agreement with Mougios & Bárány [3], we conclude that the satellites contain a distinct (and possibly non-muscle) isoform that represents as much as 20% of the total LC₂₀ in swine carotid media. This data also suggests that multiple phosphorylation of the antigenic LC₂₀ species is insignificant in intact strips under our conditions. Supported by USPHS grants 5-T32-HL07355 and 5-P01-HL19242. [1]- Driska *et al.*, *Am J Physiol* 240:222(1981) [2]- Gagelmann *et al.*, *BBRC* 120:933(1984) [3]- Mougios & Bárány, *BBA* 872:305(1986)

M-Pos202 CLONING AND CHARACTERIZATION OF SMOOTH MUSCLE MYOSIN LIGHT CHAIN* FROM CHICKEN AND HUMAN TISSUES. C. Chandra Kumar, Paul Zavodny, Mary Petro, Herinder Loinal, Satwant Narula and Paul Leibowitz. Introduced by Jeffrey P. Gardner

Department of Molecular Biology, Schering Corporation, Bloomfield, NJ

In smooth muscles, as opposed to skeletal and cardiac muscles, phosphorylation of Myosin Light Chain₂ (MLC) by MLC Kinase regulates the contraction process. To understand the regulation of smooth muscle contraction and to compare the phosphorylation sites of MLCs in human and chicken smooth muscle tissues, we have undertaken the cloning and characterization of MLCs from human vascular and chicken gizzard smooth muscle tissues. cDNA libraries were constructed in gt10 vector, using poly A⁺ RNA from human umbilical cord and chicken gizzard tissue. Using rat aortic smooth muscle MLC cDNA clone provided to us by Nadal-Ginard et al, we have isolated and characterized the respective MLC cDNA clones. Regions of high homology were found between the chicken and human MLC isoforms. S1 nuclease protection analysis is being carried out to analyze the expression of the MLC isoforms in different smooth muscle and non-muscle tissues.

*Regulatory Myosin Light Chain

M-Pos203 BRUSH BORDER MYOSIN HEAVY CHAIN PHOSPHORYLATION IS REGULATED BY A CALMODULIN-DEPENDENT KINASE. Rieker, J.P., Swanljung-Collins, H., Montibeller, J. and Collins, J.H. Dept. of Microbiology, Biochemistry and Molecular Biology, Univ. Pittsburgh Sch. of Med.

Recent findings from an increasing number of nonmuscle cell types that myosin is phosphorylated on its 200-kDa heavy chains (HC) in vivo suggests that heavy chain phosphorylation, in addition to 20-kDa light chain (LC20) phosphorylation, may regulate some aspects of myosin function. We have identified and characterized a myosin heavy chain kinase activity that is totally dependent on Ca²⁺ and CaM for activity from chicken intestinal epithelial cell brush borders. A partially purified fraction containing this kinase and an apparently distinct, CaM-insensitive light chain kinase catalyzed the incorporation of 0.8 mol P/mol HC and 1.1 mol P/mol LC20 in the presence of CaM and <0.01 mol P/mol HC and 1.1 mol P/mol LC20 in its absence. Phosphorylation in either the presence or absence of CaM activated the actin-activated ATPase activity about ten-fold, to a specific activity of ~50 nmol/min/mg. Phosphorylation of LC20 by gizzard myosin light chain kinase in the presence of CaM gave similar activation. Subsequent phosphorylation by the brush border kinase fraction (an additional 0.2 mol P/mol LC20 and 0.8 mol P/mol HC) did not change the ATPase activity of myosin. This is in contrast to the inhibition of ATPase activity found for some invertebrate myosins and suggests that the mechanism of myosin regulation by HC phosphorylation is different in vertebrate nonmuscle cells. In addition, a separate CaM-stimulated light chain kinase has been identified. Supported by NIH and March of Dimes grants to J.C., NIH Postdoctoral Training Grant to J.R.

M-Pos204 PROTECTION OF MYOSIN IB FROM TRYPSIN-CLEAVAGE BY F-ACTIN. Hanna Brzeska, Thomas J. Lynch and Edward D. Korn, Laboratory of Cell Biology, NHLBI, National Institutes of Health, Bethesda, MD 20892 (Intr. by A.N. Schechter).

Myosins IA and IB from *Acanthamoeba* consist of one light chain and one heavy chain and exhibit actin-activated Mg²⁺-ATPase activity when the heavy chain is phosphorylated. The Mg²⁺-ATPase activity of myosin I shows triphasic dependence on F-actin concentration. Myosin I does not form filaments but does cross-link F-actin. The two last properties can be explained by the existence of two actin-binding sites and their presence has been shown for the myosin IA heavy chain.

In the absence of F-actin, trypsin digests the myosin IB heavy chain (127 kDa) into an NH₂-terminal 62-kDa and a COOH-terminal 68-kDa fragment which undergo further proteolysis. In the presence of F-actin, trypsin-cleavage produces an 80-kDa fragment which is resistant to further proteolysis. This fragment originates from the NH₂-terminal region of the heavy chain, contains the ATP-binding and phosphorylation sites and retains NH₄⁺-ATPase and actin-activated Mg²⁺-ATPase activities, the last, however, being monophasic. The 80-kDa fragment binds to F-actin but does not cross-link it. These results strongly suggest that a second actin-binding site is located in the COOH-terminal 45-kDa region of the myosin IB heavy chain. Addition of ATP to the acto-80-kDa complex allows further digestion of the 80-kDa fragment into an NH₂-terminal 62-kDa fragment, which contains the phosphorylation and ATP-binding sites and possesses NH₄⁺-ATPase but not actin-activated Mg²⁺-ATPase activity. These data demonstrate that F-actin protects a functionally specific segment of myosin IB and that the region lost when the 80-kDa fragment is digested to the 62-kDa fragment is essential for actin-activated Mg²⁺-ATPase.

M-Pos205 PURIFICATION AND CHARACTERIZATION OF ERYTHROCYTE MYOSIN. Masaaki Higashihara, David J. Hartshorne*, and Mitsuo Ikebe. Dep. of Physiol. and Biophysics, Case Western Reserve Univ. *Dep. of Biochem. Nutrition and Food Sci., Univ. of Arizona.

Myosin was purified from bovine erythrocytes by chromatography on DEAE-cellulose, Sepharose CL-4B, hydroxylapatite, and TSK DEAE 5PW column. The purity was above 95% judged by densitometric scanning of the SDS polyacrylamide gel. The purified erythrocyte myosin consisted of 200,000 dalton heavy chain and two light chains whose molecular weights were 20,000 dalton and 17,500 dalton. Molecular weight of light chain of our myosin was different from the previous reports of Wont *et al* and Fowler *et al* (J. Biol. Chem. 260:46-49, 1985 and J. Cell Biol. 100:47-55, 1985) whose molecular weight of light chain was 25-26,000 dalton and 19,500 dalton. Several properties of erythrocyte myosin were studied. 20,000 dalton light chain was phosphorylated by smooth muscle myosin light chain kinase. The activities of K^+ EDTA-ATPase, Ca^{2+} -ATPase and Mg^{2+} -ATPase of myosin at 0.5MKCl and pH 7.5 were 210, 250, and 3.0 nmoles/min.mg, respectively. Mg^{2+} -ATPase activity of myosin was activated about 5 fold by skeletal muscle actin. The dependence of KCl concentration on Ca^{2+} -ATPase activity was similar to that of smooth muscle myosin. The activity (250 nmoles/min.mg at 0.5MKCl) was decreased at the KCl concentration below 0.35M and was reached to 32 nmoles/min.mg at 0.1 MKCl. This depression of Ca^{2+} -ATPase is correlated to the transition of myosin conformation from an extended (6S) to a folded (10S) in case of smooth muscle myosin. Therefore, our results suggest that the conformational transition is also occurred in erythrocyte myosin. Supported by NIH grants AR 38431 to M.I. and HL23615 and HL20984 to D.J.H.

M-Pos206 ISOLATION OF A GENE ENCODING THE NON-FILAMENTOUS MYOSIN FROM ACANTHAMOEBA: FUSION OF MYOSIN AND NON-MYOSIN SEQUENCES. G. Jung, E.D. Korn, and J.A. Hammer III, LCB, NHLBI, NIH, Bethesda, MD 20892.

Acanthamoeba myosin IB (MIB) is an actin-activated ATPase which supports analogs of contractile and motile activity *in vitro*, but which possesses very unusual structural features, the most striking of which are its low Mr heavy chain (125 kDa), its monomeric nature (1 heavy chain/molecule), its roughly globular shape, and its inability to form bipolar filaments. We have isolated and almost completely sequenced a genomic clone encoding the entire 125 kDa MIB heavy chain. The gene spans ~6 kb and contains ~21 introns; the positions of 8 out of the first 16 introns are exactly conserved relative to the rat embryonic myosin heavy chain gene. Approximately three fourths of the deduced ~1150 amino-acid-residue sequence is myosin-like while one fourth is unique. The N-terminal ~90 kDa of amino acid sequence shows strong homology (~55%) with the globular head region of conventional myosins. The C-terminal ~35 kDa of sequence shows no homology to any portion of conventional myosin sequences, is rich in glycine and proline, and clearly cannot participate in forming a coiled-coil structure. These results establish that (1) MIB is a true gene product, i.e. it is not derived from a conventional amoeba myosin by proteolysis, (2) MIB is genetically related to conventional myosins, and (3) MIB has no coiled-coil rod like tail. These results support the conclusion drawn from study of the protein that filamentous myosin is not required for force generation. The results also suggest that the MIB heavy chain may have been generated by gene fusion or exon shuffling events. This gene can now be used to search for MI-like genes in higher eukaryotes and to explore the *in vivo* function of MI.

M-Pos207 THE EFFECT OF CALCIUM ON THE AGGREGATION OF SMOOTH MUSCLE THIN FILAMENTS. W. Lehman, Department of Physiology, Boston University School of Medicine, Boston, MA 02118.

Electron microscopy demonstrates that thin filaments isolated from chicken gizzard smooth muscle in the absence of Ca^{2+} are aggregated into networks. In contrast, thin filaments isolated in the presence of Ca^{2+} are dissociated from each other. Moreover, the respective state of aggregation in each type of preparation is reversible and dependent on Ca^{2+} concentration. Viscometry, a sensitive measure of actin-filament interaction, was used to confirm and quantitate the results of our structural studies on thin filament aggregation. Viscosity measurements indicate that thin filament network formation is associated with an increase in thin filament viscosity; under our set of conditions the apparent viscosity of thin filaments isolated and maintained in EGTA is approx. 3 to 6 times that of those isolated and maintained in Ca^{2+} . Additionally, the relative difference in viscosity between thin filaments isolated in EGTA and those isolated in Ca^{2+} magnifies logarithmically as a function of thin filament concentration, suggesting that at the very high thin filament concentrations present *in vivo*, large Ca^{2+} -dependent changes in thin filament interaction may occur. An increase in viscosity is observed immediately after adding EGTA to Ca^{2+} -treated thin filaments; moreover, the magnitude of the effect is time-dependent. At appropriate antibody concentration, anti-caldesmon Fab fragments block this time-dependent viscosity increase, suggesting an involvement of caldesmon in the thin filament aggregation process. Thin filament aggregation *in vivo* may be responsible for sustaining tension and/or maintaining thin filament alignment during relaxation of smooth muscle.

M-Pos208 AUTOPHOSPHORYLATION OF SMOOTH MUSCLE CALDESMON. Gisele C. Scott-Woo, Department of Medical Biochemistry, University of Calgary, Calgary, Alberta, Canada T2N 4N1.

It is well-established that initiation of smooth muscle contraction is effected by the Ca^{2+} /calmodulin-dependent phosphorylation of the 20,000-dalton light chains of myosin. Smooth muscle contraction may also be regulated by thin filament-associated proteins such as caldesmon, a major actin- and calmodulin-binding protein. In vitro, caldesmon inhibits the actin-activated myosin Mg^{2+} -ATPase; this inhibitory capability is lost when caldesmon is phosphorylated by a copurifying Ca^{2+} /calmodulin-dependent kinase. We have identified this kinase as caldesmon itself by the following criteria: 1) Caldesmon kinase activity copurifies with caldesmon through several chromatographic steps to 97% purity. 2) Both caldesmon and the remaining 3% contaminating proteins react with a monoclonal antibody to caldesmon (generously provided by Dr. J. Bryan, Baylor College of Medicine). The contaminants therefore probably represent proteolytic fragments of caldesmon. 3) Caldesmon binds strongly to AffiGel Blue, an affinity resin which binds proteins, such as kinases, which contain a dinucleotide fold. 4) Caldesmon can be covalently labeled with [α - ^{32}P]8-azido ATP and this labeling is inhibited by the non-hydrolyzable ATP analog, AMP-PNP. Caldesmon kinase exhibits a high degree of substrate specificity. Phosphorylation is an intermolecular reaction and occurs predominantly on serine (~80%) but also on threonine (~20%) residues; no tyrosine phosphorylation is observed. Phosphorylation is stoichiometric and site-specific as revealed by tryptic and chymotryptic peptide mapping and autoradiography. Finally, phosphorylation is pH-dependent, with a pH maximum of 7-7.5, and requires free Mg^{2+} in addition to the MgATP^{2-} substrate; maximal activity is observed at 2 mM Mg^{2+} in the presence of 0.5 mM ATP. (Supported by MRC Canada and AHFMR).

M-Pos209 A 40 kDa CYANOGEN BROMIDE FRAGMENT OF CALDESMON RETAINS CALMODULIN-BINDING PROPERTIES. C.-L.A. Wang and Q. Zhan, Dept. of Muscle Research, Boston Biomedical Research Institute, Boston, MA 02114.

Smooth muscle caldesmon (CaD) binds both calmodulin (CaM) and F-actin, and is thought to play a regulatory role in the process of smooth muscle contraction. Recently Szpacenko and Dabrowska (FEBS Lett. 202, 182, 1986) reported that a 40 kDa fragment of CaD resulting from limited chymotryptic cleavage preserves all functional properties of the intact CaD molecule. We have studied the domain-structure of CaD by CNBr digestion. From the digestion mixture, the CaM-binding peptides were separated using a CaM-sepharose affinity column. The CaM-binding fraction yields three major bands (140 kDa, 95 kDa, and 40 kDa) on NaDodSO₄ polyacrylamide gel electrophoresis. While the two bands with higher molecular weight may correspond to the undigested and/or partially digested CaD, the 40 kDa fragment represents a smaller peptide that still contains the CaM-binding domain. When CaD modified with iodoacetamido-4-nitrobenz-2-oxa-1,3-diazole (IANBD) was subjected to CNBr digestion, the 40 kDa fragment also became fluorescently labeled, suggesting that this CaM-binding fragment contains at least one reactive sulfhydryl group. This fluorescent probe was then used to monitor interactions between the fragment and CaM. Upon addition of CaM in the presence of Ca^{2+} , the NBD fluorescence exhibited a small but reproducible decrease while the intrinsic (tryptophan) fluorescence increased slightly. Work is underway to further characterize this 40 kDa fragment of CaD and to determine whether it is identical with the 40 kDa chymotryptic fragment. This work was supported by grants from NIH and AHA.

M-Pos210 THE EFFECTS OF PHOSPHORYLATION OF SMOOTH MUSCLE CALDESMON. Philip K. Ngai and Michael P. Walsh, Dept. of Medical Biochemistry, University of Calgary, Alberta, Canada T2N 4N1.

Caldesmon is a major calmodulin- and actin-binding protein of smooth muscle which interacts with calmodulin in a Ca^{2+} -dependent manner or with actin in a Ca^{2+} -independent manner. Isolated caldesmon inhibits the actin-activated Mg^{2+} -ATPase of smooth muscle myosin suggesting a possible physiological role for caldesmon in regulating the contractile state of smooth muscle. Caldesmon can be phosphorylated in vitro by a copurifying Ca^{2+} /calmodulin-dependent protein kinase and dephosphorylated by a protein phosphatase, both present in smooth muscle. We have investigated further the phosphorylation of caldesmon and the effects it has on the functional properties of the protein. The kinetics of caldesmon phosphorylation were found to be similar whether the caldesmon substrate was free or bound to actin, actin/tropomyosin or thin filaments. Caldesmon containing endogenous kinase activity was rapidly phosphorylated (to ~1 mol P_i /mol in 5 min) when reconstituted with actin, myosin, tropomyosin, calmodulin and myosin light chain kinase in the presence of Ca^{2+} and MgATP^{2-} . Under conditions in which unphosphorylated caldesmon showed substantial inhibition of the actin-activated myosin Mg^{2+} -ATPase, no inhibition was observed with phosphorylated caldesmon. Binding studies revealed maximal binding of 1 mol unphosphorylated caldesmon/9.5 mol actin and 1 mol phosphorylated caldesmon/11.7 mol actin. All the bound phosphorylated caldesmon could be released by Ca^{2+} /calmodulin, with half-maximal release at 0.11 μM Ca^{2+} , whereas only 62% of the bound unphosphorylated caldesmon could be removed, with half-maximal release at 0.16 μM Ca^{2+} . These observations suggest a possible mechanism whereby caldesmon phosphorylation may prevent its inhibitory action on the actomyosin Mg^{2+} -ATPase. (Supported by MRC Canada and AHFMR).

M-Pos211 AMINO ACID SEQUENCE OF A NOVEL AND ABUNDANT 22 kDa PROTEIN (SM22) FROM CHICKEN GIZZARD SMOOTH MUSCLE. J.R. Pearlstone, M. Weber, J.P. Lees-Miller, M.R. Carpenter and L.B. Smillie, MRC of Canada Group in Protein Structure and Function, Department of Biochemistry, University of Alberta, Edmonton, Alberta, Canada T6G 2H7.

A 22 kDa protein from gizzard smooth muscle, present in a ratio of actin:SM22:tropomyosin=6.5 (± 0.8):2.0(± 0.2):1.0, was found to exist in at least three isoelectric forms, α : β : γ =14:5:1. The most basic variant, SM22 α , is a moderately asymmetrical globular molecule which has similar M_r 's and pI 's to, but different properties from myoglobin, brain 23 kDa protein and troponin-I. Using rabbit antibodies against the gizzard protein, SM22 was shown to be present in several chicken smooth muscle organs but to be absent or at very low levels in skeletal muscle and several other non-muscle tissues. Its presence in beef aorta and porcine carotid has also been demonstrated.

The complete amino acid sequence of SM22 α was elucidated by manual and automated Edman degradation procedures. Suitable fragments were generated by proteolytic and chemical cleavages. The protein, consisting of 197 residues, has a M_r of 21,978 by sequence determination. Its net charge at neutral pH is +4 $\frac{1}{2}$. Typical of a globular protein, SM22 α has alternating hydrophilic and hydrophobic portions along its length. Secondary structural analysis using several algorithms predicts approximately 31% α -helix, 24% β -sheet, 18% β -turn and 27% random coil. No significant homology was found with any previously determined amino acid sequence when SM22 α was subjected to a search against the National Biomedical Research Foundation protein sequence databank, Washington. (Supported by MRC of Canada.)

M-Pos212 Effect of Caldesmon on the Binding of Skeletal Muscle Myosin Subfragments to Actin. M. E. Hemric, C. E. Benson, N. E. Oakes and J. M. Chalovich; East Carolina University Medical School; Greenville, NC 27858.

We reported earlier that the inhibition by caldesmon of skeletal muscle S-1 catalyzed hydrolysis of ATP is correlated with decreased binding of S-1 \cdot ATP to actin (Biophys. J. 49, 67a). In contrast, the binding of smooth muscle HMM \cdot ATP has been reported to be enhanced by caldesmon (Lash *et al.*, Biophys. J. 49, 390a). We now report the results of binding studies of skeletal muscle S-1 and HMM to skeletal muscle actin saturated with smooth muscle tropomyosin and caldesmon in the presence of various nucleotides. Caldesmon was found to be a competitive inhibitor of S-1 binding in the presence of PPi, AMP \cdot PNP and in the absence of nucleotide as well as in the presence of ATP. In no case has it yet been possible to demonstrate the simultaneous binding of S-1 and caldesmon to actin. Caldesmon was found to inhibit ATP hydrolysis by skeletal muscle HMM. At 70 mM ionic strength and 50 μ M actin, the ATPase activity was 90% inhibited at 3.7 μ M caldesmon monomer. In contrast to S-1, the binding of HMM \cdot ATP actually increased 40% at this caldesmon concentration. This binding increased steadily, without evidence of saturation, reaching 220% of the initial value at 10 μ M caldesmon. The binding of HMM in the presence of PPi, AMP \cdot PNP or in the absence of nucleotide is, however, inhibited by caldesmon. It is therefore considered unlikely that the enhanced binding of skeletal muscle HMM \cdot ATP in the presence of caldesmon is directly related to inhibition of ATP hydrolysis.

M-Pos213 QUINONE-BINDING MUTATIONS IN REACTION CENTERS: DELAYED-LUMINESCENCE MEASUREMENTS AS A PROBE OF ELECTRON TRANSFER ΔG_0 IN R. SPHAEROIDES. C. C. Schenck, Department of Biochemistry, Colorado State University, Fort Collins, CO 80523 (Intr. by T. N. Solie).

We would like to know how protein structure determines the spectroscopic, thermodynamic and kinetic properties of the photosynthetic reaction center. We are focusing our attention on the effects of structural mutations in the quinone binding region of the protein. A flash fluorometer is being constructed that will enable us to measure the emission from the back reaction P^+Q^- P^*Q with sub microsecond time resolution. Thus, we can calculate the free energy change accompanying electron transfer from P^* to P^+Q^- and other relaxations. We can determine how structural perturbations in the protein alter these parameters. This instrument will be described together with our most recent experimental results.

Additionally, plasmid vectors are being constructed that will allow us to move site-directed mutant alleles of reaction center genes into appropriate recipient strains. Our progress toward establishing a generalized system of site-directed mutagenesis in R. sphaeroides will be described.

M-Pos214 THE EFFECT OF UBIQUINONE TAIL LENGTH ON QB ACTIVITY IN RECONSTITUTED PHOTOSYNTHETIC REACTION CENTER PROTEOLIPOSONES C.C. Moser and P.L. Dutton. Dept. of Biochemistry and Biophysics, Univ. of Penna., Phila., Pa. 19104

The degree of secondary quinone (Q_b) activity in bacterial photosynthetic reaction centers (RC), isolated from Rhodospseudomonas sphaeroides and co-reconstituted into proteoliposomes with ubiquinone (UQ), can be assayed by means of the biphasic relaxation kinetics of flash oxidized bacteriochlorophyll dimer. The dependence of Q_b activity on the UQ to RC ratio during reconstitution follows the behavior expected of a simple binding equilibrium between UQ bound in the Q_b site, and UQ free as pool quinone in the artificial membrane, and may be described by a dissociation constant. Reconstitution with a series of synthetic UQs with different isoprene tail lengths reveals a monotonically decreasing affinity of the Q_b site for UQ relative to the membrane as the number of isoprenes is increased from 3 to 6. This is consistent with the increasing hydrophobicity of this series increasingly favoring the partitioning of UQ into the lipid membrane relative to the Q_b site. However, this trend is reversed for UQ tails longer than 7 isoprene units, indicating that increased hydrophobicity is no longer correlated with less Q_b activity. These observations may be explained by supposing that only UQ with a tail greater than 6 isoprene units can simultaneously have both its redox reactive head in the Q_b site and the end of its tail in the hydrophobic membrane environment. Supported by NSF PCM 09202 and USPHS GM27309.

M-Pos215 EFFECT OF HYDROCARBON TAIL STRUCTURE ON THE AFFINITY OF SUBSTITUTED QUINONES FOR THE Q_A AND Q_B SITES IN REACTION CENTER PROTEIN OF RHODOPSEUDOMONAS SPHAEROIDES R26 K.Warncke, M.R. Gunner, B.S.Braun, C.-A.Yu⁺, and P.L. Dutton. Intro. by S. Meinhardt Dept. of Biochem. and Biophys., Univ. of Penn., Phila., PA 19104 and +Oklahoma St. Univ., Stillwater, OK. 74078

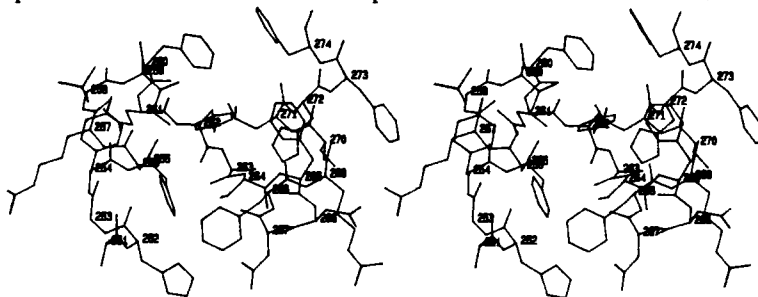
The dissociation constants (K_d) of various UQ derivatives for the Q_A site of solubilized reaction center protein (RC) have been correlated with hydrocarbon tail length and structure. Addition of 3'-methyl-2'-butene (isoprenoid) units resulted in a marked enhancement of quinone affinity ($-\log K_d$ UQ₀=5.1; UQ₁=7.3; UQ₂>10). The corresponding saturated straight-chain or methyl-branched derivatives of like carbon number bound much weaker (5 carbon aliphatic derivative 2.0 kcal>UQ₁; 10 carbon derivative 3.5 kcal>UQ₂). Desaturation at carbon 4' of UQ₂ weakens the affinity (relative to UQ₂) by 5 kcal. This indicates a requirement for rotational freedom about the C4'-C5' bond. Therefore, the first two 3'-methyl-2'-butene units are seen to interact with a binding region that is essential in generating the affinity and specificity for the quinone at the Q_A site.

In contrast, affinity of UQ for the Q_B site increases little with tail length. Thus the affinity for short-tailed UQs is comparable at the Q_A and Q_B sites but for UQs with tails greater than 5 carbons the Q_B affinity is substantially weaker. Also, there is little variation in affinity with change in tail structure, so no specificity for the isoprenoid UQs is evident. Supported by NSF Grant PCM 82-09292.

M-Pos216 A HYPOTHETICAL TERTIARY STRUCTURE FOR THE Q_B-BINDING POCKET OF THE PHOTOSYSTEM II REACTION CENTER PROTEIN D1.

Howard Robinson and Antony Crofts, Physiology and Biophysics, Univ. of Illinois, Urbana, IL 61801

The stereogram below is a preliminary model for the tertiary structure of the plastoquinone binding pocket (the Q_B-binding site) of the photosystem II reaction center protein D1 of *Anacystis nidulans* R2 based on structural and functional homologies with the L subunit of the reaction center of *Rps. viridis* (Deisenhofer, J., et al., 1984 J.Mol.Biol.180, 385-398.) Our hypothetical tertiary structure for D1 is justified by the following analogies; 1) locations of histidines; 2) herbicide resistance sites; 3) locations of hydrophobic and hydrophilic residues. The model enables us to predict the involvement of specific residues in the mechanism of plastoquinone reduction with



respect to; 1) binding of the quinone ring [residues 255, 264, 268 and 271]; 2) binding of the first member of the isoprenoid tail [residues 259, 260, 262, 265 and 274]; 3) stabilization of the semiquinone [residues 255, 262 and 264]; 4) protonation of the quinone [residues 252 and 267]; 5) electron transfer [residues 255 and 268]. The viewpoint of the figure is from the reaction center non-heme iron with the stroma-membrane interface toward the bottom.

M-Pos217 LIGHT INDUCED PROTON UPTAKE BY RCs FROM *R. SPHAEROIDES* R-26.1.* P.H. McPherson, M.Y. Okamura, G. Feher, U.C.S.D., La Jolla; M. Schonfeld, The Hebrew Univ. of Jerusalem, Israel.

Proton uptake following photo-reduction of Q_A in isolated RCs has been reported to be less than 1 H⁺/e⁻ for 6 < pH < 11 (1). This result is in disagreement with redox titrations of the Q_A/Q_A⁻ couple in chromatophores and liposomes, which predict a proton uptake of 1 H⁺/e⁻ for pH < 9. We have measured the light induced proton uptake by isolated RCs using a different method than in (1), and confirm this discrepancy. Proton uptake accompanying formation of D⁺Q_A⁻, DQ_A⁻ (Fig. 1), and D⁺Q_AQ_B⁻, DQ_AQ_B⁻ (not shown) was monitored with a glass pH electrode. The data for DQ_A⁻ was fitted with a model in which proton uptake results from positive shifts in pK_a (indicated by arrows in Fig. 1) of three titratable groups. Proton uptake of D⁺Q_A is less than that of DQ_A⁻, because of proton release associated with the formation of D⁺ (1). The difference in proton uptake between D⁺Q_AQ_B⁻ and D⁺Q_A⁻ is in good agreement with that predicted from the free energy difference between the states D⁺Q_AQ_B⁻ and D⁺Q_A⁻ in isolated RCs (2). The discrepancy in the results for isolated RCs and chromatophores/liposomes is at present not understood.

*Work supported by NSF.

(1) P. Maroti, C.A. Wraight (1986) VII Int. Cong. Photosyn. (abstract). (2) D. Kleinfeld, M.Y. Okamura, G. Feher (1984) BBA, 766, 126.

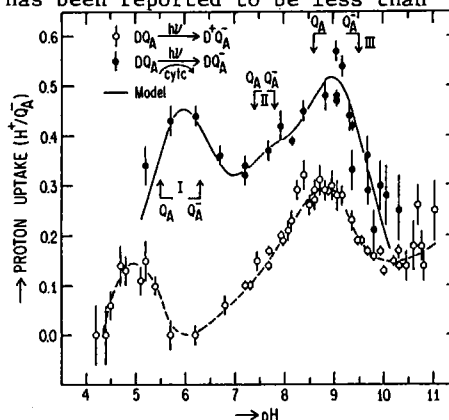


Fig. 1. Proton uptake by RCs(1Q/RC); corrected for cyto contribution.

M-Pos218 THE REACTION OF CYTOCHROME c₂ WITH RHODOPSEUDOMONAS SPHAEROIDES REACTION CENTER INVOLVES THE HEME CREVICE DOMAIN. J. Hall, F. Millett, X. Zha, B. Durham, and P. O'Brien. Dept. of Chemistry and Biochemistry, University of Arkansas, Fayetteville, AR, 72701

In order to define the interaction domain on *R. sphaeroides* cytochrome c₂ for the photosynthetic reaction center, positively charged lysine amino groups on cytochrome c₂ were modified to form negatively charged carboxydinitrophenyl (CDNP) lysines. The reaction mixture was separated into 7 different fractions by ion exchange chromatography on CM-52 and DEAE agarose. HPLC peptide mapping was used to determine that fraction A consisted of a mixture of singly labeled derivatives modified at lysines 35, 88, 95, 97, and 105. Although it was not possible to further resolve these derivatives, all of the labeled lysines are located on the front surface of cytochrome c₂ near the heme crevice. The second order rate constant for the reaction of native cytochrome c₂ with reaction centers was found to be $2.0 \times 10^8 \text{ M}^{-1} \text{ s}^{-1}$, while that for fraction A was 8-fold less, $2.8 \times 10^7 \text{ M}^{-1} \text{ s}^{-1}$. This suggests that lysines surrounding the heme crevice of cytochrome c₂ are involved in electrostatic interactions with carboxylate groups at the binding site of the reaction center. The reaction rates of horse heart cytochrome c derivatives trifluoroacetylated at single lysine amino groups were also measured. Modification of lysines 8, 13, 27, 72, 79 and 87 surrounding the heme crevice was found to significantly lower the rate of reaction, while modification of lysines in other regions had no effect. This indicates that horse heart cytochrome c also reacts at its heme crevice region. We thank Dr. Robert Bartsch for a gift of *R. sphaeroides* cytochrome c₂, and Dr. Melvin Okamura for a gift of purified reaction centers. Supported by NIH Grants GM20488 and RR07101.

M-Pos219 THE REACTION BETWEEN CYTOCHROME c_2 AND REACTION CENTERS FROM *RHODOSPIRILLUM RUBRUM*.

F. Millett, D. Knaff, H. van der Wal, and R. van Grondelle. Univ. of Arkansas, Fayetteville, AR, 72701; Texas Tech Univ., Lubbock, Texas; Univ. of Leiden, The Netherlands.

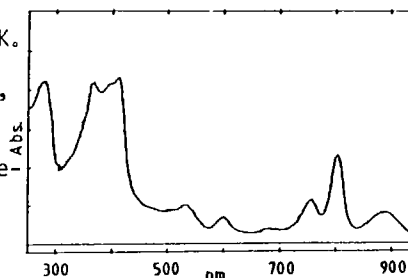
The oxidation of cytochrome c_2 by photooxidized reaction center P-870⁺ in chromatophores from *R. rubrum* followed second order kinetics at all ionic strengths, with no evidence for tight binding between the reactants even at low ionic strength. Similar results were obtained for the reaction between purified reaction centers and cytochrome c_2 . The second order rate constant was maximal at 30 mM ionic strength, and decreased with both increasing and decreasing ionic strength. The decrease in the rate constant with increasing ionic strength suggests the importance of electrostatic interactions between lysine amino groups surrounding the heme crevice of cytochrome c_2 and carboxylate groups at the binding site on the reaction center. However, the decrease in rate constant observed upon lowering the ionic strength below 30 mM is unexplained, and suggests that non-productive binding modes might be present. The reaction involving horse heart cytochrome c showed a greater dependence on ionic strength than that for cytochrome c_2 , indicating a stronger electrostatic interaction. The reactions of horse heart cytochrome c derivatives each modified at a single lysine amino group with a trifluoromethyl-phenylcarbonyl were also studied. Modification of lysines 8, 13, 27, 72, 79, and 87 surrounding the heme crevice was found to significantly lower the rate of the reaction, while modification of lysines in other regions had no effect. This suggests that the binding domain on horse heart cytochrome c is located at the heme crevice. Supported by NIH grants GM20488 and RR07101 and NSF grant DMB 84-08564.

M-Pos220 PURIFICATION AND PROPERTIES OF REACTION CENTERS FROM *Chromatium tepidum*

Tsunenori Nozawa, Jeffrey T. Trost and Robert E. Blankenship
Department of Chemistry, Arizona State University, Tempe, AZ 85287

Chromatium tepidum is a thermophilic purple sulfur photosynthetic bacterium (M. Madigan, Int., J. Syst. Bact., 36, 222-27, 1986). We have purified and partially characterized a reaction center complex from this organism. Chromatophores were treated with 0.25% LDAO at 40°C and the resulting crude reaction center fraction chromatographed on DEAE cellulose to remove light-harvesting complexes. Final purification was achieved using DEAE ion-exchange and S-300 gel filtration HPLC columns. The complex has a UV-VIS absorption spectrum characteristic of purple bacterial reaction centers, with peaks at 280, 365, 411, 531, 599, 755, 801, and 880 nm. The long wavelength band shifts to 892 nm at 77K. The complex is photoactive, with a room-temperature decay time of P880⁺ of 20 ms. SDS-PAGE analysis reveals four peptides of MW 49, 33, 28, and 22 kDa. The heaviest peptide stains positively for heme. Redox difference spectra indicate a hydroquinone-reducible c-type heme with α -band maximum at 556 nm, as well as a dithionite-reducible heme at 553 nm. Under some conditions reaction centers devoid of cytochrome can also be prepared.

Supported by grants from the Japanese Ministry of Education (T.N) and the Competitive Research Grants Office of the USDA (RB) 84-CRKR-1-1523.

**M-Pos221 INFRARED SPECTROELECTROCHEMISTRY OF BACTERIOCHLOROPHYLLS AND BACTERIOPHEOPHYTINS: MODELS FOR THE INTERACTION OF THE PIGMENTS IN REACTION CENTERS OF PHOTOSYNTHETIC BACTERIA**

W. Mäntele[†], A. Wollenweber[†], E. Nabedryk* and J. Breton* (Intr. by P. Ripoche)

[†]Institut für Biophysik und Strahlenbiologie, Universität Freiburg, D-7800 Freiburg, FRG

*Service de Biophysique, CEN Saclay, 91191 Gif-sur-Yvette cedex, France

Fourier-transform infrared (FTIR) difference spectra of the electrochemically generated radicals of isolated bacteriochlorophylls and bacteriopheophytins were used to follow molecular changes upon one-electron oxidation or reduction. With a new type of electrochemical cell developed by us, in situ electrolysis could be performed with spectroscopic control over the whole range from 200 nm to 10000 nm. Optical and infrared spectra of the oxidation and reduction processes indicate that, in the case of BChl a, more than 95 % of the cation can be formed with more than 90 % of it being reversible. For the IR-difference spectra of BChl a and b cation formation, a remarkable similarity in the carbonyl frequency region is found with the difference spectra of the photooxidation of the primary electron donor P in RC containing BChl a or b. Thus, by comparison, band assignments as well as conclusions for the interaction of the pigments in vivo are possible. At least one of the ester C=O vibrations, although not involved in the conjugated system, shows strong absorbance changes upon cation radical formation. They may be interpreted as a formation of a free C=O bond which has been ligated before. For the keto C=O vibration, a shift as well as an absorbance change is observed, indicating a transition from a ligated to a free form as well. In case of bacteriopheophytin a or b anion formation, the absorption of the ester C=O vibrations decreases. In the model compound, both esters absorb at the same position. In RC split ester C=O bands are observed indicating a different type of interaction with the protein.

M-Pos222 TEMPERATURE DEPENDENCE OF ELECTRON TRANSFER IN A MODEL FOR THE PHOTOSYNTHETIC REACTION CENTER. John Delaney and David Mauzerall, The Rockefeller University, 1230 York Avenue, New York, NY 10021 and John Lindsey, Carnegie-Mellon, 4400 5th Avenue, Pittsburgh, PA 15213.

The temperature variation of the bi-exponential fluorescence lifetime of a tetrabridged co-facial zinc porphyrin-quinone polymacrocyclic (ZnPQ) was analysed in terms of rates of electron transfer and the equilibration between two conformers. Between 100K and 190K the equilibrium constant has an enthalpy of 2.2 kcal/mole, with the conformer showing the shorter lifetime having the higher energy. Below 190K the ratio of conformers remains constant indicating a freezing out of the equilibration. The molecule is complex enough to have a glass transition. The glass transition of the solvent (methanol:ethanol; 1:4) is at about 120K. The rate constant for electron transfer from the 'slow' conformer is constant at $2 \times 10^8 \text{ s}^{-1}$ between 300K and 190K, then decreases with an activation energy of 1.2 kcal/mole. This suggests that a sub conformation along the path to isomerization with this electron tunneling time is readily available above 190K but is frozen out at lower temperature along with the equilibration of the conformers. The rate constant for the 'fast' conformer varies only slightly, 1.5 to $3 \times 10^9 \text{ s}^{-1}$, between 300K and 77K, confirming the electron tunneling mechanism. There is an indication of a break at 190K, and the overall slightly negative activation energy may be caused by sub conformers with different rotation angles along the porphyrin-quinone axis. The 'fast' conformer is assigned to the inverted conformer with the shorter porphyrin quinone distance, and the mean difference in distance between the two conformers is fit with a tunneling parameter of $1-2 \text{ \AA}^{-1}$.

This work was supported by a grant from the NSF DMB-83-16373 and by the Rockefeller University.

M-Pos223 SOLVENT DEPENDENCE OF CHLOROPHYLL AND BACTERIOCHLOROPHYLL Soret EXCITATION RESONANCE RAMAN SPECTRA Patricia M. Callahan and Therese M. Cotton, Department of Chemistry, University of Nebraska, Lincoln, NE 68588-0304

To obtain a more complete understanding of the resonance Raman (RR) spectra of native chlorophyll proteins, the vibrational spectra of a series of isolated chlorophyll pigments have been obtained. Soret excitation RR spectra contain information about the chlorophyll macrocyclic ring vibrations and the ketyl and acetyl ($\text{C}=\text{O}$) group stretching frequencies are observed in the $1600-1700 \text{ cm}^{-1}$ region. The coordination sensitive vibrations previously described for visible excitation RR for 5 and 6 coordinate Bchl *a* (1) are found to pertain also with Soret excitation. The high frequency characteristic marker bands are at 1609 and 1530 cm^{-1} for 5 coordinate and 1595 and 1520 cm^{-1} for 6 coordinate, monomeric Bchl *a*. Upon formation of aggregated Bchl *a*, the most intense band in the spectrum indicative of 5 coordinate Mg^{2+} shifts slightly to 1615 cm^{-1} and its intensity is dramatically increased. We also report here the first RR spectra of monomeric Chl *a*, Chl *b* and Bchl *a* in aqueous/detergent solvent environments. With reference to the above Bchl *a* assignments and previously reported chlorophyll coordination sensitive vibrations (2), it is concluded that the chlorophyll pigments are 5 coordinate. The ketyl and acetyl stretching vibrations are very broad and centered at 1685 and 1660 cm^{-1} , respectively, with a bandwidth of 30 cm^{-1} . The characteristics of these spectra are important to be able to distinguish protein-bound chlorophyll pigments from detergent-solubilized denatured systems.

(1) Cotton, T.M. and VanDuyne, R.P., (1981) J. Am. Chem. Soc., **103**, 6020-6026.

(2) Fujiwara, M. and Tasumi, M. (1986) J. Phys. Chem., **90**, 250-255.

M-Pos224 PHOTOVOLTAIC PROPERTIES OF SANDWICH CELLS OF CHLOROPHYLL *a*, *b* AND ZINC PORPHYRIN COMPLEXES.

A. Désormeaux^a, J.-J. Max^a, S. Hotchandani^a, M. Ringuet^b and R.M. Leblanc^a, ^a Centre de recherche en photobiophysique and ^b Département de chimie-biologie, Université du Québec à Trois-Rivières, C.P. 500, Trois-Rivières, Québec, CANADA, G9A 5H7.

The primary photochemical event in the photosynthesis is the light-induced charge separation. To better understand this phenomenon, the photovoltaic studies of sandwich cells of chlorophyll *a*, *b* and Zn-carboethoxy-2-trihexyl-7,12,17-tetramethyl-3,8,13,18-porphin have been carried out. We have used the Langmuir-Blodgett monolayer technique to simulate the orientation of the pigments *in vivo*. The cells have been prepared by sandwiching the pigment multilayers between two dissimilar semi-transparent metal electrodes, i.e. aluminum and silver, with work functions (ϕ) as $\phi_{\text{Al}} < \phi_{\text{pigment}} < \phi_{\text{Ag}}$. All cells exhibit photocurrent and photovoltage. The power conversion efficiencies of the cells measured at their respective absorption maxima have been measured for light intensity of $\sim 10 \text{ } \mu\text{W cm}^{-2}$. The action spectra of the cells illuminated through aluminum and silver electrodes are compared with their absorption spectra. The photoactive region has been found to be at the rectifying Al/pigment junction and the excitons are the precursors of charge carriers. The internal resistance calculated at the maximum power of the cells by the method of impedance matching has been obtained. The capacitance measurements have also been carried out to investigate the characteristics of the metal/semiconductor contact. The capacitive behavior at low frequencies (0.005 Hz and 0.01 Hz), in dark and under illumination, suggests the presence of large number of trapped charge carriers which are mobilized by light. The influence of the molecular structure of pigments and of the insulating layer on the photovoltaic properties of cells will also be presented.

M-Pos225 A PORTABLE DOUBLE-FLASH SPECTROPHOTOMETER FOR MEASURING THE KINETICS OF ELECTRON TRANSPORT COMPONENTS IN INTACT LEAVES

David M. Kramer, Omar Adawi, Philip D. Morse, II, and Antony R. Crofts.
Dept. of Physiology and Biophysics, Univ. of Illinois, Urbana, Illinois USA.

We are developing a portable Joliot-type spectrophotometer which uses a measuring flash to study absorbance changes induced by an actinic flash in living plant leaves. The advantages of this type of spectrophotometer are: i) the signal-to-noise ratio during measurement is high due to the intense (but brief) measuring flash; ii) the integrated intensity of the measuring flash is low, therefore no significant activation of photosynthesis occurs; iii) the time resolution is 2 usec and the noise level is independent of the experimental time range so that at times <100 usec the signal-to-noise ratio is greatly improved compared to conventional spectrophotometers. Noise levels are at present < 80 ppm. The instrument is battery-operated, computer-controlled, and has a liquid crystal display to enable graphic observation of the measured absorbance changes as a function of time. A plastic fiber-optics light guide permits measurements to be conducted in the visible region. Interchangeable interference filters with center wavelengths at 515 nm, 545 nm, 554 nm, 563 nm, and 572 nm are used to study absorbance changes associated with electrochromism, P-700, cytochrome f, cytochrome b₆, and plastocyanin (Joliot, P. and Joliot, A. *Biochim. Biophys. Acta* 765, 1984, 210-218). Data obtained from measurements conducted in the field can be transferred through a serial interface to a laboratory-based computer for storage and further analysis.

M-Pos226 REACTION OF SUBSTRATE ANALOGS, NH₂OH and H₂S, WITH THE PHOTOSYNTHETIC WATER-OXIDIZING COMPLEX. M. Sivaraja, D. Hunziker and G. C. Dismukes, Princeton University, Department of Chemistry, Princeton, NJ 08544, USA.

The reaction of the S-states of the water-oxidizing complex (WOC) in Photosystem II membranes with the substrate analogs NH₂OH and H₂S has been investigated by titration of several endogenous paramagnetic donor signals using EPR spectroscopy, steady-state O₂ rate and manganese release. In the dark, the S₁ state binds 3-4 NH₂OH/PSII reversibly by a cooperative process. This is seen as a loss of the ability to generate the S₂ multiline EPR signal at 200K, as well as by a parallel loss in the g 4.1 EPR signal produced at 150K. These two signals behave as though they arise from a single species. Following turnover by laser pulses at 277 K the reaction with NH₂OH results in a two flash delay of the characteristic quaternary oscillation pattern for the multiline signal, indicating that a 2-electron reduction has occurred. When the S₂ state is generated first by a flash and then mixed with NH₂OH the reduction reaction is completed faster than we can measure in a few seconds, indicating that S₂ is the state involved in the 2-electron reduction. The reduction of S₂ occurs even at 150K, indicating that an inner sphere mechanism is likely involved in which at least one NH₂OH molecule binds directly to Mn(III) in the dark (S₁ state). At higher concentrations (0.5 mM) NH₂OH reacts irreversibly with the S₁ state in the dark to release 3 out of 4 Mn/PSII in parallel with the loss of the multiline signal and O₂ evolution. H₂ completely inhibits steady state O₂ evolution along with release of Mn and the three extrinsic polypeptides of the WOC at around 5 mM. 50% loss of the S₂ multiline EPR signal is seen at about 100 μM H₂S, a concentration at which only 10% activity is lost. Like NH₂OH, H₂S seems to have two modes of reaction with the WOC, one reversible and the other irreversible.

Research supported by DOE Soleras Program: DE-F602-84CH10199 and the NJ Comm. on Science Tech.

M-Pos227 BINDING OF LIGANDS TO THE Cl⁻-BINDING SITE OF THE O₂-EVOLVING CENTER OF PHOTOSYSTEM II. Warren F. Beck, Thomas Zewert, and Gary W. Brudvig, Department of Chemistry, Yale University, New Haven CT 06511.

Primary amines and F⁻ inhibit photosynthetic O₂ evolution activity by displacing Cl⁻ from a site on the O₂-evolving center (OEC) of photosystem II (Sandusky and Yocum (1986) *Biochim. Biophys. Acta* 849, 85). We have employed low-temperature EPR spectroscopy to determine the effect of amines, hydroxylamines, or F⁻ on the Mn site in the OEC. When untreated spinach PSII membrane samples are illuminated at 210K, the S₂ state multiline EPR signal is produced as a result of oxidation of the Mn site. In contrast, PSII membrane samples treated at low Cl⁻ concentrations with NH₃, CH₃NH₂, or F⁻ exhibit a stable form of the S₂ state g=4.1 EPR signal at the expense of the S₂ state multiline EPR signal after illumination at 210K. The addition of Cl⁻ or Br⁻ reverses this effect of NH₃, CH₃NH₂, or F⁻ on the S₂ state EPR signals. These results show that displacement of Cl⁻ from a binding site on the OEC in the S₁ state shifts the configurational equilibrium between the forms of the OEC exhibiting the S₂ state g=4.1 and multiline EPR signals (Beck and Brudvig (1986) *Biochemistry* 25, in press) so that the form exhibiting the g=4.1 EPR signal is favored. The intensity of the S₂ state multiline EPR signal produced in PSII membranes by illumination at 210K decreases exponentially with increasing dark incubation time at 0°C in the presence of hydroxylamine or N-alkylhydroxylamines. The kinetics of this dark reaction with the Mn site in the S₁ state are slowed with increasing Cl⁻ concentration and with decreasing pH. Thus, the hydroxylamines probably bind to the Cl⁻-binding site as free base amines prior to reacting with the Mn site through an electron transfer reaction. We suggest, then, that primary amines, hydroxylamines, and F⁻ bind in the S₁ state to a common Cl⁻-binding site in close proximity to the Mn site in the OEC. (Supported by the National Institutes of Health (GM32715), the Chicago Community Trust/Searle Scholars Program, the Camille and Henry Dreyfus foundation, and a National Science Foundation Graduate fellowship to W.F.B.)

M-Pos228 **ENERGETICS OF THE WATER OXIDATION REACTION OF PHOTOSYSTEM II.** Julio C. de Paula and Gary W. Brudvig, Department of Chemistry, Yale University, New Haven, CT. 06511.

The oxidation of H_2O by Photosystem II (PSII) occurs at a tetranuclear Mn complex, the O_2 -evolving center (OEC), which exists in five intermediate oxidation states, the S_i ($i = 0$ to 4) states. Based on the interpretation of the magnetic properties of the S_2 state, it has been proposed that the OEC assumes a cubane-like Mn_4O_4 structure in the S_2 state (de Paula et al. (1986) J. Am. Chem. Soc. 108, 4002). Furthermore, studies on the binding of NH_3 to the OEC suggest that the Mn site binds substrate only after the S_2 state is formed (Beck et al. (1986) J. Am. Chem. Soc. 108, 4018). Using this information, Brudvig and Crabtree (Proc. Natl. Acad. Sci. USA (1986) 83, 4586) proposed a mechanism for photosynthetic water oxidation where the binding of two H_2O molecules during the S_2 to S_3 state transition causes the Mn site to change from a cubane-like to an adamantane-like geometry. In this contribution, we consider the energetic constraints of the four-electron oxidation of H_2O to O_2 during the S_4 to S_0 state transition. The formalism outlined by Krishtalik (Biochim. Biophys. Acta (1986) 849, 162) was used to obtain the configurational free energy change of several four- and two-electron reactions. The mechanistically important consequences of our calculations are: (i) O_2^{2-} , and not H_2O , is the species which undergoes oxidation; (ii) the concomitant release of two protons and O_2 in the S_4 to S_0 transition is coupled to a change in pK_a of OH^- groups bound to Mn; (iii) this change in pK_a is a consequence of the structural rearrangement of the Mn site from an adamantane-like S_4 state to a cubane-like S_0 state; (iv) prior to release into the intrathylakoid space, protons are bound to basic protein groups.

M-Pos229 **EFFECT OF OXYGEN EVOLUTION INHIBITORS ON Cl^- BINDING TO PHOTOSYSTEM II.** W.J. Coleman¹, Govindjee^{1,2}, and H.S. Gutowsky³, Departments of ¹Plant Biology, ²Physiology and Biophysics and ³Chemistry, University of Illinois, Urbana, IL. 61801

Treatments capable of inhibiting the oxygen-evolving complex (OEC) were used to study Cl^- binding to Cl^- -depleted PS II membranes by ^{35}Cl -NMR. In previous studies of the Cl^- NMR binding curve, linewidth maxima and minima were found and attributed to Cl^- -induced conformational changes in the OEC polypeptides. They persist even after washing with 1.0 M NaCl to remove the 18kD and 24kD proteins, if Ca^{2+} is added. Removal of all of the extrinsic polypeptides by washing with 1.0M $CaCl_2$ substantially alters the binding curve, producing narrow linewidths at low Cl^- and a single, broad linewidth maximum centered at 0.5 mM Cl^- . The presence of this residual binding indicates that intrinsic proteins (e.g. D2) must also participate in functional Cl^- binding. Mild heating (38°C 3min) partially inhibits O_2 -evolution and flattens-out the maxima and minima in the binding curve, suggesting partial denaturation of the proteins involved in Cl^- binding/ O_2 -evolution, such that conformational changes are disrupted. Treatment of PS II membranes with 1.5 mM NH_2OH shifts these features to lower $[Cl^-]$. The persistence of significant Cl^- binding after substantial removal of Mn indicates that Mn is probably not directly involved in Cl^- binding. Washing with 0.8 M Tris-phosphate (pH 8.0) produces a binding curve qualitatively similar to that for $CaCl_2$ washing, but with much narrower overall linewidths and a greatly reduced (by >50%) linewidth maximum at 0.5 mM Cl^- . This reduction in $\Delta\nu$, compared to the linewidths observed after $CaCl_2$ washing, may result from Tris-induced denaturation of intrinsic proteins. We conclude from these studies that interaction between the 33 kD polypeptide and certain intrinsic polypeptides is necessary for the Cl^- binding observed in native PS II membranes.

M-Pos230 **EVIDENCE FOR INVOLVEMENT OF AT LEAST TWO BOUND QUINONES IN FERREDOXIN MEDIATED PHOTOSYNTHETIC CYCLIC ELECTRON TRANSFER.** J.W. McGill and J.C. Salerno, Dept. of Biology and Biophysics Group, Renns. Poly. Inst., Troy NY, 12180.

Recently, we have described ferredoxin catalyzed transfer of electrons to the b cytochromes in purified cytochrome b_6f complex. We have studied the effects of various inhibitors on this reaction, which may represent part of photosynthetic cyclic electron transfer. 20 μM UHDBT was sufficient to inhibit cyt b reduction by 70%. At 100 μM , less than 15% of the cyt b could be reduced. 100 μM HHNQ caused complete inhibition of this activity. 50% inhibition was achieved at 40 μM inhibitor. We have yet to see an appreciable antimycin A effect. The possibility that these quinone analogs act allosterically seems unlikely. A large free radical signal generated during turnover, which we attribute to ubi- or plastosemiquinone, is quenched by these inhibitors. The inability of UHDBT to fully inhibit the cyt b reduction suggests the involvement of 2 quinone binding sites acting in parallel, only one of which rapidly binds UHDBT. HHNQ blocks both routes of quinone mediated b reduction, suggesting either that the electrons enter the complex through a 'Qc' type site or through a third site that also binds HHNQ. We have noted a ferredoxin-induced oxidation of both the cyt b and cyt f in the presence of NADPH. When either more ferredoxin or NADPH is added to the system in which the cyt b are partially reduced, both the cyt b and cyt f can be partially oxidized. We believe that the cyt b oxidation occurs via a semiquinone radical generated by ferredoxin, as suggested by Chain. We propose that a Reiske center oxidation by a bound semiquinone at a 'Qz' type site leads to the observed cyt f oxidation. Cyt b probably reduces that site to the radical state, since at initially low levels of cyt b reduction, the induced oxidation is smaller.

M-Pos231 **ABSORPTION AND CIRCULAR DICHROIC SPECTRA OF APO-PLASTOCYANIN.** Stewart Durell, George Anderson and Elizabeth Gross, Dept. of Biochemistry, The Ohio State University, Columbus, Ohio, 43210 and James Draheim, Dept. of Chemistry, Univ. of Toledo, Toledo, Ohio.

Plastocyanin (PC) prepared by two different methods was used to evaluate the relative contribution of charge transfer (CT) transitions and conformational changes to near-UV CD and absorption spectra. Apo-PC prepared by treatment with cyanide (CN-apo) was denatured as determined by its far-UV CD spectrum. The near-UV absorption spectrum was almost identical to that observed for oxidized PC. Apo-PC prepared by treating the mercury derivative with β -mercaptoethanol (M-apo) showed a far-UV CD spectrum similar to that for oxidized PC but reduced in magnitude. The extinction at 278 nm was $2.3 \text{ mM}^{-1} \text{ cm}^{-1}$ compared to $1.8 \text{ mM}^{-1} \text{ cm}^{-1}$ for CN-apo-PC. Thus, the extinction of the tyrosine residues is sensitive to protein conformation and that at least part of the absorbance at 278 nm observed upon reduction of PC may be due to conformational changes. The extinction of M-apo at 255 nm was the same as that for CN-apo PC suggesting that there is a CT band at this wavelength for reduced PC. The 255 nm CD band was missing in both the CN-apo and M-apo PC. In reduced parsley PC, this band titrated with a pK_a of 5.7 indicative of a Cu-His 87 CT transition. However, the 255 nm absorption band does not decrease below pH 5.7 and, thus, must be a different CT transition. Both the absorption and CD bands observed at 255 nm are sensitive to changes in species, salt concentration, and chemical modification leading to the conclusion that the copper center in reduced PC (as opposed to oxidized PC) is flexible and sensitive to changes in its environment.

M-Pos232 **IONOPHORE ACTION AND ELECTRICAL BREAKDOWN AND RECOVERY IN A BIOLOGICAL MEMBRANE CONTAINING INTRINSIC OPTICAL PROBES.** Daniel L. FARKAS, Department of Biochemistry, Weizmann Institute, Rehovot, Israel and Department of Physiology, University of Connecticut Health Center, Farmington, CT 06032

Changes in the structure and function of the photosynthetic membrane are reflected in large variations of the light absorption and emission by its functional pigments, which - under carefully controlled conditions - can thus serve as sensitive, fast responding intrinsic optical probes for membrane properties and events. An investigation of electrical phenomena at the membrane level is reported here, using the external electric field-stimulated luminescence of chloroplasts. The membrane conductivity - upon which the emission features (intensity, kinetics, polarization) critically depend - is increased by ionophore addition or induced electrical breakdown in a typical, strong, reproducible and conditions-dependent way. The ensuing changes have been used to characterize (1) Ionophore action: type (carrier vs. channel), rheogenicity, turnover time and intercationic selectivity have been determined i.a., with μs time resolution; (2) Electrical breakdown and recovery: conditions for irreversible vs. reversible breakdown have been described and the influence of field and medium parameters on the latter has been analysed.

The methodological advantages of this new approach for monitoring ionophores and breakdown in a natural membrane are discussed by comparison with a model system and illustrated by application to a number of lesser-known membrane-conductivity modifiers.

M-Pos233 **SYSTEM ANALYSIS OF PHYCOMYCES LIGHT-GROWTH RESPONSE IN MUTANTS AFFECTED IN GENES madC, madG AND madH.** Anuradha Palit, Promod Pratap, and Edward D. Lipson, Department of Physics, Syracuse University, Syracuse, NY 13244-1130

The fungus Phycomyces blakesleeianus has been studied extensively for its blue-light responses (Galland and Lipson, Photochem. Photobiol. 40:795-800, 1984). The Phycomyces sporangiophore bends towards unilateral light (phototropism) and changes its elongation rate transiently after changes of light intensity (light-growth response). Both the light-growth response and phototropism operate over the intensity range from 10^{-9} W m^{-2} to 10 W m^{-2} . The light-growth response has been studied with system analysis methods using Gaussian-white-noise stimuli (Lipson, Biophys. J. 15:989-1045, 1975; Poe and Lipson, and Poe *et al.*, Biol. Cybernetics, in press) and sum-of-sinusoids stimuli (Pratap *et al.* and Palit *et al.*, Biophys. J., in press). The nonlinear input-output relation of the light-growth response can be expressed mathematically by a set of weighting functions called kernels. The linear (first-order) kernels of wild type, and of single and double mutants affected in genes madA to madG were determined previously with Gaussian white noise, and were used to study interactions among the products of these genes (Poe *et al.*, see above). In this work, we have used the more precise sum-of-sinusoids stimulus method to extend the interaction study. Both the first- and second-order kernels were used to study interactions of the gene product of madH (hypertropic) with those of madC and madG. Experiments were performed on the Phycomyces tracking machine under control of a microcomputer. The kernels were analyzed in terms of kinetic models (Pratap *et al.*, and Poe and Lipson; see above). Our results, which reveal interactions of madH with madC and madG gene products, indicate that hypertropic mutations affect both the input and the output of the sensory transduction pathway for the light-growth response. (Supported by NIH grant GM29707)